Investigating gastrointestinal tract functional zonation in the gut microbiome and enzyme activity of *Oncorhynchus mykiss* (Rainbow Trout) with temperature and ion-poor water salinity challenge

Melanie Renee Williams

A Thesis Submitted to the Faculty of Graduate Studies in Partial Fulfillment of the Requirements for the Degree of Master of Science

Graduate Program in Biology

York University

Toronto, Ontario

January 2018

Abstract:

The regional distribution of digestion, metabolic, osmoregulatory and detoxification function along the GIT of fish are poorly understood. Several studies have shown evidence for zonation in the enzyme activity and zonation in the microbiome of the fish GIT; however, few studies have provided a more comprehensive survey of the interplay between the microbiome and enzyme activity with respect to zonation. The objective of this study was to explore functional zonation by manipulating two external environmental factors, specifically temperature and salinity, to observe zonation patterns in the bacterial communities, and corresponding digestive, metabolic, osmoregulatory and detoxification enzyme alterations along the GIT. It was found that zonation was more indicative of bacterial species communities and enzyme activity than temperature and salinity. The findings in this research will contribute to our understanding of the functionality of each region and the complexity of fish GIT physiology.

Acknowledgments:

I would like to express my deepest appreciation to my supervisor, Dr. Carol Bucking, for her guidance and support on my graduate school journey. Without her patience and mentorship, I would not have made it this far in my academic career.

I would also like to thank my lab mates Leah Turner and Vlad Kodzhahinchev for their words of encouragement and for helping with my experiments. In addition, I thank my colleague Pranav Dhakal for teaching me how to use the QIIME computer program and helping with my data analyses. I thank my undergraduate volunteers Sherry Bhan, Divya Patel, Taylor Reddi and Sandra Vigelis for their assistance with dissections and the enzyme assays. I also thank Dr. Scott P. Kelly and the members of his lab for their advice and assistance with my project as well as for allowing me to use their fish facilities and reverse-osmosis water treatment system for my salinity experiment. Special mention to Dmitry Rogozhnikov for reviewing my thesis and providing valuable feedback. Additionally, I express my appreciation to Dr. Raymond Kwong for joining my supervisory committee as my thesis advisor.

My sincerest gratitude goes to my parents, Leslie and Marcia Williams, and my brother, Austin, for always encouraging me to push myself and supporting me in the achievement of my goals.

Table of Contents:

List of Tables:

List of Figures:

List of Abbreviations

ADP – Adenosine Diphosphate
AI – Anterior Intestine
ANOVA – Analysis of Variance
ATP – Adenine Triphosphate
BAPNA – Nα-Benzoyl-L-Arginine-*P*-Nitroanilide Hydrochloride
CMC – Carboxymethylcellulose
COA – Coenzyme A
CS – Citrate Synthase
CW – Cold Water
DNS – Dinitrosalicylic Acid
DTNB – Dini-trothiobenzoate
DTT – Dithiothreitol
EDTA – Ethylenediaminetetraacetic Acid
$FADH_2$ – Flavin Adenine Dinucleotide
FW – Freshwater
GDH – Glutamate Dehydrogenase
GIT – Gastrointestinal Tract
GLN – Glutaminase
GS – Glutamine Synthetase
GTP – Guanosine Triphosphate
IPW – Ion-poor Water
LDH – Lactate Dehydrogenase
MDH – Malate Dehydrogenase
MI – Mid-Intestine
MS-222 – Tricaine Mesylate
NADH – Nicotinamide Adenine Dinucleotide
NKA – Sodium-Potassium ATPase
OAA – Oxaloacetate
OTUs – Operational Taxonomical Units
PEP – Phosphenolpyruvate
PI – Posterior Intestine
PK – Pyruvate Kinase
QIIME – Quantitative Insights into Microbial Ecology
RDA – Redundancy Analyses
SW – Seawater
TCA – Tricarboxylic Acid
WW – Warm Water
αKG – α-Ketoglutarate

Chapter 1: General Background

The gastrointestinal tract (GIT) has many critical functions. Its primary purpose is to extract essential nutrients from the animal's environment including water, macronutrients (protein, carbohydrates, and fats), micronutrients (minerals and vitamins) and phytochemicals (biologically activity plant compounds which serve as antioxidants) which aid in growth, development, and reproduction in addition to homeostatic balance (Stevens and Hume 2004; Sekirov 2010). The GIT also plays a role in osmoregulation, detoxification, and immunity (Meister et al. 1983; Abbaurrea-Equisoain and Ostos-Garrido 1996; Mommsen et al. 2003a; Scott et al. 2006; Buddington et al. 1997; Shin et al. 2005; Sekirov et al. 2010) which further aid in animal health and survival. To perform these functions, numerous biochemical reactions occur within the GIT aided by a variety of enzymes, many of which are endogenous to the enterocyte, the intestine cell, and produced by the organism itself (Lesel and Fromageot 1986; Saha and Ray 1998; Bairagi et al. 2002). These enzymes contribute to vital processes such as cellular respiration and energy metabolism, ion-balance, ammonia detoxification, and other aspects of digestion (Farell 2011; McCormick 1993; Rubino et al. 2014; Ray et al. 2012). Many studies have examined these biochemical pathways in response environmental manipulation, such as increasing temperature and altering water salinity. However, these past studies overlook two important factors. Firstly, mutualistic bacteria have been identified in the gut and the limited evidence that is currently available suggests the microbiome can contribute to enzymatic pathways in fish. However, the interplay between resident bacteria and the host in regards to enzymatic pathways is currently unclear. If bacteria are contributing to the various roles of the GIT, manipulating the microbiome could be an avenue for optimizing the functions of the GIT, such as nutrient assimilation. This would be beneficial for industries, such as aquaculture, as growth could be increased through increased nutrient assimilation. Secondly, anatomical

differences along the GIT exist, and functional differences are often reflected by these structural changes. For example, the trout has several specific organs within the GIT, all with specific functions. However, often studies combine these zones into one homogenous GIT, despite the possibility for functional differences. This approach may obscure alterations in the GIT in response to specific treatments. Identifying which zones are responding to environmental manipulation can aid in predicting functions that would be altered.

1.1 Enzymes in the GIT

1.1.1 Cellular respiration and energy metabolism

Cellular respiration is a process in which ATP (adenosine triphosphate), the main energy carrying molecule of the cell, is produced via the catabolism of biomolecules such as sugars, fats, and proteins (Farrell 2011). ATP fuels many of biological processes and is an essential component of cellular homeostasis and cell function (Farrell 2011). Cellular respiration consists of three major steps including glycolysis which occurs in the cytosol, and the citric acid or tricarboxylic acid (TCA) cycle and oxidative phosphorylation or the electron transport chain, both of which occur in the mitochondria. In glycolysis, glucose is catabolized into pyruvate and energy in the form of NADH (nicotinamide adenine dinucleotide, a proton carrier) is produced (Farrell 2011). Pyruvate is then shuttled into the TCA cycle where energy molecules including NADH, $FADH_2$ (flavin adenine dinucleotide) and GTP (guanosine triphosphate) are produced (Farrell 2011). In aerobic respiration, oxidative phosphorylation stage is the final step; here ATP is produced by the oxidation of the NADH and $FADH_2$ and water is produced from the reduction of oxygen (Farrell 2011). In anaerobic respiration, when oxygen concentrations are low or when no oxygen is present to accept protons in oxidative phosphorylation, pyruvate is shuttled away from the TCA cycle and stored in the form of lactic acid (Farrell 2011).

Lactate dehydrogenase (LDH), pyruvate kinase (PK) and citrate synthase (CS) are examples of key metabolic enzymes involved in cellular respiration.

LDH is a cytosolic enzyme that converts lactate to pyruvic acid in a reversible reaction and can provide either energy for the TCA cycle or glycolysis; this enzyme is associated with anaerobic respiration (Yancey and Somero 1978; Feron 2009). PK also contributes to the TCA cycle is a cytosolic enzyme that catalyzes the final step of glycolysis, converting phosphoenolpyruvate to pyruvate and producing ATP for use in the TCA cycle; it is involved in aerobic and anaerobic respiration (Locasale et al. 2011). Finally, CS is a mitochondrial enzyme which catalyses the conversion of oxaloacetate and Acetyl-CoA to citrate for the TCA cycle and is involved in aerobic respiration (Kelly et al. 2015).

1.1.1.1 Sodium-potassium ATPase

Sodium-potassium ATPase (NKA) is a plasma membrane antiporter protein that pumps 3 Na^+ extracellularly and 2 K^+ intracellularly and hydrolyses ATP (McCormick 1993). It is involved in sodium excretion in the epithelia of tissues such as in the intestine, kidney and gills, ion-balance, and cell volume regulation as well as action resting potential in nerve cells and the transport of substances across the epithelial membrane such as glucose through secondary active transport (Jampol 1970; McCormick 1993; Randall et al. 2002). Evidence suggests that NKA can influence the activity of enzymes involved in cellular respiration (Langdon and Thorpe 1985; McCormick et al. 1989; Soengas et al. 1995; Le Francois and Blier 2003; Le Francois et al. 2004). For example, during seawater exposure increased NKA activity was correlated with increased energy metabolism in the activities of LDH, PK and CS in both brook charr (Le Francois and Blier 2003) and wolfish (Le Francois et al. 2004). A functional relationship between osmoregulation (NKA) which requires high levels of energy and lactate oxidation

(LDH) has been proposed as glucose and lactose are the main fuel sources in the performance of osmoregulatory processes (Le Francois et al. 2004; Perry and Walsh 1989; Soengas et al. 1995). In contrast, CS did not show any adjustments with increased salinity and increases in NKA activity (Le Francois and Blier 2003; Le Francois et al. 2004) suggesting differences in the regulatory pathways of these enzymes (Thibault et al. 1997; Belanger et al. 2002; McCormick et al. 1989; Blier and Lemieux 2001).

1.1.2 Local ammonia detoxification in the gut

Carnivorous fish such as rainbow trout have high-protein diets; a by-product of protein digestion is the toxin ammonia (Murai et al. 1987; Bucking and Wood 2012; Wright and Wood 2009; Bucking et al. 2013; Karlsson et al. 2006; Rubino et al. 2014). Following feeding, ammonia levels in the chyme of rainbow trout increase six times higher than in the blood plasma of the intestine which was proposed to be a result of dietary protein catabolism into excess ammonia and amino acids (Bucking and Wood 2012), the latter being used for energy production in other processes (Ballantyne 2001; Stone et al. 2003; Bucking and Wood 2012). Since ammonia is toxic, mechanisms must exist to detoxify the body of ammonia; one such way is through the synthesis of amino acids (Rubino et al. 2014).

Two major enzymes, glutamate dehydrogenase (GDH) and glutamine synthetase (GS), have been implicated in ammonia detoxification processes (Wicks and Randall 2002; Wright et al. 2007; Rubino et al. 2014). GDH catalyzes the reaction of α-ketoglutarate and free ammonia to glutamate (Chew et al. 2010; Ip et al. 2010; Tok et al. 2009; Bunik et al. 2016). The GS enzyme is also involved in ammonia detoxification and protein metabolism through the conversion of free ammonia and glutamate to glutamine.

Though much ammonia detoxification occurs via excretion through the gills and kidneys, localized enzymatic detoxification of excess ammonia in the intestine of fish is also possible. GDH and GS activity, and mRNA expression of these proteins, have been identified in the guts of salmonids and midshipman (Wood 1995; Wright 1995; McDonald et al. 2012; Bucking et al. 2012; Chamberlin et al. 1991; Mommsen et al. 2003b; Murray et al. 2003; Bucking et al. 2013b). This local ammonia detoxification process in the gut may be an essential function of the gut as it serves to reduce uptake of toxic ammonia into the blood and surrounding tissues.

1.1.3 Digestive enzymes

The lumen of the GIT contains a suite of enzymes responsible for the catabolism of complex dietary molecules into smaller subunits that are readily absorbed in the GIT (Furne and Sanz 2005). Cellulase, trypsin and lipase are enzymes of interest as they are associated with carbohydrate, protein, and fat digestive processes; key functions of the GIT.

Cellulase is a digestive enzyme that breaks down cellulose, an important component of the cell wall of plant cells, into glucose monomers to be used in downstream metabolic processes such as glycolysis (Stickney and Shumway 1974; Bairagi et al. 2002; Saha and Ray 1998; Ray et al. 2012). Carnivorous fish are thought to lack the ability to produce significant levels of cellulase activity endogenously. Observed cellulase activity in the gut of carnivorous fish is present but negligible (Bairagi et al. 2002; Liu et al. 2016). Bairagi et al. (2002) proposed that this may be because carnivorous fish do not produce a significant amount of cellulase enzyme; ingestion of very small quantities of plant material may induce small levels of cellulase activity.

Trypsin is an enzyme that is involved in the catabolism of the peptide bond in polypeptides producing amino acid monomers (Lauff and Hofer 1984; Liu et al. 2016). Rainbow

trout are carnivorous fish that require a high protein diet for growth and survival; proteases such as trypsin are essential for extracting protein from their diet (Torrissen 1984). Trypsin is produced endogenously by the pancreas and secreted into the intestinal lumen in an inactive form before being activated by brush border enzymes in the intestine (Stevens 1982).

The lipase enzyme functions to break down fatty acid chains into lipid monomers that are more easily absorbed into the body (Nayak 2010). Lipase is endogenously secreted in the stomach, pancreas, and intestine (De Silva and Anderson 1994; Ray et al. 2012). Carnivorous fish like the rainbow trout have lipid-rich diets requiring lipase activity to aid in the extraction of these high energy molecules (Furne and Sanz 2005). Furne and Sanz (2005) observed that rainbow trout had higher lipase activity than the omnivorous Adriatic sturgeon indicating the importance of this enzyme to nutrient extraction in the carnivorous diet.

1.2 The contribution of GIT bacteria to digestion and metabolism

The microbiome of the GIT consists of a variety of bacteria, archaea, and fungi; these communities are termed the "gut microbiome" because they live commensally within the host (Sekirov 2010; Sommer and Backhed 2013; Liu 2016). The bacterial communities within the GIT can impact the host's physiology in a variety of ways including aiding with host digestion and absorption of nutrients, breakdown of otherwise indigestible materials, contribution of essential vitamins, and influencing host epithelial permeability and transport (Turnbaugh et al. 2006; Backhed et al. 2004; Sullam et al. 2012; Sommer and Backhed 2013). In return, the microbiome is provided a habitat to grow and reproduce as well as nutrients from their host's ingested meals and secretions by the GIT (Lesel 1991; Bairagi et al. 2002).

There are three major evolutionarily conserved bacterial phyla amongst eukaryotes which consistently populate the gastrointestinal tract (commonly referred to as "core gut bacteria"): Firmicutes, Bacteroidetes and Proteobacteria (Sullam et al. 2012; Xia et al. 2014; Lowrey 2014; Ratten et al. 2017). Species of bacteria in these groups have been shown to have an impact on digestion and absorption of nutrients and can serve as an indicator for changes in host physiology (Xia et al. 2014, Shin et al. 2015, Ley et al. 2006). Firmicutes (often grouped with the Tenericutes bacterial phyla due to phylogenetic similarity) have been associated with high protein and calorie diets as well as with processes related to lipid uptake (Semova et al. 2012; Carmody and Turnbaugh 2012); Li et al. (2015) has also suggested Firmicutes utilizes complex polysaccharides including cellulose, xylan and hemicelluloses. Bacteroidetes is associated with low calorie diets and the fermentation of plant material and protein in fish (Xia et al. 2014; Ruth et al. 2006; Ley et al. 2006; Shin et al. 2015; van Kessel et al. 2011; Ratten et al. 2017). Finally, Proteobacteria has been associated with protein-rich diets and processes related to the modulation of the microbiome; for instance, starved Asian seabass were shown to have decreased Proteobacteria and an increase in Bacteroidetes compared to the control fed fish (Bairagi et al. 2002; Ray et al. 2012; Xia et al. 2014; Shin et al. 2015).

The gut microbiome and its relationship to host metabolism has been previously studied in mammals particularly in relation to the role of bacteria in nutrient extraction and obesity. For example, there is evidence suggesting that a difference exists in the microbiome of obese and lean individuals and this variation can influence the ability of the host to extract and process dietary nutrients; the microbiome of obese individuals enhances energy harvest and is associated with increased Firmicutes while leaner individual's microbiome is dominated by Bacteroidetes (Backhed et al. 2004; Turnbaugh et al. 2006). Piscine studies are lacking however there is

anecdotal evidence for fish. For example, Stickney and Shumway (1974) detected low levels of cellulase activity in omnivorous and carnivorous fish and postulated that this was perhaps a result of the ingestion of invertebrates containing cellulase-producing microflora.

1.3 Evidence for zonation along the GIT

Morphological zonation has been identified in the rainbow trout gut. Their GIT is divided into four anatomically distinct regions: the stomach, anterior intestine (AI) – which includes small, numerous, finger-like projections known as pyloric ceca, the mid-intestine (MI) and posterior intestine (PI) (Figure 1). Each of these zones can contribute specific functions to the GIT. For example, the stomach aids in acid digestion while the AI aids in lipid digestion (Bik et al. 2006; Semova et al. 2012; Carmody and Turnbaugh 2012). These specific functions are often overlooked, and the GIT is treated as a uniform organ. However, with anatomical zonation along with functional zonation, this approach may obscure specific responses of each section to treatments such as environmental manipulation.

Different enzymes show patterns of activity zonation along the GIT of fish as was explored by Mommsen et al. (2003a) who investigated metabolic zonation in the gut of fish. They reported the activities of the mitochondrial enzymes, GDH and CS, as well as cytosolic LDH decreased along the GIT of the rainbow trout where the stomach followed by the pyloric ceca had the highest activities (Mommsen et al. 2003a). This corroborated the findings of a study by Walsh et al. (1991) where it was observed there was increased mitochondrial density in the anterior portion of the GIT suggesting a specialization of this region for energy metabolism. Mommsen et al. (2003a) also identified zonation patterns in other enzymes, including malic enzyme, 6-phoshogluconate dehydrogenase, isocitrate DH, glucose-6 phosphate DH as well as

alanine and aspartate aminotransferases. In addition to rainbow trout, they also examined Nile tilapia and copper rockfish which also exhibited regional enzyme differences along the gut.

There is also evidence to support zonation of digestive enzyme activity, particularly with regards to trypsin. Stevens (1982) investigated trypsin activity in the pyloric ceca of rainbow trout and found that the anterior ceca had higher trypsin activity compared to the posterior ceca. He proposed that this increase in activity in the anterior portion of the ceca was due to the closer association between the ceca and the pancreas which secretes this digestive enzyme (Stevens 1982). Conversely, Torrissen (1984) reported rainbow trout had the highest level of trypsin activity in the mid-intestine followed by pyloric ceca, the stomach, posterior intestine, and the anterior intestine. Finally, Uematsu et al. (1992) state that lipase activity occurs primarily in the pyloric ceca and the proximal intestine in the red sea bream (Olsen and Ringo 1997).

Zonation of the GIT microbiome has been examined, however most of these studies have focused on mammals. In mammals, the density of bacterial populations increases along the anterioposterior axis of the gut (Sekirov et al. 2010; Sommer and Backhed 2013). Additionally, in the stomach and small intestine, bacteria of *Enterococci* and *Lactobacilli* (of phyla Firmicutes) and *Enterobacillae* (of phyla Proteobacteria) predominate (Sarma-Rapuvtarm et al. 2004; Macpherson and Harris 2004; Corbitt 2011). In contrast, in the large intestine, *Bacteroides* (of phyla Bacteroidetes), *Bifidobacteria* (of phyla Actinobacteria), *Clostridium*, *Fusobacteria* and *Peptostreptococci*, all strict anaerobes, predominate in mice (Sarma-Rapuvtarm et al. 2004; Macpherson and Harris 2004; Corbitt 2011). Zonation of bacteria within fish GITs has only been examined in the brown trout (Al-Hisnawi et al. 2015), and the pyloric ceca appeared to have the highest bacterial diversity of all sections. However, this study did not explore the effects of these bacterial populations on host physiology.

Interaction between region-specific intestinal function and bacteria has been postulated. Rubino et al. (2014) hypothesized zonation in ammonia handling and the activity of GDH, GS and GLN (glutaminase; converting glutamate to glutamine) along the GIT of rainbow trout in response to feeding. GS and GDH but not GLN activity showed evidence of zonation where GS showed increased activity along the anterioposterior axis in the unfed condition where the PI had 10-fold higher activity than the AI; conversely, GDH activity decreased over the anterioposterior axis in the fed condition where the AI had 3-fold higher activity than the PI which corresponds to the findings of Mommsen et al. (2003b). This increased GS activity in the PI was postulated to be a result of the localization of ammonia-fixing bacterial flora via GS (ammonia is their preferred nitrogen source) or glutamine synthesis for processes related to energy production in intestinal cells (Magasanik 1977; Taylor et al. 2011; Rubino et al. 2014). Thus, enzymes with similar processes do not necessarily correlate in their patterns of zonation but may instead be influenced by exogenous factors such as the microbiome or other complex regulatory processes.

Bacteria have a multitude of functions within the gut and contribute in various ways to host physiology. The region-specific localization of certain bacterial communities and the ways in which they contribute to gut function and health can provide insights into functional zonation along the gut. Additionally, morphological and histochemical zonation has also been established in the GIT of rainbow trout and there is a great deal of evidence for enzymatic zonation (Harder 1975; Stevens 1982; Torrisen 1984; Wilson and Castro 2010; Mommsen et al. 2003a; Mommsen et al 2003b; Bucking and Wood 2007; Bucking and Wood 2012; Rubino et al. 2014). However, the relationship between the microbiome and enzyme activities in the context of functional zonation have not been well established in fish. Understanding patterns of zonation in the GIT

can contribute to our understanding of the multifunctionality of the gut and its importance to fish physiology.

1.4 Study objectives

Previous studies have examined zonation in the microbiome and the activity of GIT associated enzymes separately. The objective of this novel study was to investigate the interactive effect of the gut microbiome on functional zonation in the rainbow trout, assayed through genetic identification of GIT bacteria and the measurement of enzyme activities. It was hypothesized that patterns of zonation along the GIT would be detected in the composition of the bacterial communities and the activities of important metabolic and digestive enzymes and that these patterns may indicate a synergistic relationship between the gut bacteria and enzyme activity in each region thus elucidating functional zonation in rainbow trout gut physiology (Figure 1). Two external environmental stressors, temperature and salinity, have been previously been shown to affect both the microbiome and enzyme activity separately in fish (Lesel and Peringer 1981; Al-Hisnawi et al. 2015). The effects of these stressors on functional zonation and the microbiome was explored to determine the possible role of zonation modalities on fish physiology. In Chapter 2, I will discuss the effect of temperature on the microbiome and enzyme activity zonation relationship. Chapter 3 will focus on the effect of salinity on these factors. Finally, in Chapter 4, I will compare my findings from these experiments and draw conclusions about functional zonation in the rainbow trout GIT.

This work will contribute to our understanding of regionalized function in the gut and the contribution of the GIT bacteria. Characterization of the gut microbiome and relation to gut functions, such as nutrient assimilation and metabolism would be of great use to aquaculture, an industry worth an estimated $99.2 billion USD worldwide (FAO 2016), where microbiome

alterations through environmental manipulations such as diet or in husbandry conditions can be controlled to optimize growth and health. Additionally, considering the GIT as a regionalized organ system in future studies will expand on our knowledge of the function and complex relationship of this system and its contribution to overall fish physiology.

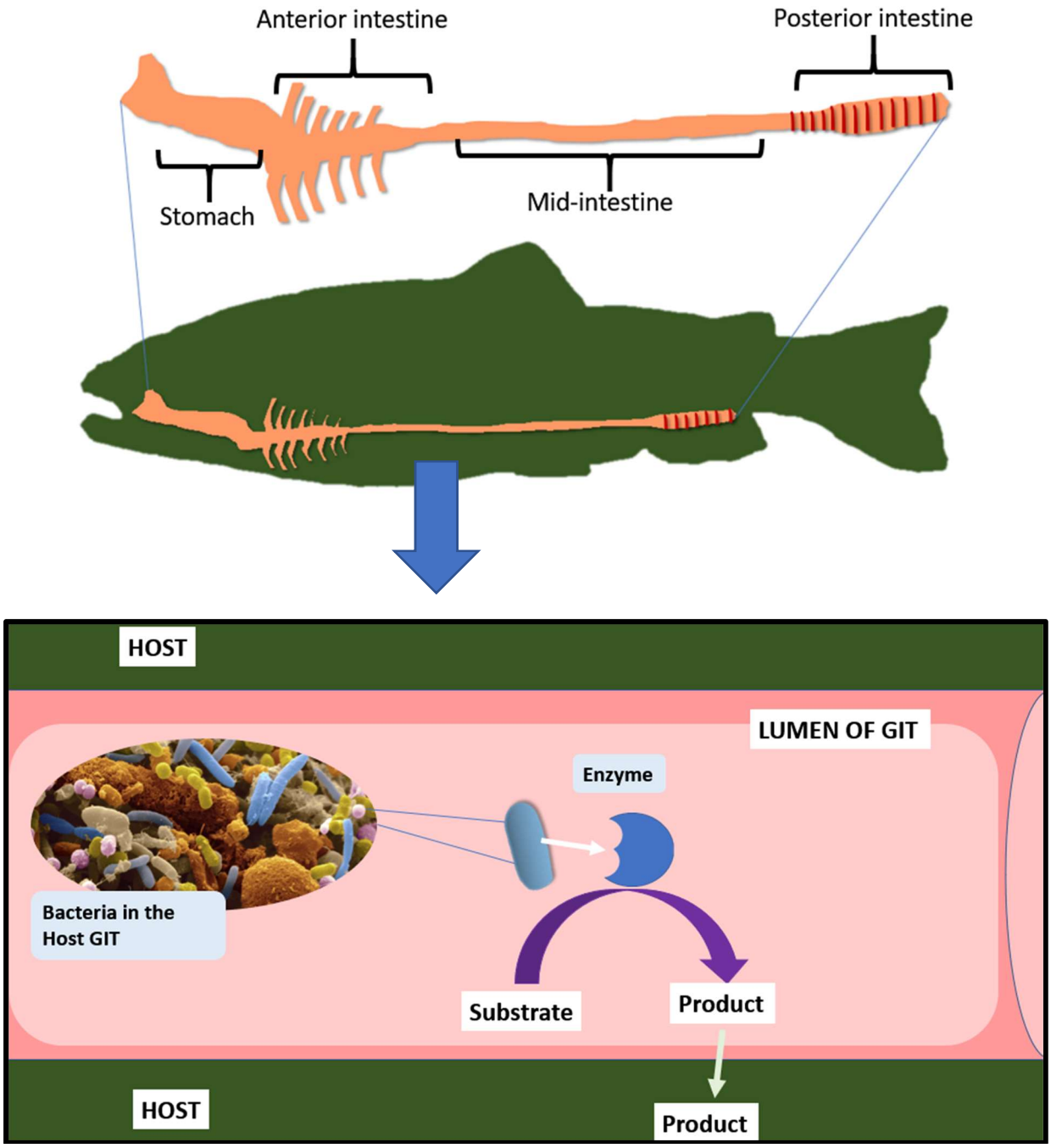

Figure 1. Exploring bacterial and enzyme activity zonation in the GIT of the rainbow trout. The GIT consists of four major anatomically distinct regions which include the stomach, anterior intestine (AI), middle intestine (MI), and posterior intestine (PI). The relationship between bacterial composition in each region of the GIT and enzyme activity will be investigated to establish patterns of functional zonation.

Chapter 2: The effect of temperature on the microbiome, and metabolic and digestive enzyme activities along the GIT of the rainbow trout

Introduction:

2.1 Overview

Most fish are poikilotherms meaning that they lack mechanisms which would enable them to regulate their body temperature; as a result, any endogenous heat that they manage to produce is lost to their external environment via the gills and body surface (Hazel and Prosser 1974; Stevens and Sutterlin 1976; Currie and Schulte 2014). The microbiome of the gut can be influenced by temperature which may allow for the proliferation of bacteria that can influence fish physiology in a variety of ways (Lozupone and Knight 2007; Nayak 2010; Givens 2014; Zarkasi et al. 2016). Therefore, temperature has a tremendous impact on the physiological processes regulating homeostatic balance such as the microbiome as well as the rate of chemical reactions via the alteration of thermal energy, changes to the structure and functioning of proteins, and membranes properties such as permeability (Schulte et al. 2011; Currie and Schulte 2014).

2.2 The effects of temperature on the GIT microbiome

Temperature can affect the bacterial populations of the microbiome in fish (Lesel and Peringer 1981; Lozupone and Knight 2007; Nayak 2010; Givens 2014; Zarkasi et al. 2016). Lesel and Peringer (1981) performed a bacterial count in the major regions of the whole GIT in rainbow trout and observed that temperature increase had positive effect on the counts of bacteria in each region; however, the implications of these changes were not investigated. Furthermore, Al-Hisnawi et al. (2015) examined the resident bacterial populations along the anterior, posterior, and pyloric ceca regions of the intestine in brown trout; the pyloric ceca had the highest bacterial diversity followed by the anterior region, but this group did not explore the

physiological aspects of the microbiome on the host or temperature responses. Studies suggest that sporadic proliferation of some bacterial taxa may be due to host physiological responses to temperature stress (Zarkasi et al. 2014). In addition, Proteobacteria abundance increases at higher temperatures in the gut of fish indicating that this phylum may have a physiological significance (Givens 2014; Al-Hisnawi et al. 2015).

2.3 The effects of temperature on enzyme activity and compensatory responses

Temperature impacts the kinetic activity of biological and physiological processes (Currie and Schulte 2014). Factors such as enzymatic maximum velocity and enzyme-substrate affinity influence the activity levels of enzymes and transporters, the former of which has been well-studied in poikilotherms (Licht 1967; Mutchmor 1967; Rasmussen and Rasmussen 1967; Read 1967; Somero and Hochachka 1968).

Animals can have different types of compensatory metabolic responses to stressors such as temperature. Precht (1958) proposed five patterns of metabolic compensation including ideal compensation, partial compensation, supraoptimal compensation, inverse compensation, and no compensation. In ideal compensation, the original metabolic activity level is restored following stressor exposure. In partial compensation, the original activity level is not fully restored while in supraoptimal compensation the original activity is overshot. If the activity level follows the direction of the stressor, that is, an increase or decrease with increasing or decreasing temperature, this is considered no compensation. In inverse compensation, the activity level response is greater than in no compensation such that it is the inverse of the supraoptimal compensation response (Precht 1958; Prosser 1969). In this work, the compensatory patterns in metabolic activity along the GIT in response to increasing temperature will also be explored to detect zonation patterns.

Enzymes involved in energy metabolism such as LDH and PK are stable within a limited range of their thermal tolerance range displaying perfect compensation; similar behaviour is expected with CS activity as this enzyme is also involved in cellular respiration like LDH and PK (Smith and Ellory 1971; Yancey and Somero 1978; Coppes and Somero 1990; Low and Somero 1976; Prosser 1991; Ozernyuk et al. 1994; Eddy 2005). It is important for organisms to regulate the activity of certain enzymes such as LDH, PK and CS to maintain stable levels of function under environmental stress as this aids in ensuring homeostatic balance (Low and Somero 1976). Overcompensation in the activities of NKA and lipase have been reported in the intestinal tissues of some fish species (Smith and Ellory 1971; Borlongan 1990). Other enzymes, such as cellulase and trypsin have shown metabolic adaptation or an inverse compensatory response to decreased temperature where their activities are elevated to maintain metabolic rates against decreased thermal kinetic energy (Kristjbnsson 1991). GDH and GS, involved in ammonia detoxification, are likely to increase in warmer water as higher temperatures are correlated with increased permeability of epithelial surfaces in fish to ammonia from the water; an increased requirement for local ammonia detoxification in the GIT epithelia is required to mitigate this effect (Prosser 1991; Eddy 2005).

2.4 Hypotheses

The effect of seasonal temperature changes and lab-simulated alterations of water temperature on fish physiology and the gut microbiome have been explored in previous studies, however, functional patterns along the GIT of fish in response to temperature have not been well documented. Understanding the way in which temperature changes the microbiome and enzymatic activity will aid in elucidated functional zonation in the fish gut.

The eurythermal rainbow trout has a thermal tolerance range of 0°C – 25°C where their optimal performance temperature is 11°C making it an excellent model for temperature stress studies (Threader and Houston 1983; Taylor et al. 1996; Aho and Vornanen 2001).

In this study, long-term exposure (6 weeks) to elevated temperature (17ºC) was used to investigate the acclimation capacity in enzyme activity and perturbations to the bacterial populations along the GIT of the rainbow trout to explore functional zonation. An analysis of metabolic and digestive enzymes as well as bacterial populations along the GIT were also used to performed to determine the interrelationship between temperature, the microbiome, and the host physiology in zone-specific regions.

Firstly, it was hypothesized that *increasing temperature will lead to the proliferation of Proteobacteria over the other core gut bacteria phyla*. This is because in previous studies the proportion of Proteobacteria has been found to increase in the gut of fish when tank water temperature was increased (Givens 2014; Al-Hisnawi et al. 2015).

Furthermore, it was hypothesized that *some enzymes would not be as affected by temperature as other enzymes due to compensatory mechanisms which aid in the regulation and stabilization of their activities*.

Enzymes including sodium-potassium ATPase (NKA), cellulase, trypsin, lipase, glutamate dehydrogenase (GDH), glutamine synthetase (GS) have been shown to be affected by changes to ambient temperature while lactate dehydrogenase (LDH) and pyruvate kinase (PK) have demonstrated relatively stable activities with increased temperature in fish; citrate synthase (CS) activity is also expected to exhibit similar behaviour to LDH and PK as they belong to a class of enzymes involved in cellular respiration. GDH and GS activity might become more

important at higher temperatures due to increased dietary protein catabolism for energy production. The interrelationship between enzyme activity and the microbiome was explored to understand how these factors together may contribute to functional zonation in the stomach, AI, MI and PI.

Materials and Methods

3.1 Fish care:

Rainbow trout (Humber Springs Trout Farm, Orangeville, Ontario) were kept in three 200L aerated, flow-through tanks at 6°C (~25 individuals per tank) with dechlorinated freshwater supplied through the City of Toronto. Fish were fed UV-sterilized 3-point pelleted fish food (Tropica Aquaria Limited, Brampton, Ontario; see composition in Appendix D) every 48 hours during acclimation and for the duration of the experiment. Fish health and water temperature were monitored each day; the water quality was monitored on a weekly basis to ensure the levels of ammonia, nitrate and chlorine were within a safe limit.

3.2 Initial dissections, sampling, and tissue storage

To prepare for aseptic dissection, forceps, scissors, and 2 ml microcentrifuge tubes for sample collection were UV-sterilized for 15 minutes and the bench surface was sprayed and wiped with 70% ethanol to reduce foreign bacterial contamination during dissection. At t=0, five fish euthanized with an overdose of tricaine methane sulfonate (MS-222; Sigma Aldrich, Oakville, Ontario) in a bucket of water (pH 7.4), their length and mass were recorded, and the exterior surfaces of the animal were sprayed with 70% ethanol. Fish were dissected by lateral incision starting posterior to the operculum along the ventral surface and ending at the anus to expose internal organs. Samples of tissue and stool from the stomach, AI, MI, and PI were aseptically collected, ensuring rotation of dissection tools into the 70% ethanol tube after each major incision. Samples were stored in 2 ml microcentrifuge tubes and snap-frozen and kept on dry ice until freezer storage at -80°C.

3.3 Temperature experiment and sampling periods

The water temperature of three tanks holding the experimental fish were adjusted to 6°C, 12°C and 17°C over a period of 24 hours and the water temperatures were monitored daily. At 6 weeks exposure, four fish were sampled from the 6°C, 12°C and 17°C tanks. Samples were collected to be used in the microbiome analysis as well as in the enzyme activity analysis.

3.4 Stool and tissue bacterial sample gDNA extraction

Bacterial gDNA extraction was performed by combining two commercial extraction kits. First, the QIAGEN QIAamp DNA Stool Mini Kit (QIAGEN; Toronto, Ontario) was used as per manufacturer instructions to isolate DNA from each of the stool samples collected from each fish GIT zone. Prior to extraction, kit contents, pipettes and tips, and microcentrifuge tubes were UV-sterilized for 20 minutes. Samples were homogenized using a hand-held power homogenizer to aid in the lysis of cells. A blank (a 2-ml microcentrifuge tube with no stool or tissue sample) was prepared using the kit reagents alongside the gDNA extraction of the samples to ensure that the extraction process was sterile (Appendix C, Table 3). The isolated DNA from each sample were then stored at -20°C until further analysis.

Then, the QIAGEN DNeasy Blood and Tissue kit was used as per manufacturer instructions to isolate DNA from each intestinal content, stool and tissue sample collected from each fish GIT zone. Buffer ATL and Proteinase K were added to each sample and incubated on a 56°C rocking heater block overnight to facilitate lysis of cells in the sample. A blank (a 2-ml microcentrifuge tube with no stool or tissue sample) was prepared alongside the extraction of the samples to ensure that the extraction process was sterile (Appendix C). The isolated DNA from each sample were then stored at -20°C until further analysis.

3.5 Bacterial gDNA quantification, pooling, and packaging:

The isolated DNA from each sample was quantified using the BIOTEK Synergy HT spectrophotometer using the Take3 plate and Gen 5 v3.02 software (BIOTEK Instruments Inc.; Winooski, Vermont) and each extraction kit sample was pooled before being stored at -20°C until further analysis. For the microbiome analysis, samples from each fish in each treatment were pooled into a single stomach, AI, MI, and PI sample containing a minimum of concentration of 80 ng/uL isolated gDNA with a quality ratio (260 nm to 280 nm) ~2. The AI and MI were combined because I had not been able to detect distinguishable bacterial compositions in my initial method validation study; AI+MI are considered one sample in this analysis. Pooled stomach, AI and MI combined, and PI gDNA samples from each treatment group were placed into appropriately labelled individual zip-locked bags, placed in one package, and sent to Mr. DNA (Shallowater, Texas) in for bTEFAP ® Illumina sequencing of 16S RNA. Briefly, universal 16S RNA primers were used in PCR to amplify a short region of 16sRNA (~ 300 bp) that contained species-specific nucleotide sequences bracketed between the universal regions. Hence, the primers amplified all bacterial sequences present in the extracted gDNA during PCR, which were then individually sequenced using Illumina sequencing. These individual sequence files were then analyzed as outlined below.

3.6 Bacterial DNA sequence analysis

DNA sequence data sets including a fasta sequence file, a qual quality file and a mapping file in addition to analysis pipeline files containing the counts of bacteria in each sample were obtained from Mr. DNA following Illumina sequencing. Since the temperature experiment was repeated twice and the 6°C and 12°C results were the same, the fasta, qual and mapping files from each Illumina sequencing run were concatenated, resulting in a pooled 6-12°C cold water (CW) and 17°C warm water (WW) samples. Data were analyzed using QIIME ® (Quantitative

Insights into Microbial Ecology), R Studio and Microsoft Excel. QIIME was used to filter sequences to remove low quality reads (<25 base pairs), short and long sequences (<200 nucleotides; >1000 nucleotides), gaps, sequences with homopolymer runs exceeding 6 nucleotides, and zero primer sequence mismatches. Chimeras were identified and removed from the filtered sequences using UCHIME in USEARCH v5.2.236 (Edgar et al. 2011). Sequences with a minimum of 97% similarity were organized into OTUs (operational taxonomical units), essentially similar to biological species, using USEARCH (Edgar 2010); OTUs were then compared to the bacterial 16S rRNA Green Gene database using a closed-reference OTU picking protocol and assigned taxonomy for downstream analysis (Caporaso et al. 2010; Caporaso et al. 2011; Kuczynski et al. 2012). Unassigned bacterial species were removed from the data set prior to downstream analysis. To remove uneven sampling depth impacts on diversity analyses, the sequences from each sample were rarefied to the lowest sequence number detected.

For the alpha diversity analysis, which examines diversity (richness and abundance) within individual sample's sequences, the following rarefaction curves were generated with QIIME: observed OTUs detected in each sample per sequence subset, phylogenetic diversity (PD) whole tree (which depicts the likelihood of a new OTUs being identified in the sample), Shannon (showing the abundance of OTUs in each sample) and Chao1 (representing the likelihood of finding a rare species).

Beta diversity analyses, comparing diversity between samples, were performed by generating unweighted (OTU identity-based) and weighted (OTU identity and abundance-based) Unifrac metric which was based on the abundance data that had been normalized (Lozupone and Knight 2010). Principle coordinate analyses representing the degree of variation in sample sequences between samples were generated from these metrics. The metrics were used to create

a jackknifed beta diversity analysis (Caporaso et al. 2010; Caporaso et al. 2011) to examine the similarity of OTU diversity between samples. Bootstrap consensus trees were generated using Unweighted Pair Group Method with Arithmetic mean (UPGMA) clustering based on the jackknifed analysis. A bacterial phylum % identity stacked bar graph was generated in Microsoft Excel from the OTU sequences assigned taxonomy from Green Genes library in QIIME.

Finally, multivariate redundancy analyses (RDA) were generated using the vegan package in R Studio from the OTU biome table generated in QIIME (Oksanen et al. 2015). The RDA plot is generally used to depict the variation in the response variables (in this case the bacterial species abundance) that can be explained by the explanatory variables (the GIT zones and treatments).

The description of the scripts used in QIIME and R Studio for these analyses are in Appendix A and B.

3.7 Enzyme assay analysis tissue preparation:

Assays of nine enzymes, NKA, LDH, PK, GDH, CS, GS, cellulase, trypsin, and lipase, were used to measure zone-specific changes in activity in response to varying temperature. Maximal activities were measured in this experiment which were optimized beforehand. The Bio-Rad Bradford Assay was used to measure protein content as per manufacturer protocol using 5 µl of sample homogenate and 200 µl of Bradford Dye Reagent. Enzyme activities were normalized by protein concentrations in the final calculations of specific enzyme activity.

Each zone of the GIT tissue (stomach, AI, MI, and PI) was homogenized using an ice-cold glass homogenizer and pestle in the corresponding homogenization buffer. A BIOTEK

Synergy HT spectrophotometer with BIOTEK Gen 5 v3.02 software was used to measure enzyme activities (BIOTEK Instruments Inc.; Winooski, Vermont).

3.7.1 Sodium-potassium ATPase

The NKA activity assay protocol was adapted from McCormick (1993). Two types of homogenization buffer were prepared: one was SEI buffer (150 mM sucrose, 10 mM EDTA, and 50 mM imidazole in ddH_2O at pH 7.5) and the other was SEID buffer (5g/L deoxycholate added to an aliquot of SEI buffer), the latter of which was prepared daily. Both homogenization buffers were kept chilled on ice. Frozen tissue was homogenized in a 150 µl SEI and 50 µl SEID mixed homogenization buffer. Homogenate was transferred to a 1.5 ml microcentrifuge tube and centrifuged for at 4°C (1 min. at 10000 RPM) and the resulting supernatant was used in the assay.

Two primary reactions buffers, prepared fresh daily: Solution A (2.8 mM Na^+-PEP, 0.7 mM ATP, 0.22 mM NADH, 4U/µl LDH, 5U/µl PK and 50 mM imidazole in ddH_2O at pH 7.5) and Solution B (0.5 mM ouabain in an aliquot of Solution A at pH 7.5). Solution B was covered with aluminum foil to prevent photo-degradation of ouabain. A salt solution was prepared from 50 mM NaCl, 10.5 mM $MgCl_2$, 42 mM KCl and 50 mM imidazole in ddH_2O at pH 7.5. The final two reaction mixtures containing a 4:1 ratio of Solution A: salt solution and Solution B: salt solution was made. A 96-well microplate was pre-chilled on an ice pack prior to sample loading. Sample reactions using Solution A: salt mix and Solution B: salt mix were run in duplicates and contained 10 µl homogenate and 200 µl reaction buffer each. Immediately following well loading, the microplate was placed in the spectrophotometer at 26°C and absorbance was read at 340 nm for the decrease in NADH (which is coupled with the hydrolysis of ATP) over 12 minutes. NKA activity was calculated based on the difference between the rate of ouabain-

insensitive (Solution A: salt mix) and ouabain-sensitive (Solution B: salt mix) ATP hydrolysis and was expressed as μmol ADP mg^{-1} protein h^{-1}.

3.7.2 Lactate dehydrogenase

The LDH assay performed was adapted from McClelland et al. (2008). The homogenization buffer was composed of 20mM HEPES, 1mM EDTA and 0.1% Triton X-100 in ddH_2O pH 7.4. Frozen tissue was homogenized in ice-cold homogenization buffer and samples were stored on ice. The reaction buffer, prepared fresh daily, was composed of 0.15 mM NADH, 0.2 mM pyruvate-Na, 50 mM imidazole in ddH_2O at pH 7 was chilled on ice. A 96-well microplate was pre-chilled on an ice pack prior to sample loading. Sample reactions were run in triplicates and contained 10 μl homogenate and 200 μl reaction buffer each. Immediately following well loading, the microplate was placed in the spectrophotometer at 26°C and absorbance was read at 340 nm for the decrease in NADH over 6 minutes. LDH activity was calculated based on the conversion of pyruvate to lactic acid coupled to the oxidation of NADH to NAD^+, and was expressed as μmol min^{-1} g^{-1} protein.

3.7.3 Pyruvate Kinase

The PK assay performed was adapted from McClelland et al. (2008). The homogenization process was the same as was used for LDH and used the same buffer. The reaction buffer, prepared fresh daily, was composed of 0.15 mM NADH, 5 mM ADP, 0.01 ml LDH and 50 mM imidazole in ddH_2O at pH 7.4 and was chilled on ice. For each sample assayed two reactions were prepared: one with and one without phosphoenolpyruvate (PEP) to measure the net decrease in NADH as PEP was reduced by PK. For the reaction with PEP, 5mM PEP was added an aliquot of the stock reaction buffer described above and chilled on ice. A pre-chilled

96-well plate was loaded with the reactions where the with and without PEP reactions were each run as duplicates consisting of 10 µl homogenate and 200 µl reaction buffer each. The absorbance was read at 340 nm for the decrease in NADH in a spectrophotometer at 26°C for 6 minutes. PK activity was calculated from the difference in the rates of NADH oxidation in the with and without PEP reactions and expressed as µmol min^{-1} g^{-1} protein.

3.7.4 Glutamate dehydrogenase

The GDH assay performed was adapted from Walsh (1995). The homogenization process was the same as was used for LDH. The reaction buffer, prepared daily, was composed of 0.12 mM NADH, 1 mM ADP, and 50 mM imidazole in ddH_2O at pH 7.4 and was kept chilled on ice. For each sample assayed there were two reactions prepared: one with and one without α-ketoglutarate to measure the net decrease in NADH as α-ketoglutarate (αKG) was converted to glutamate. For the reaction with αKG, 14 mM α-ketoglutarate was added an aliquot of the stock reaction buffer described above and chilled on ice. A pre-chilled 96-well plate was loaded with the reactions where the with and without αKG reactions were each run as duplicates consisting of 10 µl homogenate and 200 µl reaction buffer each. The absorbance was read at 340 nm for the decrease in NADH in a spectrophotometer at 26°C for 10 minutes. GDH activity was calculated from the difference in the rates of NADH oxidation in the with and without αKG reactions and expressed as µmol min^{-1} g^{-1} protein.

3.7.5 Citrate synthase

The CS assay performed was adapted from McClelland et al. (2008). The homogenization was the same as was used for LDH except 1 mM DTT was added to the buffer during daily preparation and kept chilled on ice. The homogenized samples were then frozen at -

20°C overnight prior to the assay. The reaction buffer, prepared daily, was 50 mM Tris-HCl, 0.1 mM DNTB, 0.3 mM Acetyl-CoA and 0.5mM oxaloacetate at a pH 8 in ddH_2O and was chilled on ice; the solution was covered with aluminium foil to protect the DTNB from photo-degradation. For each sample assayed there were two reactions prepared: one with and one without oxaloacetate (OAA) to measure the net decrease in DTNB as OAA was converted to citrate. For the reaction with OAA, 0.5 mM OAA was added an aliquot of the stock reaction buffer described above and chilled on ice. A pre-chilled 96-well plate was loaded with the reactions where the with and without OAA reactions were each run as duplicates consisting of 10 µl homogenate and 200 µl reaction buffer each. The absorbance was read at 412 nm for the increase in DNTB in a spectrophotometer at 26°C for 10 minutes. CS activity was calculated from the difference in the rates of Acetyl-CoA reduction to CoA-DTNB in the with and without OAA reactions and expressed as µmol min^{-1} g^{-1} protein.

3.7.6 Glutamine synthetase

The colorimetric GS activity assay was based on the method of Shankar and Anderson (1985). The homogenization buffer was composed of 20 mM K_2HPO_4, 10 mM HEPES, 0.5 mM EDTA and 1 mM DTT in ddH_2O at pH 7.5 and kept chilled on ice. Tissue was homogenized in an ice-cold homogenizer and homogenate was stored in a 1.5 ml microcentrifuge tube and chilled on ice. The reaction cocktail was composed 60 mM glutamine, 15 mM hydroxylamine, 0.4 mM ADP, 20 mM KH_2AsO_4, 50 mM HEPES and 3 mM $MnCl_2$ in ddH_2O at pH 6.7 and kept chilled on ice. The ferric chloride stopping agent (which halts the reaction) was composed of 50% HCl, 24% Trichloroacetic acid and 10% $FeCl_3$ in 0.2 N HCl all prepared in ddH_2O and combined in a 1:1:1 ratio. The ferric chloride stopping agent reacts with the intermediate molecule in the reaction mechanism, acyl-phosphate, resulting in a red-brown colour change in

the solution; the darker the colour, the more robust the reaction. Two 1.5 ml microcentrifuge tubes were prepared for each sample: for the control 200 µl cocktail, 80 µl tissue supernatant and 60 µl ferric chloride stopping agent was immediately added and vortexed, and for the experimental run the reaction was allowed to run for 20 minutes before 60 µl ferric chloride stopping agent was added and vortexed. A 96-well plate was loaded 200 µl with the control and experimental runs for each sampled and read in the spectrophotometer at 540 nm to measure the concentration of acyl-phosphate and expressed as µmol min^{-1} g^{-1} protein.

3.7.7 Cellulase

The cellulase assay performed was adapted from Denison and Koehn (1977) and Saha et al. (2006). The homogenization buffer was 0.1M PBS buffer in ddH_2O at pH 6.8 which was kept chilled on ice. The homogenate was centrifuged prior to assay preparation at 12000G for 20 minutes. The reaction buffer was with or without 1% carboxymethylcellulose (CMC) in 0.1M PBS buffer at pH 6.8 which was kept chilled on ice. A dinitro salicylic acid (DNS) stopping reagent was prepared from 0.2M DNS and 2M NaOH in ddH_2O. 125 µl homogenate was combined with 125 µl reaction mixture in a 1.5 ml microcentrifuge tube which was vortexed and incubated at 37°C for 1 hour. Immediately following incubation, 750 µl DNS stopping reagent was added to each tube, vortexed and incubated at 90°C for 10 minutes. A 96-well plate was loaded with 200 µl of the with and without 1% CMC solution reactions, absorbance was measured at 574 nm for the appearance of glucose and compared against a glucose standard curve. Cellulase activity was measured as the difference in the rate of reaction with and without 1% CMC expressed as mg glucose min^{-1} mg^{-1} protein (Liu et al. 2016).

3.7.8 Trypsin

The trypsin assay performed was adapted from Stevens (1982). The homogenization buffer was prepared with 50 mM Tris-HCl at pH 7.5 in ddH_2O chilled on ice. Following homogenization, the homogenate was centrifuged at 12000 G for 15 minutes. Two reaction buffers were prepared: one with 2 mM Nα-benzoyl-L-arginine-*p*-nitroanilide hydrochloride (BAPNA) and one without BAPNA in aliquots of 50 mM Tris-HCl; solutions were kept chilled on ice. A chilled 96-well plate was loaded 10 µl homogenate and 200 µl of reaction buffer either with or without BAPNA; reactions were run in duplicates and absorbance was measured at 410 nm for the appearance of p-nitroaniline from catalysis of BAPNA over a period of 10 minutes at 37°C. The difference in activity with and without BAPNA in reaction solution was used to calculate the activity of trypsin and was expressed in µmol min^{-1} g^{-1} protein.

3.7.9 Lipase

The lipase assay was performed on GIT tissue samples with the Sigma Aldrich Lipase Activity Assay Kit as per manufacturer instructions (Sigma Aldrich; Toronto, Ontario). Activity was expressed as nmol of triglyceride converted to glycerol min^{-1}.

3.8 Data analysis and statistics

Data was expressed as mean specific enzyme activity ± standard error of mean (SEM) for all enzyme assays. Data for changes in an enzyme activity between GIT sections within each temperature were analyzed using analysis of variance (ANOVA) with repeated measures because the groups (the GIT sites), while data for changes in enzyme activity within one GIT section between temperatures was analyzed with a one-way ANOVA. Variation that was significant between means was further analyzed using the Tukey post-hoc test. Only significant data and findings are discussed in this section.

Results

4.1 Bacterial identities and abundance

Figure 2 visualizes the % of bacterial phylogeny abundance in each sample. Table 1 presents the % of core bacteria phyla was considered in this analysis.

In the stomach, Tenericutes was the most abundant phyla and was impacted by the WW treatment; the proportion of Tenericutes decreased from 60.2% to 46.7% (Figure 2, Table 1). The abundance of Bacteroidetes was also impacted by WW treatment as the proportion increased from 7.5% to 18.5%. The proportion of Firmicutes bacteria was relatively unchanged with WW treatment (7.3%) when compared to the CW sample (9.9%) (Figure 2, Table 1). The proportion of Proteobacteria was similarly unchanged by temperature in the stomach (CW = 18.3% and WW = 19.4%).

In comparison, the AI+MI also had a high abundance of Tenericutes bacteria in the CW treatment (96.6%) which similarly decreased with WW treatment to 50.7% (Figure 2, Table 1). Additionally, Bacteroidetes also increased from 0.1% in the CW treatment to 11.9% in the WW treatment. In contrast, Proteobacteria increased in this region with increased temperature (CW = 2.8% to WW=29.9%) while Firmicutes also increased 10-fold from 0.3% in the CW treatment to 3.1% in the WW treatment (Figure 2, Table 1).

Finally, in the PI, Tenericutes was again the most abundant bacterial phyla in the CW treatment and similarly fell to 38.2% in the WW treatment from 88.4%. As in the AI+MI section, Proteobacteria increased with WW treatment to become the most abundant in this region (CW=10.2% to WW=61.5%) (Figure 2, Table 1). Unlike the stomach and AI+MI, Bacteroidetes (CW=1.0%, WW=0.2%) were relatively unchanged with temperature increase though there was

a small decrease detected (Figure 2, Table 1). The abundances of Firmicutes (CW=0.2%, WW=0.0%) decreased as seen in the stomach, but in contrast to the AI+MI.

4.2 Alpha diversity in the GIT

The bacterial species (represented by OTUs) richness and abundance in each sample were explored with the rarefaction curves seen in Figure 3. The observed OTU plot (Figure 3A) shows the 6-12ºC cold water (CW) stomach has the highest number of detected OTUs (950) followed by the 17ºC warm water (WW) stomach (745), the WW AI+MI (604), the CW AI+MI (275), the CW PI (238), and the WW PI (226). The PD whole tree (Figure 3B) predicted that the WW stomach was the least phylogenetically similar sample based on phylogenetic distance followed by the CW stomach, WW AI+MI, CW AI+MI, CW PI and WW PI which was similar to the observation of sample order of richness (Figure 3A) except the WW stomach is ranked above the CW stomach. The Shannon plot (Figure 3C) showed that the WW stomach, CW stomach, WW AI+MI had the highest OTU number and evenness, followed by the WW PI, CW PI and CW AI+MI samples. Finally, the Chao1 plot (Figure 3D) predicted that the likelihood of detecting a single or rare bacterial species was highest in the CW stomach followed by the WW stomach, WW AI+MI, CW AI+MI, CW PI, and WW PI samples.

4.3 Beta diversity in the GIT

The jackknife unweighted bootstrap tree (Figure 4), which is based on the presence or absence of OTUs only (identity-driven), shows a strong distinction (>75% support) in the presence of OTU communities in the WW PI, CW PI and CW AI+MI (first major cluster) compared to the CW stomach, WW AI+MI and WW stomach (second major cluster) meaning that the first cluster and second cluster share fewer bacterial species in common than within

clusters. In the first major cluster, the CW PI and CW AI+MI show 50-75% support for distinct bacterial compositions with this cluster of samples showing higher support for distinction (<75%) from the WW PI meaning the CW PI shared more species in common with the CW AI+MI than the WW PI (Figure 4). In the second major cluster, the WW stomach, and WW AI+MI cluster more closely together sharing more species in common than the CW stomach; all relationships in this cluster show >75% support for distinct bacterial communities (Figure 4). This suggests that CW PI, CW AI+MI and WW PI share a higher number of species when compared to the CW stomach, WW stomach and WW AI+MI, where the WW stomach and WW AI+MI share more species in common.

Examining the jackknife weighted bootstrap tree (Figure 5), based on both the presence and absence as well as the OTU abundance data (abundance-driven), it was observed that the CW PI and WW PI samples (first major cluster) showed strong support (>75%) for distinct OTU richness and abundance composition when compared to the stomach and AI+MI samples indicating that the PI samples shared fewer species in common than the rest of the samples. Secondarily, the CW and WW stomach samples, cluster more closely to one another compared to the CW AI+MI, and these samples showed >75% support for distinct compositions compared to the WW AI+MI sample sharing fewer common species (Figure 5). The evidence here suggests the CW PI and WW PI share a higher number of OTUs with similar abundances compared to the rest of the samples and are thus more like each other. The CW and WW stomach share a higher number of OTUs with a similar abundance profile than the CW AI+MI and WW AI+MI, respectively, indicating the stomach samples are more like each other compared to the AI+MI samples regardless of treatment.

In both the weighted or unweighted analyses, it appears that zonation along the GIT (particularly in the PI versus the stomach and AI+MI) is more predictive of OTU communities than temperature.

4.4 Enzyme zonation along the GIT with increased temperature

4.4.1 Sodium-potassium ATPase

A significant increase in activity in PI (0.5±0.2 μmol ADP mg^{-1} protein h^{-1}) compared to the AI was seen at 6°C (0.1 μmol ADP mg^{-1} protein h^{-1}) as seen in Figure 6A. At warmer temperatures, no significant zonation patterns were detected (Figure 6B), and individual regions did not show any evidence of NKA activity perturbation with temperature.

4.4.2 Lactate dehydrogenase

In the whole GIT, no significant zonation patterns were detected along the stomach, AI, MI and PI at any temperature and temperature stress did not appear to induce any changes. The average activity across the stomach, AI, MI, and PI at 6°C was 161.8±20.2 μmol min^{-1} g^{-1} protein and at 17°C was 170.6±13.6 μmol min^{-1} g^{-1} protein.

4.4.3 Pyruvate kinase

In the whole GIT, no zonation patterns were detected along the anteroposterior axis based on the statistical analysis; the average activity across the stomach, AI, MI, and PI at 6°C was 1935.2±789.7 μmol min^{-1} g^{-1} protein and at 17°C was 150.5±12.4 μmol min^{-1} g^{-1} protein. Activity of PK in the MI showed a 4-fold decrease as the temperature went from 6°C (396.5±60.0 μmol min^{-1} g^{-1} protein) to 12°C (76.6±21.5 μmol min^{-1} g^{-1} protein), but began to

return to cold water activity levels of activity at 17°C (114.3±39.8 μmol min^{-1} g^{-1} protein) as seen in Figure 7. No other region exhibited a temperature-induced change in activity.

4.4.4 Glutamate dehydrogenase

In the GIT, activity of GDH across the anteroposterior axis remained the same at CW temperatures; the average activity was 7383.8±713.3 μmol min^{-1} g^{-1} protein. When the temperature was 17°C, it was observed that the stomach (2067.7±425.2 μmol min^{-1} g^{-1} protein) and MI (1292.4±167.8 μmol min^{-1} g^{-1} protein) showed lower GDH activity in comparison to the AI (3767.9±278.4 μmol min^{-1} g^{-1} protein) and PI (3686.9±636.4 μmol min^{-1} g^{-1} protein) regions (Figure 8A). When the activity of GDH was compared across temperatures in each region it was seen that in the PI (Figure 8B), the activity at 12°C (2929.3±813.6 μmol min^{-1} g^{-1} protein) and 17°C (3686.9±636.4 μmol min^{-1} g^{-1} protein) was significantly lower than at 6°C (9256.3±1410.1 μmol min^{-1} g^{-1} protein).

4.4.5 Citrate synthase

In the whole GIT, significant CS activity zonation patterns were observed at 17°C where the MI (5.9±1.6 μmol min^{-1} g^{-1} protein) had significantly lower activity than the stomach (16.2±3.4 μmol min^{-1} g^{-1} protein) while the AI (8.9±1.3 μmol min^{-1} g^{-1} protein) and PI (15.7±2.8 μmol min^{-1} g^{-1} protein) were not significantly different from either the stomach or MI as seen in Figure 9A. In addition, it was observed that the stomach and AI showed a significant decrease in activity at 12°C (11.4±2.4 and 5.0±0.7 μmol min^{-1} g^{-1} protein, respectively) and 17°C (16.8±3.4 and 8.9±1.3 μmol min^{-1} g^{-1} protein, respectively) compared to at 6°C (52.0±5.2 and 39.5±9.4 μmol min^{-1} g^{-1} protein, respectively) (Figure 9B-C).

4.4.6 Glutamine synthetase

Along the GIT at 6°C (Figure 10A), it was observed that GS activity was significantly elevated in the PI (131.9±57.6 μmol min^{-1} g^{-1} protein) compared to the AI (3.7±1.4 μmol min^{-1} g^{-1} protein) while the stomach (16.7±1.9 μmol min^{-1} g^{-1} protein) and MI (13.6±6.2 μmol min^{-1} g^{-1} protein) GS activities were not significantly. Temperature stress did not induce any significant changes in activity in any GIT zone but the trend in the data suggests the zonation pattern is maintained (Figure 10B).

4.4.7 Cellulase

The GIT did not exhibit any pattern of zonation in cellulase activity at any temperature nor did temperature induce any significant changes in the activity of the enzyme in any zone. The average activity across the stomach, AI, MI, and PI was 1828.4±244.9 mg glucose min^{-1} mg^{-1} protein at 6°C and 451.9±116.0 at 17°C mg glucose min^{-1} mg^{-1} protein.

4.4.8 Trypsin

In the whole GIT at 6°C, it was observed that the AI (150.0±17.3 μmol min^{-1} g^{-1} protein) and MI (136.3±42.8 μmol min^{-1} g^{-1} protein) had significantly higher trypsin activities than the stomach (28.6±11.6 μmol min^{-1} g^{-1} protein) and PI (6.9±2.7 μmol min^{-1} g^{-1} protein) as seen in Figure 11A; no significant activity zonation patterns were observed at warmer water temperatures. In the AI and MI, elevated trypsin activity was observed at 6°C (150.0±17.3 and 136.3±42.8 μmol min^{-1} g^{-1} protein, respectively) while the activity at 12°C (346.6±93.9 and 303.1±111.1 μmol min^{-1} g^{-1} protein, respectively) and 17°C (39.6±9.1 and 30.3±15.2 μmol min^{-1} g^{-1} protein, respectively) was significantly lower (Figure 11B-C).

4.4.9 Lipase

There was no evidence of zonation or temperature-induced lipase enzyme activity changes in the whole GIT. The average activity across the stomach, AI, MI, and PI was 49.3±9.1 nmol of glycerol min^{-1} at 6°C and 109.5±17.4 nmol of glycerol min^{-1} at 17°C.

4.5 Correlations between the microbiome and enzyme activity in the GIT

Figure 12 shows the relationship between bacterial species in each GIT zone treatment and how highly correlated they are with specific zones. It was observed that the abundance of bacterial species in the CW stomach and WW stomach sample vectors were within the 90° cut-off range for sample bacterial compositions to be considered similar. The CW AI+MI was distinct from the CW and WW stomach samples, and the WW AI+MI and WW PI samples. The WW stomach and AWW AI+MI clustered together in one quadrant. The CW PI and WW PI remained within the range of the definition of similar sequence compositions although they appear in distinct quadrants.

Figure 13 represents the relationship between the variation in bacterial abundance and the activity of the enzymes of interest and how these are both correlated to the GIT treatment zones. In Figure 13, it was observed that the elevated activities of Trypsin, PK, and CS in the CW AI+MI are associated with Proteobacteria and Firmicutes. Cellulase and GDH (vectors which appear overlapped in the figure) have elevated activity associated with the CW PI and these activities in this GIT zone are associated with Proteobacteria and Bacteroidetes. Elevated GS, NKA and LDH activities detected in the WW PI are associated with Proteobacteria. The CW stomach, WW stomach and WW AI+MI are highly associated with bacterial phyla including Cyanobacteria and Proteobacteria and elevated lipase activity is associated with the WW AI+MI and stomach. Highly elevated lipase activity is more strongly associated with the WW AI+MI which is weakly associated with the any particularly abundant bacterial phyla.

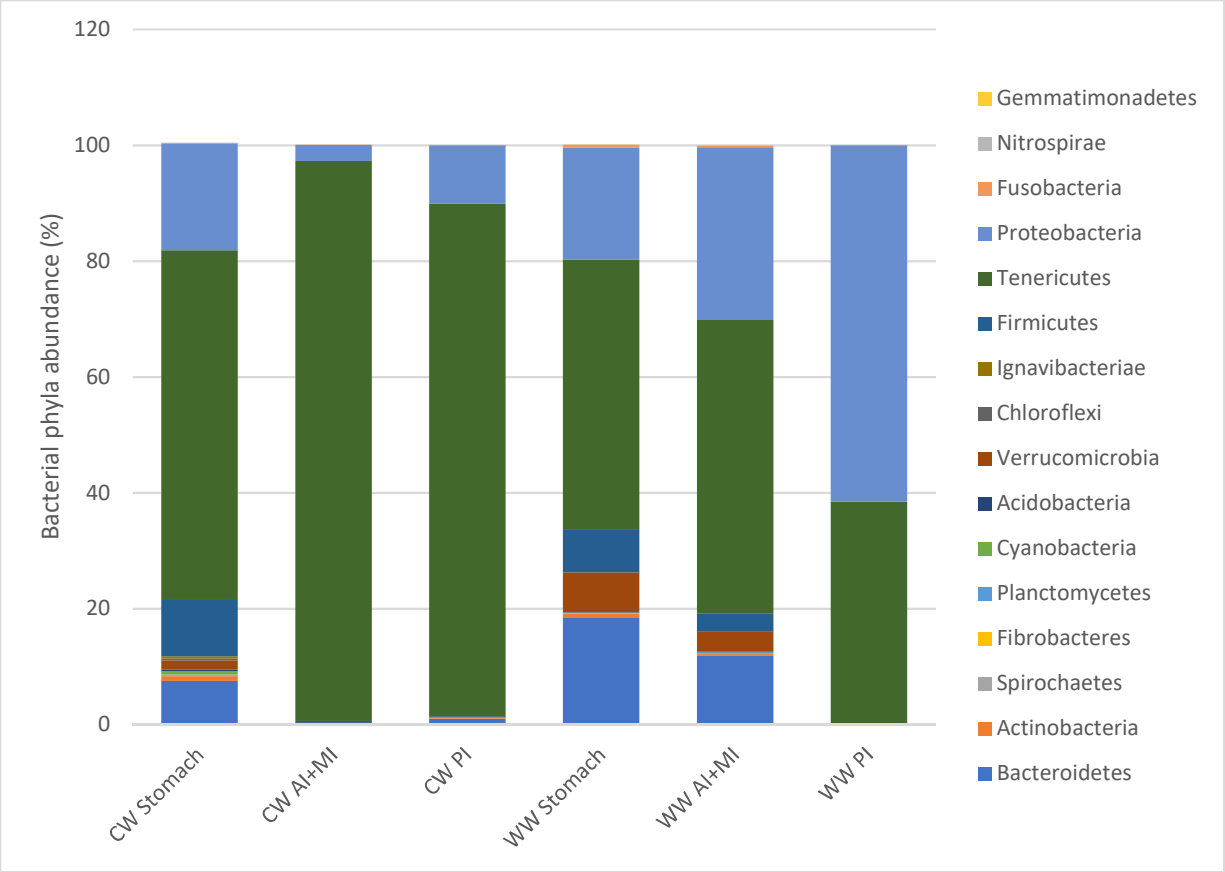

Figure 2. Bacterial community phyla abundance (%) assigned to OTUs using the Green Genes library in QIIME ® in the 6-12°C cold water (CW) and 17°C warm water (WW) stomach, AI+MI (anterior and middle intestine combined) and PI (posterior intestine) samples. The ratio of core gut bacteria (Firmicutes/Tenericutes, Bacteroidetes, and Proteobacteria) appeared to be affected by increased temperature in all GIT zones.

Table 1. Bacterial phylogeny abundance of core gut bacteria (%) detected in the rainbow trout GIT samples in CW (cold water) and WW (warm water) conditions

Bacterial phyla	Stomach	AI+MI	PI
Firmicutes	CW – 9.9% WW – 7.3%	CW – 0.3% WW – 3.1%	CW – 0.2% WW – 0.0%
Tenericutes	CW – 60.2% WW – 46.7%	CW – 96.6% WW – 50.7%	CW – 88.4% WW – 38.2%
Proteobacteria	CW – 18.3% WW – 19.4%	CW – 2.8% WW – 29.9%	CW – 10.2% WW – 61.5%
Bacteroidetes	CW – 7.5% WW – 18.5%	CW – 0.1% WW – 11.9%	CW – 1.0% WW – 0.2%

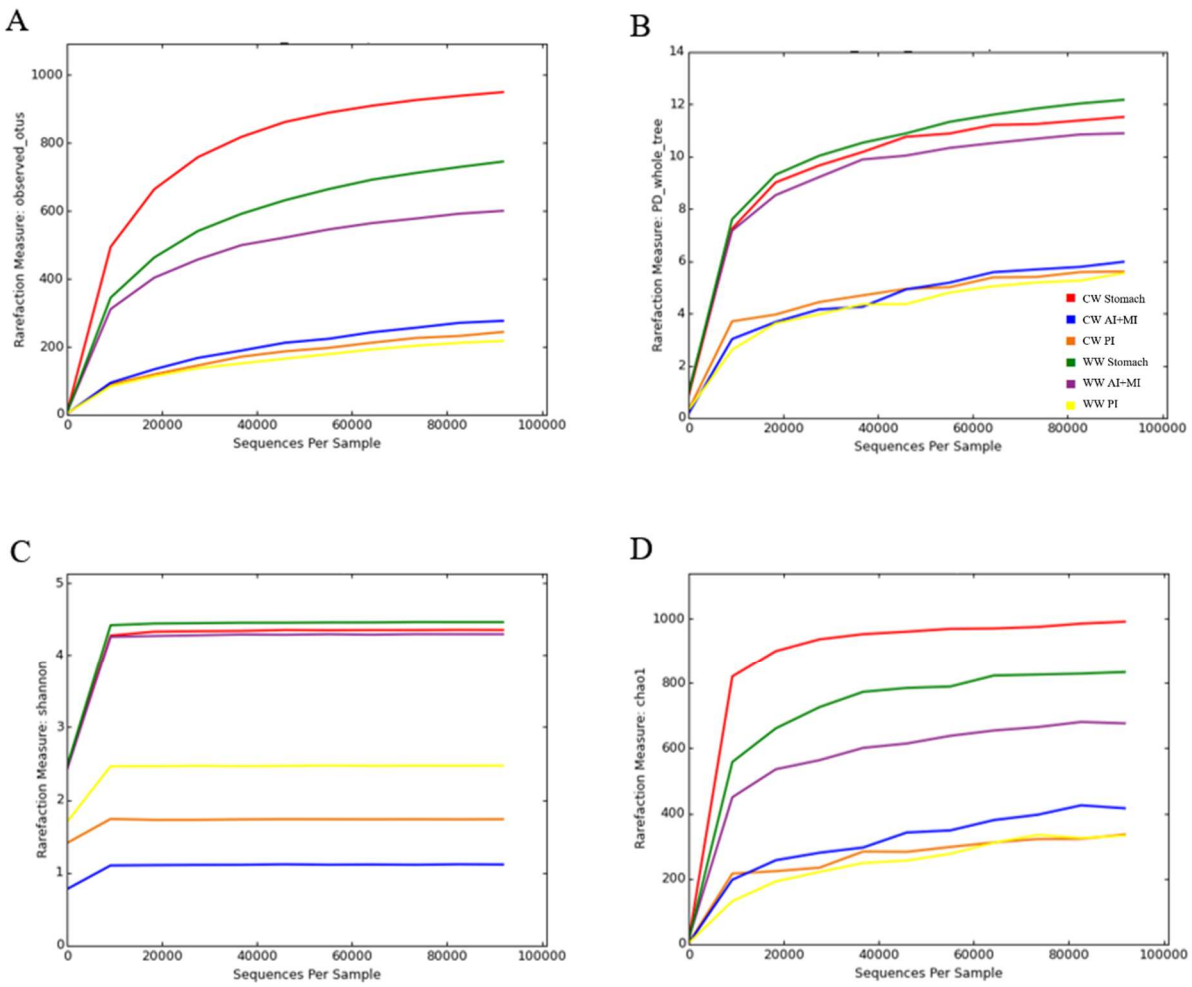

Figure 3. OTU alpha diversity in the rainbow trout stomach, AI+MI (anterior and middle intestine combined) and PI (posterior intestine) samples in 6-12°C (CW = cold water) and at 17°C (WW = warm water) conditions at a sampling depth of 20000 sequences per sample for a total of 91,787 random sequences in each sample (which was the minimum number of sequences detected across samples). A) Observed OTUs curves B) Phylogenetic diversity (PD) whole tree plot C) Shannon plot and D) Chao1 plot generated with QIIME ®. N=8

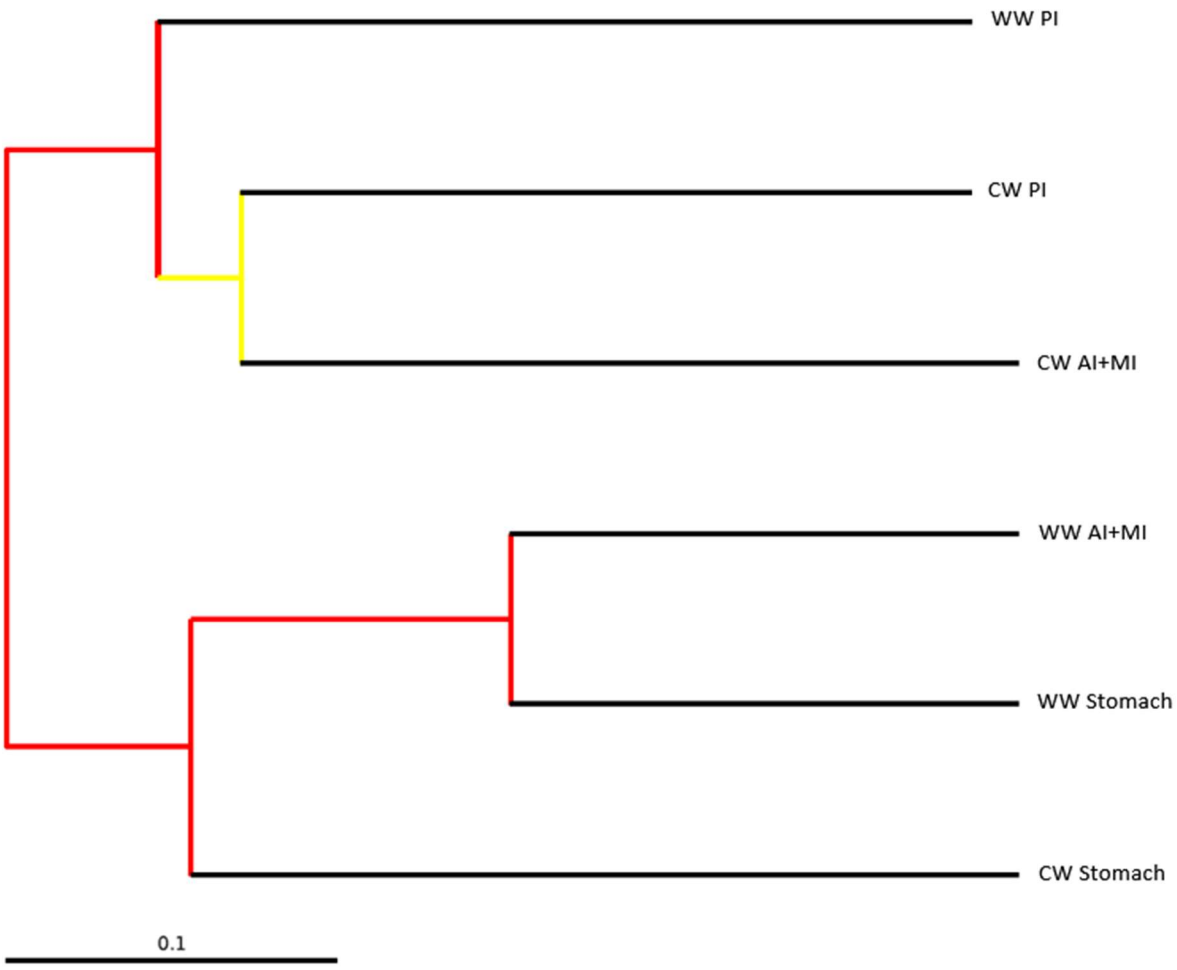

Figure 4. Unweighted (identity-based) jackknifed bootstrap tree depicting relationship between OTUs across cold water (CW, 6-12°C) and warm water (WW, 17°C) stomach, AI+MI (anterior and middle intestine combined) and PI (posterior intestine) samples at 0.1. Red indicates >75% and yellow 50-75% support for distinct bacterial compositions between samples. Jackknifed beta analysis performed using 90% of the random sequences based on the sample containing the smallest number of unique OTUs. Generated with QIIME ®.

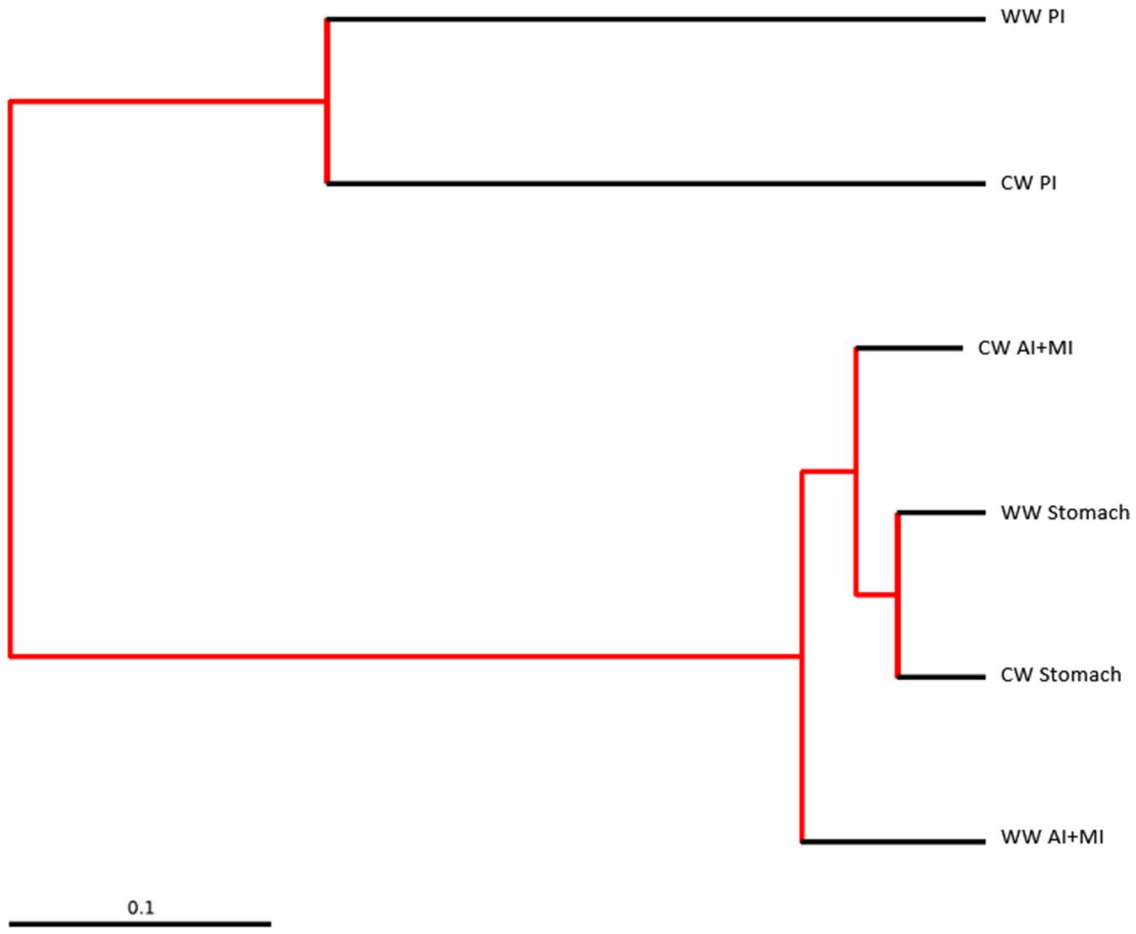

Figure 5. Weighted (abundance-based) jackknifed bootstrap tree depicting relationship between OTUs across cold water (CW, 6-12°C) and warm water (WW, 17°C) stomach, AI+MI (anterior and middle intestine combined) and PI (posterior intestine) samples at 0.1. Red indicates >75% support for distinct bacterial compositions between samples. Jackknifed beta analysis performed using 90% of the random sequences based on the sample containing the smallest number of unique OTUs. Generated with QIIME ®.

A

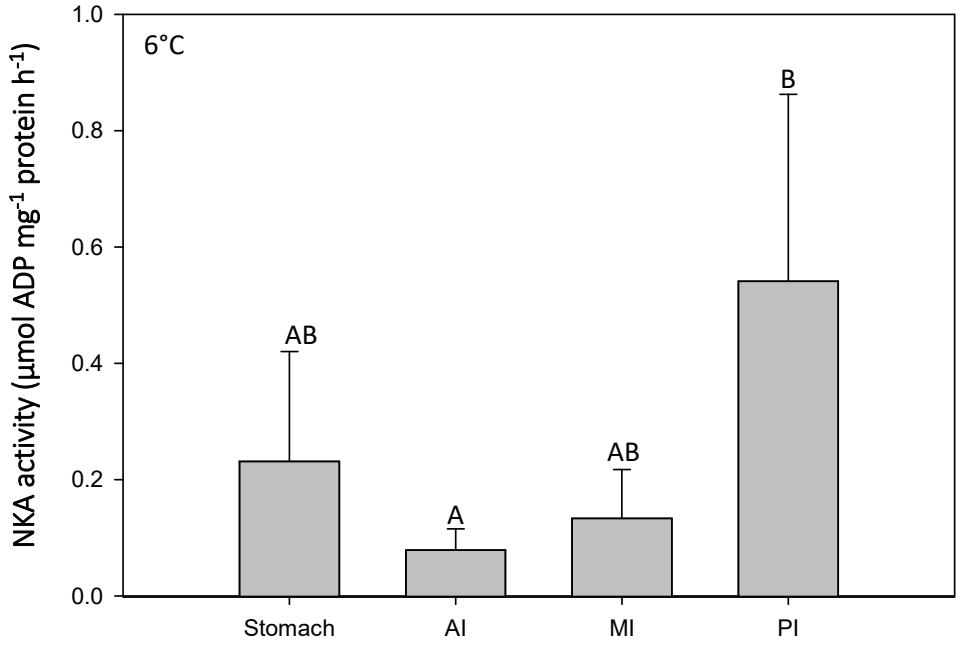

B

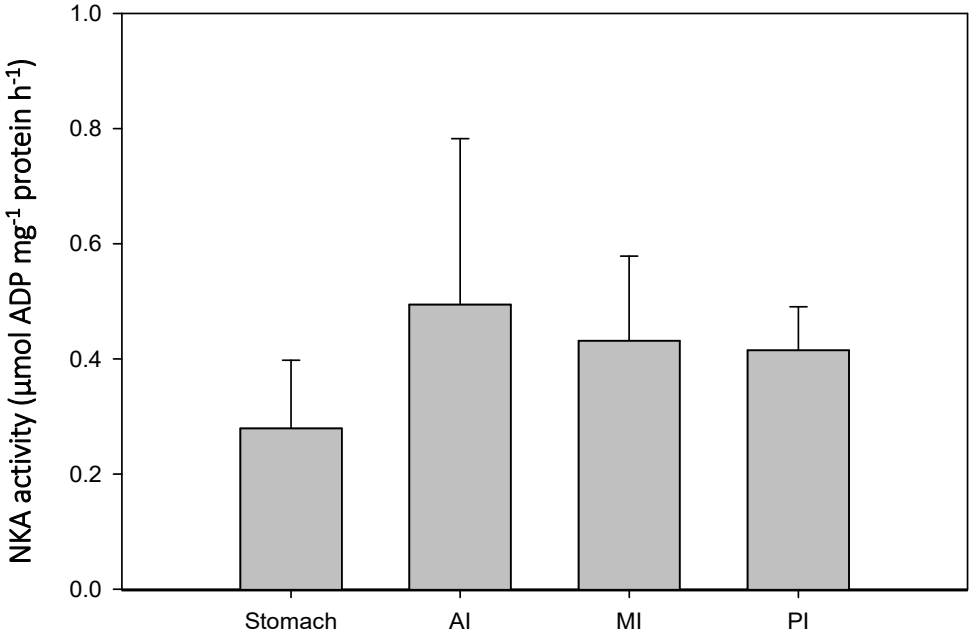

Figure 6. Sodium-potassium ATPase activity in the stomach, AI (anterior intestine), MI (middle intestine) and PI (posterior intestine) of rainbow trout exposed to A) 6ºC (one-way repeated measures ANOVA, p = 0.023, n=4) and B) 17 ºC (one-way repeated measures ANOVA, p = 0.448, n=4) water. Bars that share the same letter are not significantly different.

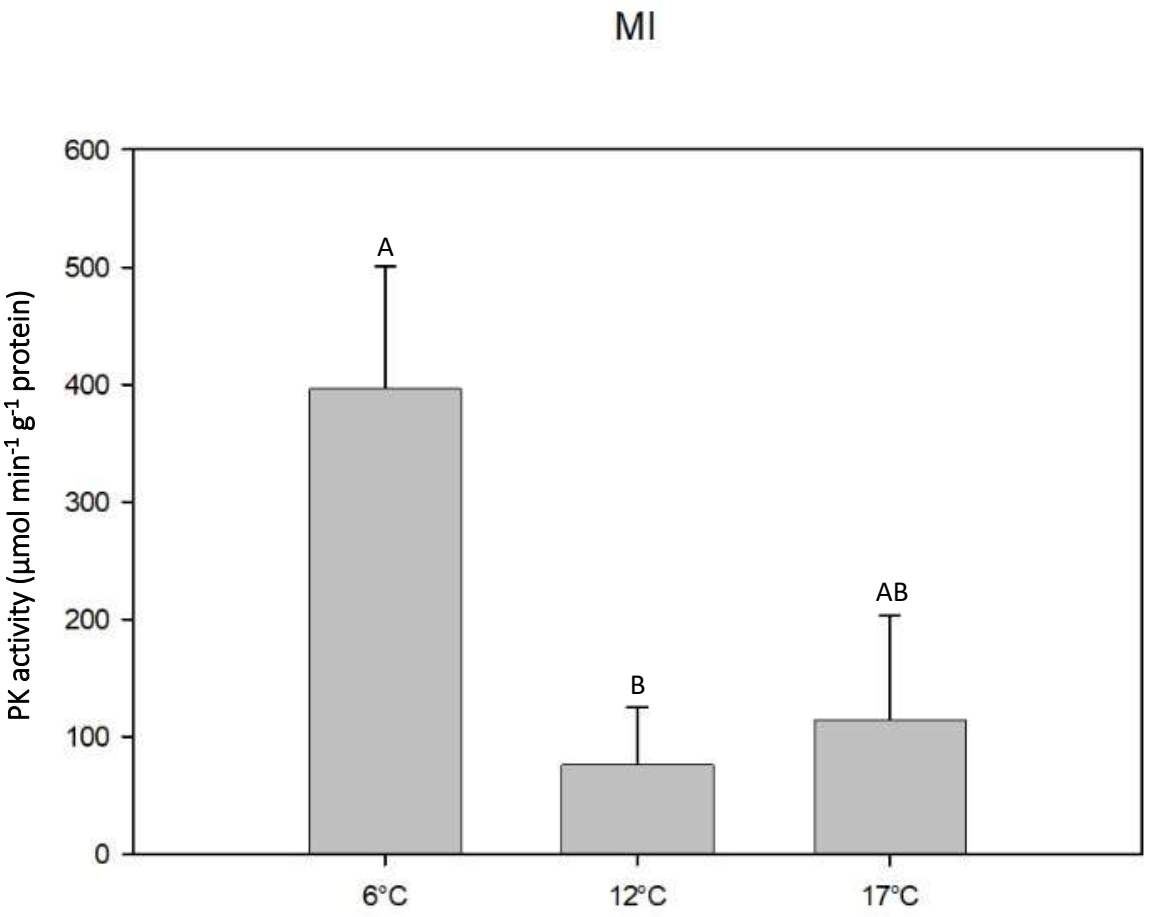

Figure 7. Pyruvate kinase activity in the MI (middle intestine) in water temperatures of 6ºC, 12ºC and 17 ºC. Bars that share the same letter are not significantly different (one-way repeated ANOVA, $p<0.001$, $n=3,5,5$).

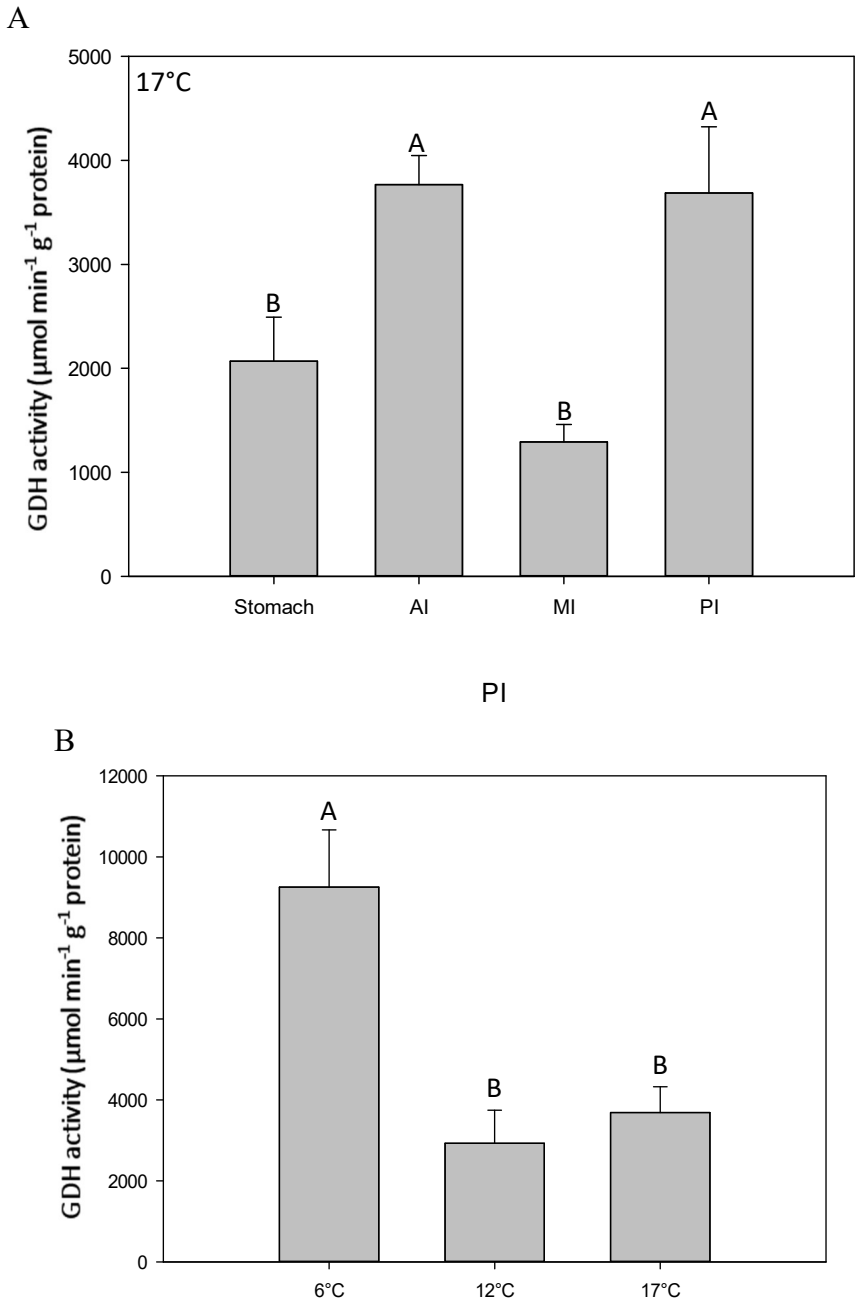

Figure 8. Glutamate dehydrogenase activity in the A) stomach, AI (anterior), MI (middle) and posterior (PI) intestines at 17°C (one-way repeated measures ANOVA, p=0.002, n=4), and the B) PI at 6°C, 12°C and 17°C water temperature conditions (one-way repeated ANOVA, p=0.004, n=5,4,4). Bars that share the same letter are not significantly different.

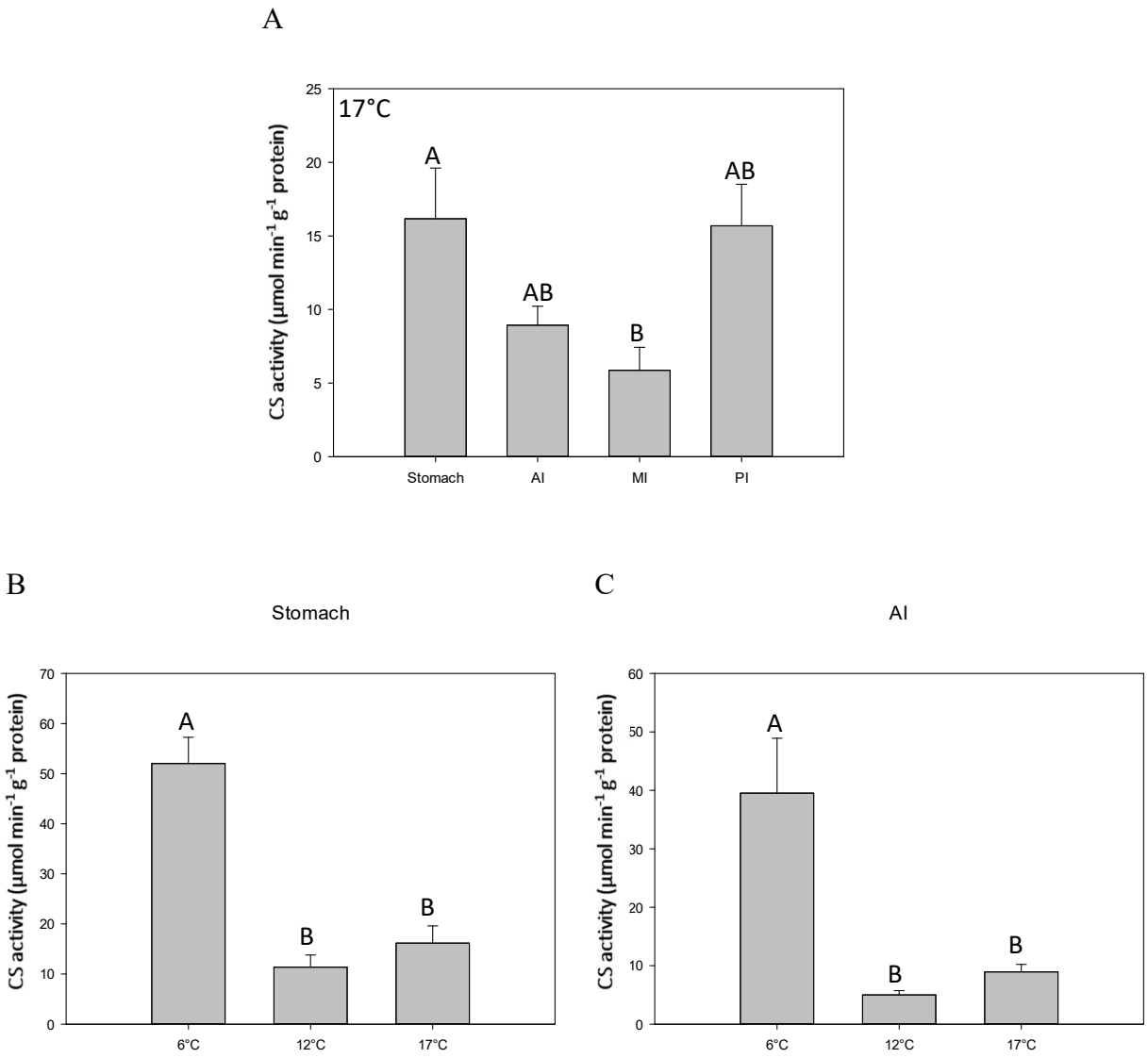

Figure 9. Citrate synthase activity in the A) the stomach, AI (anterior), MI (middle), and PI (posterior intestine) of rainbow trout exposed to 17ºC water (one-way repeated measures ANOVA, p=0.028, n=4), B) stomach (one-way ANOVA, p<0.001, n=4) and the C) the AI at 6°C, 12°C and 17°C water temperature conditions (one-way ANOVA, p= 0.018, n=5,4,4). Bars that share the same letter are not significantly different.

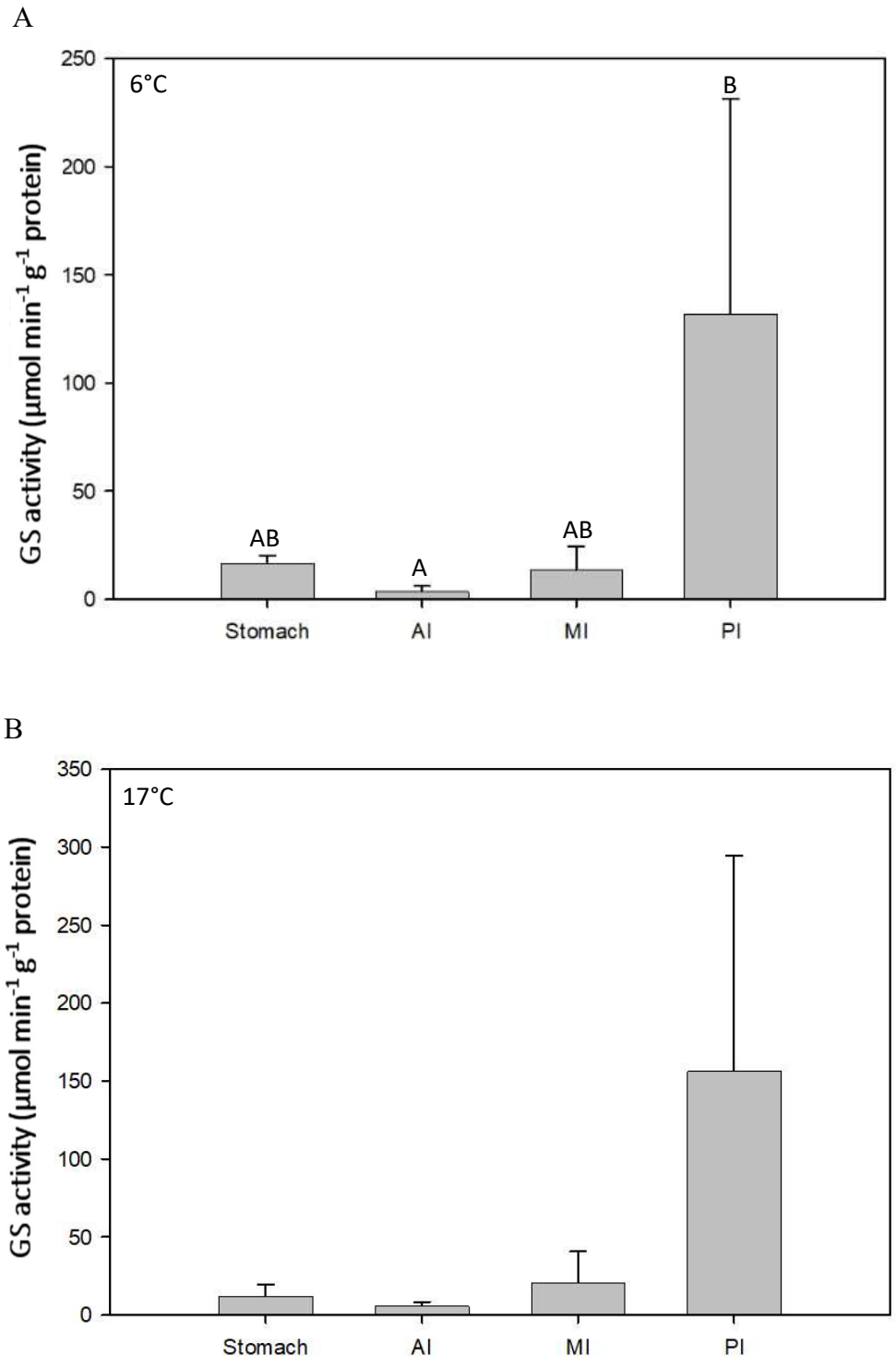

Figure 10. Glutamine synthetase activity in the stomach, AI, MI, and PI of rainbow trout exposed to A) 6ºC (one-way repeated measures ANOVA, p=0.026, n=3) and B) 17ºC (one-way repeated measures ANOVA, p=0.248, n=3) water. Bars that share the same letter are not significantly different.

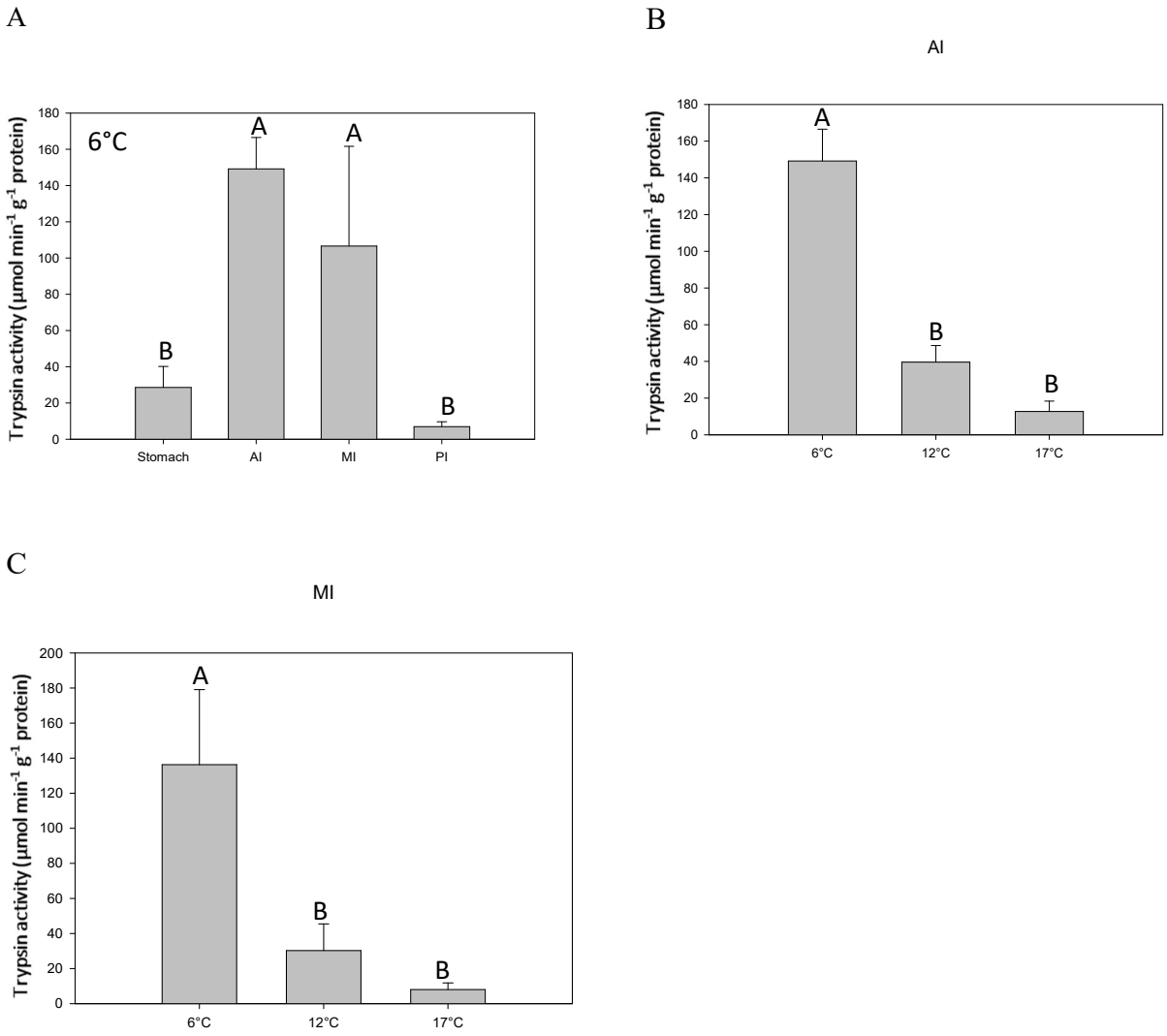

Figure 11. Trypsin activity in the A) stomach, AI (anterior), MI (middle) and PI (posterior intestine) of rainbow trout exposed to 6ºC water (one-way repeated measures ANOVA, $p<0.001$, n=5), B) the AI at 6°C, 12°C and 17°C water temperature conditions (one-way ANOVA, $p<0.001$, n=5,4,4), and C) the MI at 6°C, 12°C and 17°C water temperature conditions (one-way ANOVA, $p=0.020$, n=5,4,4). Bars that share the same letter are not significantly different.

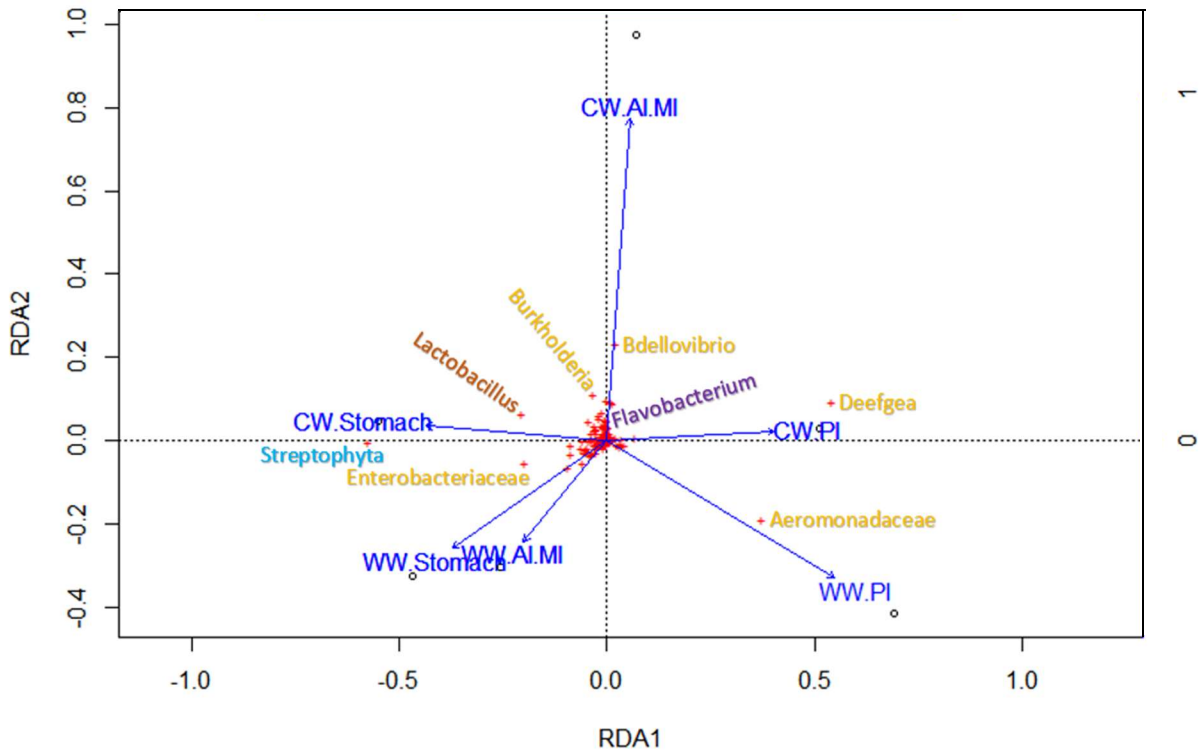

Figure 12. Multivariate redundancy analysis (RDA) depicting the variation of bacterial species abundance (represented by the red cross) in the 6-12°C cold water (CW) and 17°C warm water (WW) stomach, AI (anterior), MI (middle) and PI (posterior intestine) zone samples (shown in dark blue). Bacterial taxa identities labelled near closest red cross: genus Lactobacillus (of phylum Firmicutes shown in orange); order Streptophyta (of phylum Cyanobacteria shown in light blue); family Enterobacteriaceae, genus Burkholderia, genus Bdellovibrio, genus Deefgea and family Aeromondaceae (all of phylum Proteobacteria shown in yellow); genus Flavobacterium (of phylum Bacteroidetes shown in purple). Generated with R Studio.

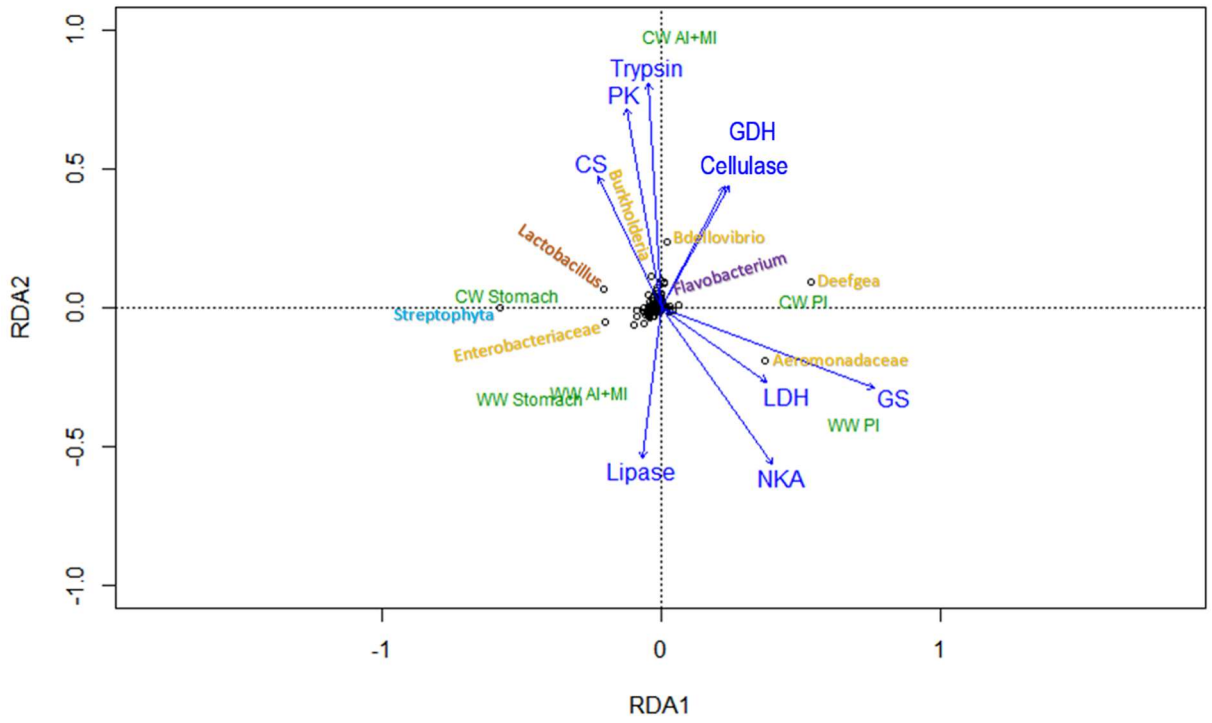

Figure 13. Multivariate RDA depicting the distinct separation and the correlation between the bacterial taxon abundance (represented by open circles) in the 6-12°C cold water (CW) and 17°C warm water (WW) stomach, AI (anterior), MI (middle) and PI (posterior intestine) zone samples (shown in green) and maximal enzyme activities (shown in dark blue). NKA = sodium-potassium ATPase; LDH = lactate dehydrogenase; PK = pyruvate kinase; CS = citrate synthase; GDH = glutamate dehydrogenase; GS = glutamine synthetase. Bacterial taxa identities labelled near closest open circle: genus Lactobacillus (of phylum Firmicutes shown in orange); order Streptophyta (of phylum Cyanobacteria shown in light blue); family Enterobacteriaceae, genus Burkholderia, genus Bdellovibrio, genus Deefgea and family Aeromondaceae (all of phylum Proteobacteria shown in yellow); genus Flavobacterium (of phylum Bacteroidetes shown in purple). Generated with R Studio.

Discussion

Environmental perturbations such as alterations in temperature impact both the microbiome and enzyme activity in the gut. In this chapter, zonation in the microbiome was more predictive of bacterial communities and seemed to influence the activities of the associated enzymes more so than temperature. The evidence here suggests a mutualistic relationship between the microbiome and enzyme activity along the zones of the GIT.

5.1 Analysis of the gut microbiome and temperature

Region-specific differences in the microbiome along the GIT of the rainbow trout were expected as has been reported in the brown trout (Al-Hisnawi et al. 2015). In the control CW fish, regional differences in the microbiome were detected across the stomach, AI+MI and PI region. The CW stomach was the most diverse region of the GIT, followed by the AI+MI and PI regions (Figure 2, Table 1, Figure 3A). Each region was shown to have distinct species composition (>75% support) in CW conditions based on taxa identity and abundance (Figure 4).

In the Al-Hisnawi et al. (2015) study where brown trout kept at 13°C, Proteobacteria comprised most of the bacterial identities in the pyloric ceca region which is associated with the AI (84.8%), the MI (88.4%) and PI (93.2%) which is higher than what was detected in the present study where Proteobacteria comprised 29.9% of the AI+MI and 61.5% of the PI sample at 12°C (Figure 3) in rainbow trout; this indicates a species-specific pattern of zonation. These data support our hypothesis that zonation in the microbiome exists in the gut of the rainbow trout.

Additionally, temperature can influence the gut microbiome of fish (Lozupone and Knight 2007; Nayak 2010; Givens 2014; Zarkasi et al. 2016), although zonation has not been concurrently examined.

The first major trend was in the proliferation of Proteobacteria in the gut. In the control CW treatment, Tenericutes/Firmicutes bacteria predominated all sections of the gut, which is common in fish with high calorie diets such as the carnivorous rainbow trout (Semova et al. 2012; Carmody and Turnbaugh 2012; Li et al. 2015), though to different degrees (stomach=70.1%; AI+MI=97.0%; PI=88.6%; Figure 2, Table 1). It was expected overall that the proportion of Proteobacteria would increase with increasing temperature due to physiological mechanisms that favour this bacterial phylum (brown trout: Al-Hisnawi et al. 2015; various species: Givens 2014; Atlantic salmon: DePaola et al. 1994; Zarkaski et al. 2016). In the present study, Proteobacteria experienced the greatest abundance increase with increased temperature (17°C) in the AI+MI and PI regions: a 10x and 6x increase in abundance was observed in the AI+MI, and PI regions, respectively (Figure 2; Table 1). A high abundance of Proteobacteria is associated with the higher temperatures of the fish's thermal range as was hypothesized. It has been proposed that the gut may serve to support the growth of this psychotolerant (extreme temperature-tolerant) bacteria and its survival may thus be affected by other host factors associated with homeostasis or that these bacteria have a competitive advantage over more temperature-sensitive bacteria (DePaola et al. 1994; Zarkasi et al. 2016). The increase in Proteobacteria shows little evidence of strong zone-specific responses to temperature. It appears that temperature drives the abundance of these phyla more so that regionalization indicating the proliferation of these bacteria are not controlled by the morphological or histochemical properties of the gut.

5.2 The effect of temperature in the stomach microbiome and the implications on enzyme zonation

The stomach was the most bacterially diverse region of the gut overall compared to the intestinal samples (Figure 2, Figure 3A). Despite the acidic conditions of the stomach, an environmental which was previously believed to be inhospitable to bacteria, this region can be extremely diverse in bacterial communities however the exact reason for this is unknown (Bik et al. 2006).

In the CW stomach, Enterobacteriaceae (of phylum Proteobacteria), Streptophyta (of phylum Cyanobacteria) and Lactobacillus (of phylum Firmicutes) were highly correlated (Figure 11); these bacteria have also been identified in the stomach of humans (Ratten et al. 2011). These bacteria were weakly correlated with maximal CS activities in CW stomach which was not as hypothesized (Figure 9B-C). It was expected that CS, a metabolic enzyme, would be relatively stable within the organism's thermal range as has been found in other metabolic enzymes including LDH and PK (Smith and Ellory 1971; Yancey and Somero 1978; Coppes and Somero 1990; Low and Somero 1976; Prosser 1991; Ozernyuk et al. 1994; Eddy 2005). Several authors have proposed an inverse relationship between temperature and CS activity in cold-acclimated fish (Antarctic vs. temperate fish: Crockett and Sidell 1990; thresspine stickleback: Gurdely and Leroy 2001; Atlantic cod: Dutil et al. 2008). Is it thought that colder temperatures might induce higher oxidative capacity and increased CS activity at lower temperatures aids in the activity transport of nutrients as the energy production capacity increases (Crockett and Sidell 1990; Dutil et al. 2008). Enterobacteriaceae and Lactobacillus, anaerobic carbon-fixing bacteria populations, are associated with sugar fermentation and the production of acids (Rachman et al. 1997; Ratten et al. 1997). The production of acids such as lactic acid may serve as to supplement

lactic acid conversion to pyruvate which is then shuttled into the TCA cycle resulting in the observed enhanced CS activity (Kelly et al. 2015). Streptophyta bacteria was highly abundant in the CW treatment (Figure 12); these bacteria are nitrogen-fixing bacteria that converts nitrogen to ammonia (Falcon et al. 2010) and are likely associated with protein digestion in the stomach although trypsin activity is not highly correlated with this region.

In contrast, the WW stomach was weakly correlated with lipase activity and Enterobacteriaceae and Streptophyta continue to be highly associated with this stomach though there is no clear relationship between lipase and these bacterial taxa. Elevated temperature increased the bacterial evenness in the stomach meaning that bacterial species that had previously comprised a relatively low proportion of the sample in CW increased in the WW treatment making the bacterial phyla more evenly distributed; this increase in bacterial evenness was greater in the stomach than the intestinal samples (Figure 3B, D). Lesel and Peringer (1981) noted a similar trend in bacterial count across the anteroposterior axis of the gut in rainbow trout: elevated temperature increased the counts in all regions, particularly the stomach. More specifically, Firmicutes/Tenericutes bacteria abundance decreased with increased temperature in the stomach while Bacteroidetes increased (Figure 2, Table 1). This relative increase in bacterial diversity in the WW stomach, most notably in the ratio of bacteria belonging to Bacteroidetes (2x increase) at the expense of Tenericutes and Firmicutes (a 25% and 28% decrease in both phyla), indicate that temperature may be inducing changes in the environment of the stomach lumen which favour certain phyla over others.

Overall, the general diversity of the stomach samples indicates a more diverse metagenome than previously thought which may contribute in various ways to gut physiology (Bik et al. 2006).

5.3 The effect of temperature in the anterior and middle intestine microbiome and the implications on enzyme zonation

The AI+MI region had the highest proportion of Tenericutes bacteria (96.6%) compared to the PI (88.4%) and the stomach (60.2%). Flavobacterium (Bacteroidetes), Bdellovibrio (Proteobacteria) and Burkholderia (Proteobacteria) abundance was also highly associated with the CW AI+MI region (Figure 12). Species of Flavobacterium, particularly *Flavobacterium psychrophilum*, have been implicated as the causative agent of cold-water disease in salmonid species which includes the rainbow trout (Madsen and Dalsgaard 1999; LaFrentz et al. 2003). Evidence suggests Bdellovibrio are involved in the control of other bacterial populations including *Aeromonas* pathogens as they can lyse cells (Snyder et al. 2002; Qi et al. 2009; Cao et al. 2012). It is possible that Bdellovibrios is controlling the proliferation of the potentially pathogenic Flavobacterium in the CW AI+MI sample. No specific function of Burkholderia bacteria in the gut has yet been identified to the author's knowledge, however, the Proteobacteria phylum to which these bacteria belong has been associated with protein-rich diets (Bairagi et al. 2002; Ray et al. 2012). Thus, the AI+MI region may be highly involved in protein digestion as is indicated by the maximal activity of trypsin and GDH for local ammonia detoxification following protein digestion (Figure 13). GDH is supplied the energy needed to catalyze this reaction by NADH; it is possible that the metabolic increase in PK and CS activities is providing the energy needed to fuel these processes (Rubino et al. 2014; Locasale et al. 2011; Kelly et al. 2015).

The AI and MI regions in the present study exhibited the largest degree of change in the bacterial diversity with increased temperature exposure (Figure 3C, D). A 198.3% increase in Bacteroidetes, a 10.7% increase in Proteobacteria and 1.9% decrease in Tenericutes bacteria was

observed in the WW AI+MI sample treatment compared to the CW control sample (Figure 2; Table 1). Although Proteobacteria and Bacteroidetes abundance increased in the intestine with temperature in the present study, Firmicutes/Tenericutes still predominated in the AI+MI (Figure 2; Table 1) which is supported by the findings of a previous study in rainbow trout by Lowrey (2014). This increase in Proteobacteria and the significantly high GDH activity in this region with WW treatment further (Figure 8A) supports the AI+MI region may be specialized in protein degradation processes and this is enhanced by warmer temperatures likely for increased energy extraction to fuel increased metabolic demand (Lauff and Hofer 1984; Liu et al. 2016). Although maximal cellulase activity was highly correlated with the CW AI+MI (Figure 12), no statistically significant difference in cellulase activity was identified across the GIT which was not expected. It is possible that basal cellulase activity is occurring in this region providing glucose used by the Firmicutes/Tenericutes and Bacteroidetes in this region for energy (Semova et al. 2014; Carmody and Turnbaugh 2012; Li et al. 2015; Ratten et al. 2017). With increased temperature, bacterial richness and abundance increased in the AI+MI (Figure 3C; Figure 5; Figure 12). This was correlated with maximal lipase activity (Figure 13) though lipase activity was not found to be significantly different across the GIT which was not hypothesized; the activity here is likely related to the Firmicutes/Tenericutes bacterial community presence, which continues to predominate the region with increased temperature (Semova et al. 2014; Carmody and Turnbaugh 2012; Li et al. 2015). Thus, there appears to be support for a mutualistic relationship between the microbiome and enzyme activity in the AI+MI, particularly with regards to protein digestion.

Interestingly, the PI experienced a decrease in GDH activity at 12 and 17°C compared to at 6°C which indicates that this may be a host-specific response.

5.4 The effect of temperature in the posterior intestine microbiome and the implications on enzyme zonation

The PI was dominated by Tenericutes at cooler temperatures (Figure 2, Table 1, Figure 12) which was also correlated with significantly increased NKA, GDH and GS (Figure 6A; Figure 10A; Figure 11). In the present study, NKA overcompensation to cooler temperatures in the posterior regions of the whole GIT were observed where the PI had the highest activity at cooler temperatures which was not hypothesized (Figure 6). Environmental temperature affects the mechanisms responsible for passive and active ion-transport which in turn influences the ion-water balance in the body (Metz et al. 2003). Therefore, the enhanced NKA activity in the PI may indicate a region-specific requirement for hydromineral balance at cooler temperatures which may be related to the transport of other ions, increased epithelial permeability to Na^+ molecules across the epithelia or NKA may be an indicator for increased energy production for other processes in that region (Metz et al. 2003). The *Deefgea* and *Aeromonadaceae* (Firmicutes) that are highly associated with PI (Figure 12) have been previously identified in the gut of fish and are involved in sugar fermentation and the production of acids (Jung and Jung-Schroers 2011; Esteve 1995; Kim et al. 2007; Li et al. 2015) which may reflect the increased though not significant activity of cellulase here (Figure 13). GS activity was elevated in the PI regardless of temperature treatment which suggests the region is particularly important for ammonia detoxification which supports the findings of Rubino et al. (2014) in rainbow trout.

The PI experienced the next largest shift in bacterial communities after the AI+MI region with WW treatment Figure 3C) but this shift was more so between Tenericutes and Proteobacteria abundance. The PI experienced a 2.3% decrease in Tenericutes abundance and a 6.2% increase in Proteobacteria with increased temperature (Figure 5, Table 1). GDH activity

decreased (Figure 8B) with WW treatment which may be correlated with decreased Tenericutes, but its activity remained significantly elevated in the PI compared to other regions (Figure 8A). It appears that this shift in bacterial communities did not result in any major changes in GS as elevated activity persisted in the PI (Figure 10). It may be possible that the increased LDH (though not significant) observed in this region (Figure 12) is related to increased energy production *via* lactic acid conversion to pyruvate that is shuttled to the TCA cycle resulting in increased ATP production to fuel activities such as local ammonia detoxification in the PI *via* GS (Figure 13; Rubino et al. 2014).

5.5 Conclusions

Zonation in the gut microbiome and enzyme activity were detected as hypothesized. Overall, the stomach microbiome and enzyme activity profile reflected a region that was very bacterially diverse but not strongly correlated with any specific enzyme activity in this survey. The intestinal regions became less diverse over the anteroposterior axis; the data also suggests the AI+MI has a more plastic microbiome than the PI which may be reflected in the dynamic enzyme activity of this region and is more specialized for processes related to protein and fat digestion as is suggested by the trypsin and lipase activity profiles and its association with high Firmicutes/Tenericutes abundance which have previously been linked to these processes (Semova et al. 2012; Carmody and Turnbaugh 2012). The stomach and PI have lower abundance of Firmicutes/Tenericutes compared to the AI+MI and are not associated with maximal trypsin and lipase activity which indicates that the high population of these bacteria may affecting enzyme activity profiles in this region. The PI showed elevated levels of GS activity consistent with ammonia detoxification likely due to bacteria contributing to the activity of the enzyme. Temperature was found to impact the bacterial composition of the gut, most notably in the core

gut bacteria where Proteobacteria and Bacteroidetes increased at the expense of Firmicutes/Tenericutes as was expected. However, strong zone-specific changes to temperature were not detected since temperature seemed to amplify major zone trends already observed in the CW control. Temperature did not seem to have a direct effect on enzyme activity as hypothesized general trends in processes such as digestive enzyme and enzymatic ammonia detoxification increase, and LDH, PK and CS perfect compensation did not appear to consistently correlate with increased temperature. It is likely a more complex relationship between temperature and the microbiome along with other more complex host regulatory mechanism which influence the activities of these enzymes. Thus, our initial hypothesis that there was a mutualistic relationship between the bacteria in the gut and enzyme activity is supported by these findings. These results also highlight the importance of zonation in studying the GIT of fish; differences in microbiome and enzyme activity might have been missed had the GIT been homogenized and considered as one unit.

Chapter 3: The effect of salinity on the microbiome, and metabolic and digestive enzyme activities along the GIT of the rainbow trout

Introduction:

6.1 Overview

Rainbow trout are a euryhaline fish meaning they can tolerate a wide range of salinities including that of freshwater (FW), brackish and seawater (SW) environments compared to stenohaline fish which can only tolerate a small range of salinities (Kultz 2015). Some varieties of rainbow trout are anadromous, spending parts of their lifecycle in freshwater and seawater (Kultz 2015). It is known that in salmonid varieties, a variety of physiological changes occur in the gut to accommodate the changing homeostatic balances that must be established to allow for their survival in different salinities such as with transition between freshwater and seawater environments over their life cycles, with changing seasons, and with natural variations in ion availability in freshwater environments (Flores and Shrimpton 2012). Most notably, fish physiology transitions to salt secretion and water retention in SW environments to active salt absorption and water excretion in FW environments to maintain ion balance and cell volume (Kultz 2015). The microbiome is affected by salinity and alterations in the activities of important metabolic, detoxification and digestive enzymes have been previously identified as was discussed in Chapter 1.

6.2 The effects of salinity on the GIT microbiome

Salinity can impact the bacterial populations and cause physiological changes in the gut of the host which in turn can indirectly impact the bacterial composition and alter their influence on host physiology (Schmidt et al. 2015). Salinity impacts the gut microbiome assembly of fish. The gut bacterial compositions of SW, estuarine and FW fish varieties show that SW fish had gut

microbiomes more like one another than to FW fish (Sullam et al. 2012). *Aeromonas* and *Plesiomonas* of the phyla Proteobacteria are the most prevalent in freshwater and anadramous fish while in marine fish, *Vibrio* (also of phyla Proteobacteria) was present in majority (Sullam et al. 2012). Similarly, Schmidt et al. (2015) reported that within a single fish species, the Mexican molly, *Aeromonas* was more prevalent in the gut of FW acclimated fish compared to increased *Vibrio* in the gut of fish of the same species in SW. In addition, the composition of gut bacteria in the Mexican molly was different from that of the surrounding tank water indicating that bacterial community composition is not only impacted by the direct effects of salinity but on the selective properties of the gut lumen and physiological changes leading to selection of certain bacterial species (Schmidt et al. 2015).

6.3 The effects of saltwater salinity challenge on enzyme activity

Much of the literature regarding salinity and enzyme activity has focused on the changes in activity with seawater (SW) salinity challenge.

Metabolic energy requirements increase with increased salinity challenge and metabolic enzymes exhibit increased activity consistent with an overcompensation response to SW challenge. LDH in the gill, liver, and muscle tissue of the Arctic char (*Salvelinus alpus*) and the gill of Atlantic wolfish (*Anarhichas lupus*) increase when the fish were moved from FW to SW (Bystriansky et al. 2007; Le Francois et al. 2004). Kirchner et al. (2005) identified a similar trend in PK with salinity challenge; an increase in intestinal PK activity of the juvenile short nose sturgeon (*A. brevirostrum*) was observed when the fish were moved from 0‰ and 20‰ water salinity. The activity of CS increased in the gills of the stickleback fish (*Gasterosteus aculeatus*) and juvenile coho salmon (*Oncorhynchus kisutch)* with increasing water salinity (Schaarschmidt et al. 1999; Shrimpton and Bernier 1994). Increased CS activity was accompanied by increased

NKA activity in the gills at higher salinities as metabolic demand increases (Shrimpton and Bernier 1994).

NKA, which plays a key role in osmoregulatory processes related to salinity challenge, increases at higher salinities in the gills of the Atlantic wolfish and the freshwater marble goby (Le Francois et al. 2004; Chew et al. 2009). NKA pumps sodium across the epithelia as has been identified in the gills and kidney and increasing this active transport at higher salinities to maintain cell volume across the body in hyperosmotic environments (Jampol et al. 1970; McCormick 1995). The intestine also plays an important role in osmoregulation indicating that similar patterns of NKA activity upregulation may occur in the GIT (Shehadeh and Gordon 1969; Abbaurea-Equisoain and Garrido 1996).

Cell volume regulation is also mediated through the intracellular concentrations of free amino acids (Ballantyne and Chamberlin 1994; Jarvis and Ballantyne 2003). GDH increases with increasing salinity while GS decreased in the intestine of the juvenile marble goby (*Oxyeleotris marmorata*) indicating that GS may act independently of GDH in certain situations (Chew et al. 2010). Other studies have reported an increase in GS activity with salinity challenge (stomach, Asian freshwater stingray: Tam et al. 2003; liver and muscle, Amazon stingray: Ip et al. 2009; liver, Asian swamp eel: Tok et al. 2009). Thus, changes in the activities of GDH and GS may also indicate osmoregulatory regulation activities in the form of increased production of amino acids as osmolytes used to maintain cell volume in hyperosmotic environments. Increased activity may also indicate increased ammonia detoxification; as the metabolic demand increases, energy sources such as protein may become more important and degradation of these molecules liberates toxic ammonia which must be removed from the system (Wicks and Randall 2002; Wright et al. 2007; Rubino et al. 2014).

Salinity alters the activities of the digestive enzymes trypsin and lipase. Trypsin activity decreases with increased salinity exhibiting an inverse compensation to salinity challenge (golden-line sea bream: Woo and Kelly 1995; gilthead seabream: Moutou et al. 2004; Tsuzuki et al. 2007). It is known that drinking rates are altered with changing salinity wherein SW acclimated fish increase drinking to increase water retention which could in turn affect enzyme activity (Bath and Eddy 1979; Moutou et al. 2004). In the case of trypsin, it is thought that salinity can affect the activation of the inactive trypsin zymogen by proteolysis although the exact mechanism of deactivation with increased salinity is poorly understood (Moutou et al. 2004). No studies have investigated cellulase activity and salinity in fish to the author's knowledge; however, in *Saprolegnia parasitica*, a parasitic cotton mould, low and moderate salt concentrations caused cellulase activity to increase while high concentrations resulted in decreased activity producing an inhibited inverse compensation effect (Hardin and Hill 1999; Mahdy et al. 2004; Ali 2005). Lipase activity increases in coho and chinook salmon following SW exposure; it is thought that increased lipolysis contributes increased energy production to fuel osmoregulation processes in SW environments reflected by the increase in metabolic enzyme activity (Sheridan 1989).

6.4 Ion-poor water and Sodium-potassium ATPase

NKA activity is unchanged with decreasing salinity to maintain the level of activity required in FW to balance the concentrations of Na^+ and K^+ cell volume (Flores and Shrimpton 2012). Flores and Shrimpton (2012) studied the physiological effect of the abrupt exposure of freshwater-acclimated rainbow trout to either SW or ion-poor water (IPW) in their gill tissue. They reported that in seawater conditions, NKA activity levels increased while in IPW conditions, NKA activity remained unchanged although the mRNA transcripts of one NKA

isoform (NKA α1b) increased as it had in abrupt seawater exposure conditions (Flores and Shrimpton 2012). Similar results were observed by Chasiotis et al. (2009) in the intestine of goldfish exposed to IPW for 14 days. This indicates that while IPW does not impact the activity of the enzyme, physiological changes occur to ensure that NKA activity remains the same as in freshwater conditions. These changes might then alter the physiological conditions and functioning of other enzymes and perhaps the microbiome. It also indicates that physiological responses with changing ion-levels do not necessarily share salinity-dependent linear correlation (i.e. increased activity with seawater exposure does not result in a decrease activity with IPW exposure).

There is evidence that the activity of NKA may influence the activities of other enzymes such as LDH and PK as was discussed in section 1.5. The extent to which NKA influences other enzymes or vice versa and the reasons for its influence on certain enzymes over others is not well established however. The relationship between NKA and the activity of other enzymes will also be briefly explored.

6.5 Objectives and Hypotheses

IPW was utilized to investigate the effects of decreased salinity on zonation patterns in the gut microbiome and physiology of fresh-water acclimated rainbow trout.

As mentioned in sections 1.2 and 1.3, regionalization of the microbiome and zonation patterns in enzyme activity have been previously been investigated; however, the mutualistic effect of the microbiome and changes in salinity on the enzyme activity zonation have not been explored.

Patterns of zonation in bacterial populations and enzyme activities are expected to be observed along the gut. It was hypothesized that the stomach would have the highest bacterial diversity followed by the anterior intestinal region and posterior region as has been previously reported in fish (Lesel and Peringer 1981; Bik et al. 2006; Al-Hisnawi et al. 2015). It was predicted that with lower salinity conditions, the bacterial diversity would decrease in the gut of the rainbow trout due to reduced ion availability. This decreased competition may lead to a change in the percent composition of each region and may influence community reorganization and assembly in such a way that certain bacterial phyla become more prevalent (Schmidt et al. 2015). Regions of the gut with decreased bacterial diversity such as the PI might be more impacted by decreased salinity as the populations of bacteria are reduced further; enzyme activity in this region is also expected to be most impacted by salinity decrease due to the change in the bacterial population composition.

It has been established that water salinity can also influence the microbial populations of the gut of fish though few studies have investigated the effect of ion-poor water salinity on the gut microbiome. It is expected that while NKA activity will not be affected by ion-poor water as was other physiological responses and perhaps changes in the microbiome in response to decreased salinity may induce changes in other enzymes' activities.

Many studies have measured enzyme activity in seawater conditions but few investigating the effect of ion-poor water exist. Whether the behaviour of the enzyme in ion-poor water follows a linear relationship with the previously documented enzyme behaviour in SW or exhibits a unique activity profile indicating more complex physiological regulatory mechanisms in IPW will be explored. Re-establishment of homeostatic balance in IPW may result in increased metabolic demand which might increase the activity of metabolic enzymes such as

LDH, PK and CS as well as GDH and GS which aid with cell volume regulation and ammonia detoxification. Proteolytic and lipolytic activity through trypsin and lipase is expected to decrease as the contribution from the microbiome is reduced. Reduced bacterial diversity may also decrease the activity of cellulase which is mostly contributed by the gut microbiome.

Materials and Methods

7.1 Ion-poor water salinity challenge experiment

Rainbow trout (Humber Springs Trout Farm, Orangeville, Ontario) were kept in two 200L aerated, flow-through tanks at 6°C (~10 individuals per tank) with dechlorinated freshwater (FW) supplied through the City of Toronto (composition was approximately in μM: Na^+ 590; Cl^- 920; Ca^{2+} 900; K^+ 50; pH 7.4). Fish acclimation and basic fish husbandry protocols were the same as described in section 3.1. Immediately prior to the experiment, fish were net-captured and sampled for the t=0 time-point with the same method as was described in section 3.2. For the experimental treatment, the water salinity in one tank was reduced to 75% ion-poor water (IPW) supplied through a reverse-osmosis system supplemented daily with Sifto Crystal Plus Water Softener Salt (Compass Minerals; Mississauga, Ontario) and 25% FW (approximate composition in μM: Na^+ 163, Cl^- 99, Ca^{2+} 227, and K^+ 13, pH 6.5) flow-through over a period of about 30 minutes to allow for gradual exposure for the fish. Experimental fish were fed fish feed pellets (Tropica Aquaria, Orangeville, Ontario; composition on Table 4) every 24 hours for a period of 2 weeks. At 24 hours and 2 weeks of IPW exposure, fish were sacrificed, and samples were collected to be used in the microbiome analysis as well as in the enzyme activity analysis as described in section 3.2. Data processing and analysis followed the same general workflow as was discussed in section 3.4-3.9.

Results

8.1 Bacterial identities and abundance in decreased salinity

Figure 14 visualizes the % of bacterial phylogeny abundance in each sample also quantified in Table 2; only the % of core bacteria phyla was considered in this analysis.

Firmicutes/Tenericutes made up most of the bacterial composition in the stomach (70.7%), AI+MI (97.4%) and PI (74.3%) samples (Figure 14, Table 2).

The stomach exhibited more bacterial phyla evenness than other samples. In this sample, the bacterial composition remained relatively unchanged with IPW treatment. Firmicutes and Tenericutes bacteria, which are in majority in this region, make up 65.8% and 5.1% of the sample in the FW treatment and 69.0% and 2.8% in the IPW treatment, respectively. Proteobacteria comprises 14.2% of the sample in the FW treatment while in the IPW it is 15.7%. Bacteroidetes composition remains around 10% in both samples (FW=10.6%; IPW = 9.8%).

The AI+MI region had the highest abundance of Tenericutes bacteria regardless of salinity (FW=97.0%; IPW=93.8%) while Firmicutes was low (FW=0.4%; IPW=0.1%) in the samples. Proteobacteria (FW=2.1%; IPW=6.1%) and Bacteroidetes (FW=0.2%; IPW=0.0%) levels remained low in this region with IPW.

Finally, the PI had the second highest proportion of Tenericutes (FW=74.2%; IPW=86.3%) after the AI+MI region which was slightly increased with IPW treatment. Firmicutes bacteria remained low in both treatments (FW=0.1%; IPW=0.1%). Proteobacteria slightly decreased from 25.7% in the FW treatment to 13.6% in IPW. Bacteroidetes remained low in both treatments (FW=0.0%; IPW=0.0%).

8.2 Alpha diversity in the GIT with ion-poor water challenge

The bacterial species (represented by OTUs) abundance and diversity was explored using the observed OTU, phylogenetic diversity (PD) whole tree, Shannon and Chao1 plots (Figure 15). The highest number of unique OTUs observed in a sample (richness) was detected in the 2-week 75% ion-poor water exposed (IPW) stomach sample (652), followed by the freshwater (FW) stomach (622), the FW AI+MI (134) and the IPW AI+MI (91) while the IPW and FW PI samples both appeared to have the lowest number of observed unique OTUs (63 and 58, respectively) over the sequence subset sampled (Figure 15A). The phylogenetic diversity whole tree (PD) in Figure 15B shows that the ranking of samples with a high number of OTUs with a large phylogenetic distance between sequences is similar to the ranking seen in the observed OTUs plot (Figure 15A) which shows that the observed OTUs in the stomach samples have a higher degree of distinctness than the AI+MI and PI samples. In the Shannon plot shown in Figure 15C it is observed that the IPW stomach has the highest evenness and richness index followed by the FW stomach, FW PI, IPW PI, FW AI+MI and the IPW AI+MI. In the Chao 1 plot (Figure 15D) it was observed that the IPW stomach had the highest likelihood of containing a rare OTU, followed by the FW stomach, FW AI+MI, IPW AI+MI, IPW PI and FW PI.

8.3 Beta diversity in the GIT with ion-poor water challenge

The jackknife unweighted bootstrap tree (Figure 16) showed strong support (>75%) for distinct sequence compositions between the stomach samples and the intestinal samples where the stomach samples clustered more closely together and thus were more like one another than the intestinal samples; this means that the stomach samples contain more similar bacterial species compared to the intestinal samples. Among the intestinal samples, the FW AI+MI sample was strongly distinct from the IPW AI+MI, FW PI and IPW PI; the FW AI+MI shared fewer

species in common with these samples. The IPW AI+MI and the IPW PI showed moderate support (50-75%) for distinct sequences compared to the FW PI which showed stronger support for distinct sequences indicating that the IPW AI+MI and IPW PI shared more species in common.

The jackknife weighted bootstrap tree (Figure 17) showed clustering similar to the unweighted bootstrap tree (Figure 4), except that there is now stronger support (>75%) for distinct OTU composition in the AI+MI samples (both the FW and IPW exposure) and the PI samples meaning they share fewer species; this indicates that these differences are abundance-driven: the amount of bacterial species in each sample is different between each region. The lengthening of the red lines between samples also indicates that abundance is driving the differences between sections indicating greater support.

8.4 Enzyme zonation in the GIT with ion-poor water challenge

8.4.1 Sodium-potassium ATPase

In the GIT (Figure 18), it was observed that significant differences in NKA activity between zones existed in the FW treatment but not the 24h IPW or 2-week IPW treatments. In the FW treatment (Figure 18A), the stomach (0.36 μmol ADP mg^{-1} protein h^{-1}) had the lowest activity while the AI (2.46±0.6 μmol ADP mg^{-1} protein h^{-1}) had the highest; the NKA activities of the MI (1.27±0.2 μmol ADP mg^{-1} protein h^{-1}) and PI (1.12±0.5 μmol ADP mg^{-1} protein h^{-1}) were indistinguishable from the activities in the stomach and AI. In the MI, the FW and 24h IPW treatment tissue had significantly higher activity than the 2-week IPW treated tissue (Figure 18B).

8.4.2 Lactate dehydrogenase

The stomach (FW: 509.6±167.7 μmol min^{-1} g^{-1} protein, IPW:468.1±114.9 μmol min^{-1} g^{-1} protein) had a significantly lowered LDH activity compared to the intestinal segments in the FW and 24h IPW treatments (Figure 19B). These differences were diminished after 2-week IPW exposure and there were no significant differences in LDH activity between GIT zones.

8.4.3 Pyruvate kinase

Significant changes in PK activity were not detected in the freshwater (FW) or 75% ion-poor water (IPW) treated whole GIT tissue sampled. The average activity in 1159.4±595.1 μmol min^{-1} g^{-1} protein in FW, 755.1±295.8 μmol min^{-1} g^{-1} protein at 24-hour IPW exposure and 1921.2±502.8 μmol min^{-1} g^{-1} protein at 2-week IPW exposure.

8.4.4 Glutamate dehydrogenase

The stomach (FW: 7507.5±2546.6 μmol min^{-1} g^{-1} protein, 24-hour IPW: 8071.0±2076.5 μmol min^{-1} g^{-1} protein, 2-week IPW: 9243.5±65.9 μmol min^{-1} g^{-1} protein) showed the highest activity when compared to the AI, MI and PI at all salinities and time points sampled (Figure 20A-C). In both the FW and 24h IPW treated fish, the stomach activity was 4x higher while at 2-week IPW exposure, the stomach had 9x higher activity than the AI, MI, and PI.

8.4.5 Citrate synthase

A zonation pattern along the whole GIT was detected in the freshwater (FW) and 24-hour exposure to 75% IPW (24h IPW) tissues tested (Figure 21); these changes between GIT zones disappeared at 2 weeks of exposure to 75% ion-poor water (2-week IPW). The activities of CS in the freshwater (FW) tissues at time=0 in the stomach, anterior intestine (AI), middle intestine (MI), and posterior intestine (PI) was 51.6±6.6, 18.8±5.7, 15.8±3.9 and 29.7±7.3 μmol min^{-1} g^{-1} protein, respectively, following a U-shaped activity pattern along the GIT wherein the stomach

had the highest activity (Figure 21A). A similar pattern was detected at 24 hours exposure to 75% ion-poor water (24h IPW) where the activities in the stomach, AI, MI and PI were 54.9±14.5, 44.1±14.9, 9.9±3.0 and 91.3±20.8 μmol min^{-1} g^{-1} protein (Figure 21B). There was a correlation between decreased salinity and CS activity in the PI only where the 24-hour IPW PI had CS activity three-fold higher than the FW (Figure 21C). At 2-week IPW, this elevated activity in 75% IPW decreased by 17% to 15.7±4.5 μmol min^{-1} g^{-1} protein (Figure 21C); no changes were detected over salinity and time in the stomach, AI, or MI.

8.4.6 Glutamine synthase

The stomach (75.7±13.6 μmol min^{-1} g^{-1} protein) showed the highest activity compared to the intestinal segments in FW conditions as seen in Figure 22A (AI: 20.1, MI: 31.4±10.3, and PI: 31.4±12.5 μmol min^{-1} g^{-1} protein, respectively), while in the 24h IPW treatment (Figure 22B), this pattern was reversed: the PI (50.9±7.7) had the highest activity and the activities in the stomach (14.44±4.0 μmol min^{-1} g^{-1} protein), AI (25.4±3.5 μmol min^{-1} g^{-1} protein), and MI (16.6±3.5 μmol min^{-1} g^{-1} protein) were depressed. At 2-week IPW, the differences in activities between zones was significantly diminished.

8.4.7 Cellulase

Cellulase activity changes were not detected in the freshwater (FW) or 75% ion-poor water (IPW) treated whole GIT tissue sampled. The average activity was 1803.7±717.2 mg glucose min^{-1} mg^{-1} protein in the FW treatment, 303.5±157.6 mg glucose min^{-1} mg^{-1} protein at 24-hour IPW exposure and 447.8±189.6 mg glucose min^{-1} mg^{-1} protein at 2-week IPW exposure.

8.4.8 Trypsin

The AI (149.2±17.3 μmol min^{-1} g^{-1} protein) had higher trypsin activity than the PI (6.6±2.4 μmol min^{-1} g^{-1} protein) while the activity in the stomach (28.6±11.6 μmol min^{-1} g^{-1} protein) and MI (106.6±55.0 μmol min^{-1} g^{-1} protein) were not significantly different to either the AI or PI in the FW treatment (Figure 23A). The same pattern was observed in the GIT tissues in the 24h IPW treatment (Figure 23B) where the stomach, AI, MI and PI had activities of 30.1±9.8, 124.8±32.4, 123.7±49.9 and 5.3±1.5 μmol min^{-1} g^{-1} protein, respectively. No significant differences in trypsin activity between the zones of the whole GIT were detected at 2-week IPW.

8.4.9 Lipase

Lipase activity changes were not detected in the freshwater (FW) or 75% ion-poor water (IPW) treated whole GIT tissue sampled. The average activity was 49.3±9.5 nmol of triglyceride converted to glycerol min^{-1} in FW, 90.8±38.7 nmol of triglyceride converted to glycerol min^{-1} at 24-hour IPW exposure and 99.6±28.2 nmol of triglyceride converted to glycerol min^{-1} at 2-week IPW exposure.

8.5 Correlations between the microbiome and enzyme activity in the GIT

The RDA (Figure 24) shows that bacterial species abundance in the stomach, AI+MI and PI sample vectors appear in distinct quadrants of the plot indicating their bacterial abundances are divergent from one another regardless of treatment. At each GIT zone, the FW and IPW samples had similar bacterial abundances such that the vectors appear close to each other in their respective quadrants.

In the multivariate RDA in Figure 25, it was observed that elevated lipase activity in the PI (both FW and IPW) is associated with an increased abundance in Tenericutes. Elevated

cellulase and LDH activity, associated with both PI samples, is closely associated with Proteobacteria. Elevated trypsin found in the FW and IPW AI+MI samples is highly associated with Tenericutes while elevated activities of GDH, CS and PK, which occurs in both stomach samples, are strongly associated with Cyanobacteria and Firmicutes, respectively.

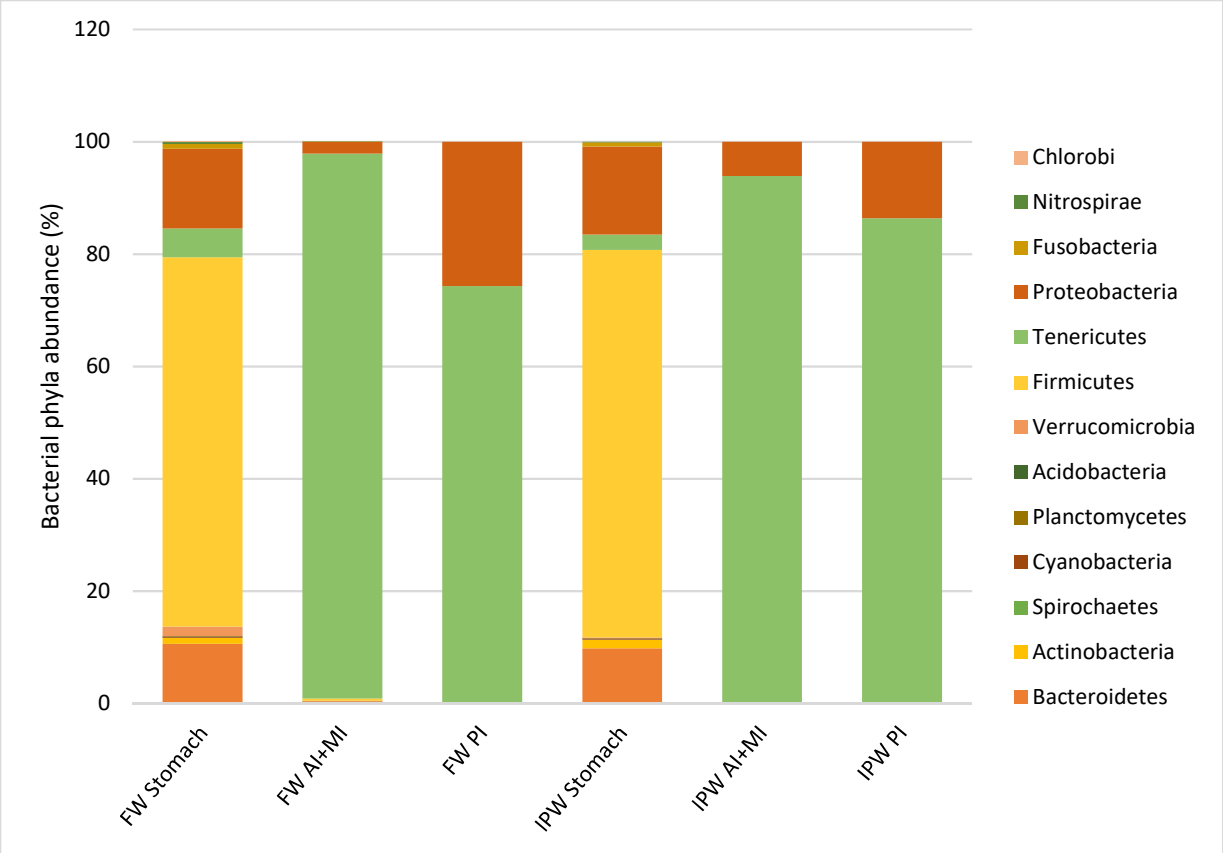

Figure 14. Bacterial community phyla abundance (%) assigned to OTUs using the Green Genes library in QIIME ® in the freshwater (FW) and 2 week exposure to 75% ion-poor water (IPW) stomach, AI+MI (anterior and middle intestine combined) and PI (posterior intestine) samples. The ratio of core gut bacteria (Firmicutes/Tenericutes, Bacteroidetes, and Proteobacteria) appeared to be affected by increased temperature in all GIT zones.

Table 2. Bacterial phylogeny abundance of core gut bacteria (%) detected in the rainbow trout GIT samples in freshwater (FW) and ion-poor water (IPW) conditions

Bacterial phyla	Stomach	AI+MI	PI
Firmicutes	FW – 65.8% IPW – 69.0%	FW – 0.4% IPW – 0.1%	FW – 0.1% IPW – 0.1%
Tenericutes	FW – 5.1% IPW – 2.8%	FW – 97.0% IPW – 93.8%	FW – 74.2% IPW – 86.3%
Proteobacteria	FW – 14.2% IPW – 15.7%	FW – 2.1% IPW – 6.1%	FW – 25.7% IPW – 13.6%
Bacteroidetes	FW – 10.6% IPW – 9.8%	FW – 0.2% IPW – 0.0%	FW – 0.0% IPW – 0.0%

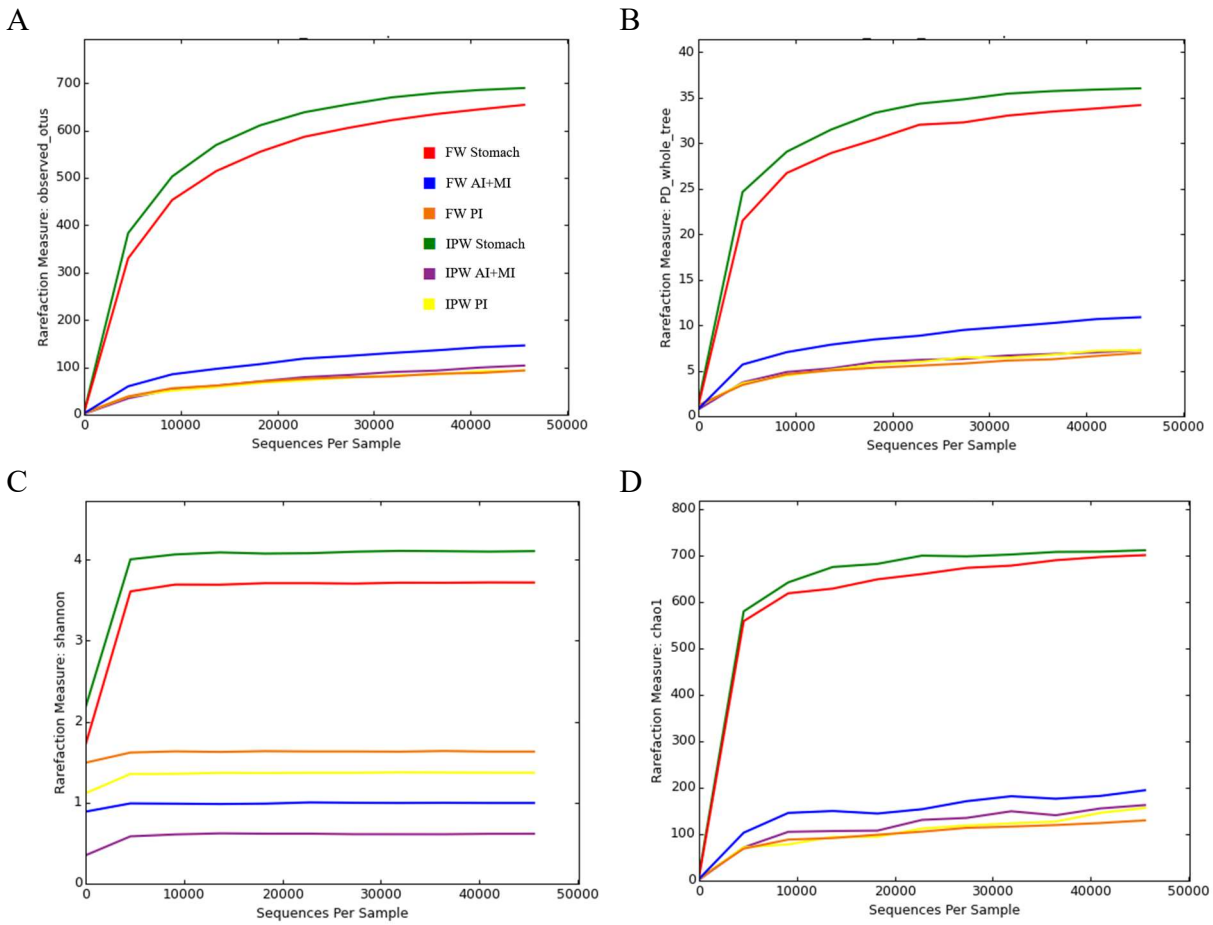

Figure 15. OTU alpha diversity in the rainbow trout stomach, AI+MI (anterior and middle intestine combined) and PI (posterior intestine) samples in freshwater (FW) and after 2 weeks exposure to 75% ion-poor water (IPW) conditions at a sampling depth of 10000 sequences per sample for a total of 45,321 random sequences in each sample (which was the minimum number of sequences detected across samples). A) Observed OTUs curves B) Phylogenetic diversity (PD) whole tree plot C) Shannon plot and D) Chao1 plot generated with QIIME ®. N=8

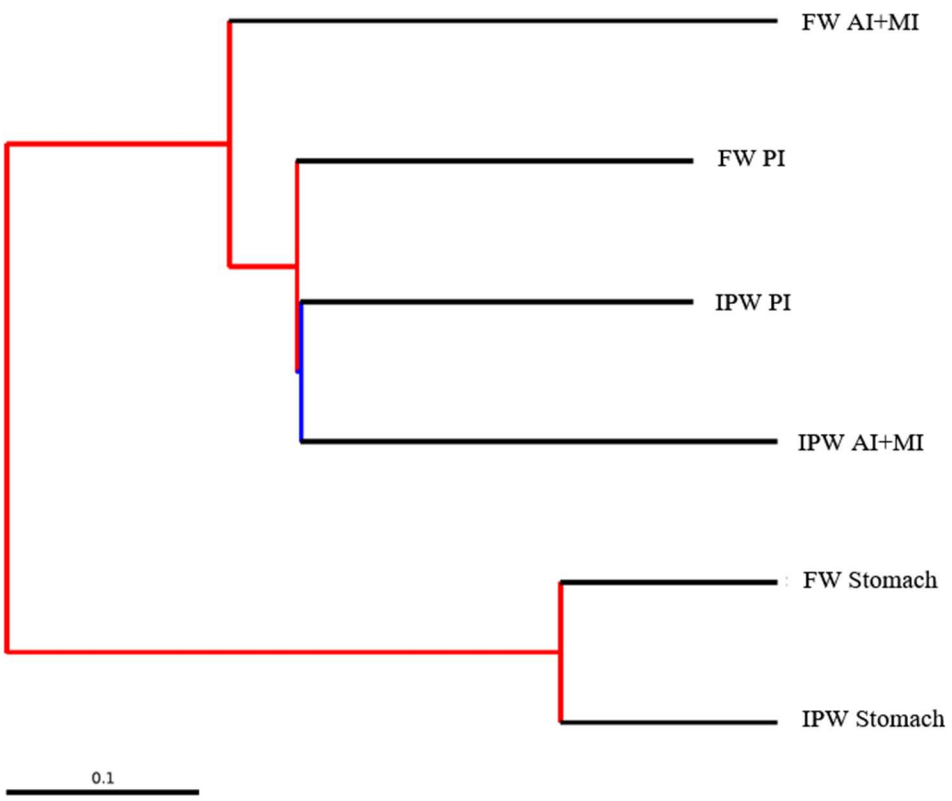

Figure 16. Unweighted (identity-based) jackknifed bootstrap tree depicting relationship between OTUs across freshwater (FW) and 75% ion-poor water (IPW) stomach, AI+MI (anterior and middle intestine combined) and PI (posterior intestine) samples at a distance of 0.1. Red indicates >75%, and blue <25% support for distinct bacterial compositions between samples. Jackknifed beta analysis performed using 90% of the random sequences based on the sample containing the smallest number of unique OTUs. Generated with QIIME ®.

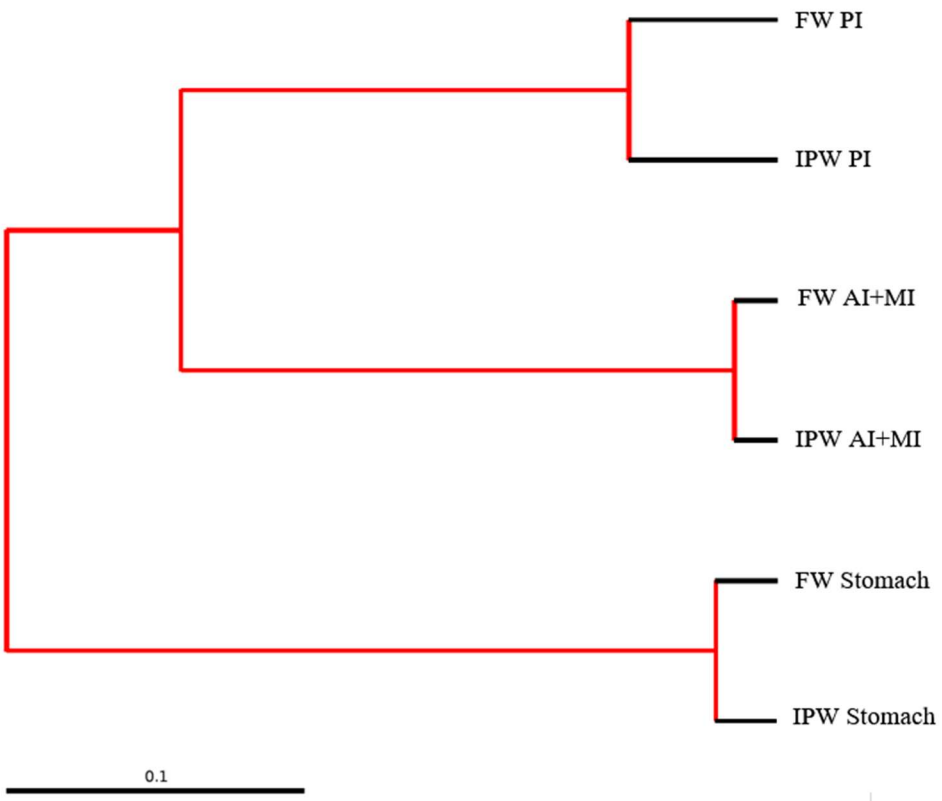

Figure 17. Weighted (abundance-based) jackknifed bootstrap tree depicting relationship between OTUs across freshwater (FW) and 75% ion-poor water (IPW) stomach, AI+MI (anterior and middle intestine combined) and PI (posterior intestine) samples at a distance of 0.1. Red indicates >75% support for distinct bacterial compositions between samples. Jackknifed beta analysis performed using 90% of the random sequences based on the sample containing the smallest number of unique OTUs. Generated with QIIME ®.

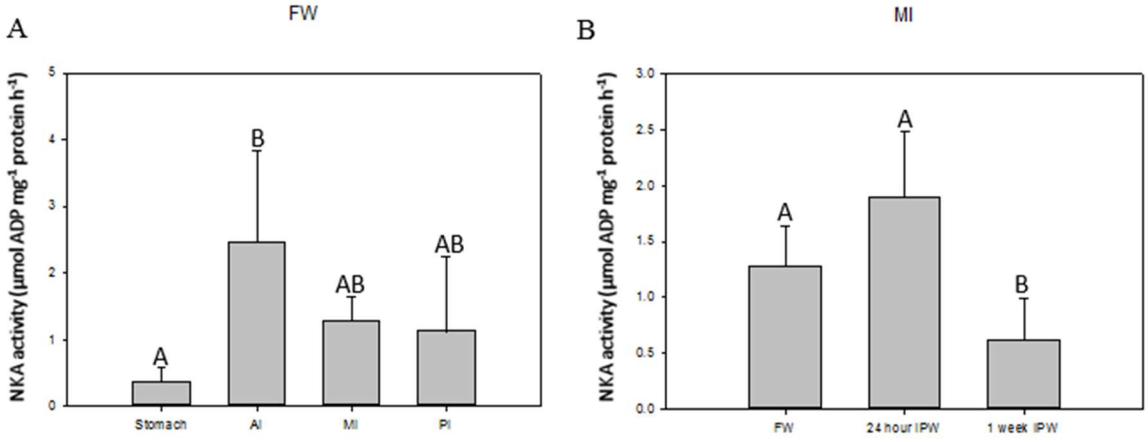

Figure 18. Sodium-potassium ATPase activity in the A) stomach, AI (anterior intestine), MI (middle intestine) and PI (posterior intestine) in FW (one-way repeated measures ANOVA, p=0.029, n=4) and B) in the MI with IPW exposure (one-way ANOVA, p=0.002, n=5,5,6). Bars that share the same letter are not significantly different.

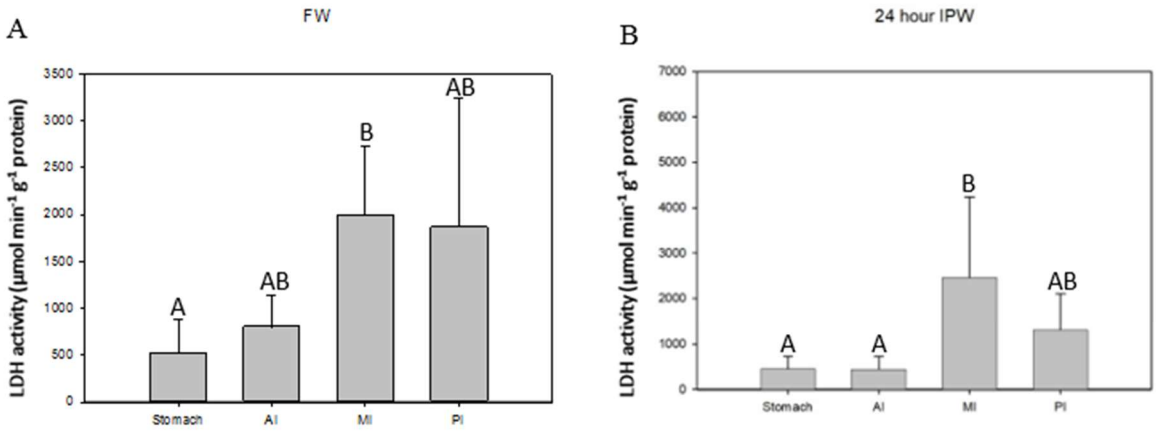

Figure 19. Lactate dehydrogenase activity in the stomach, AI (anterior), MI (middle) and PI (posterior intestine) of rainbow trout exposed to A) FW (one-way repeated measures ANOVA, $p=0.0021$, n=5,6,5,7) and B) 24-hour IPW (one-way repeated measures ANOVA, $p<0.001$, n=5,6,8,6). Bars that share the same letter are not significantly different.

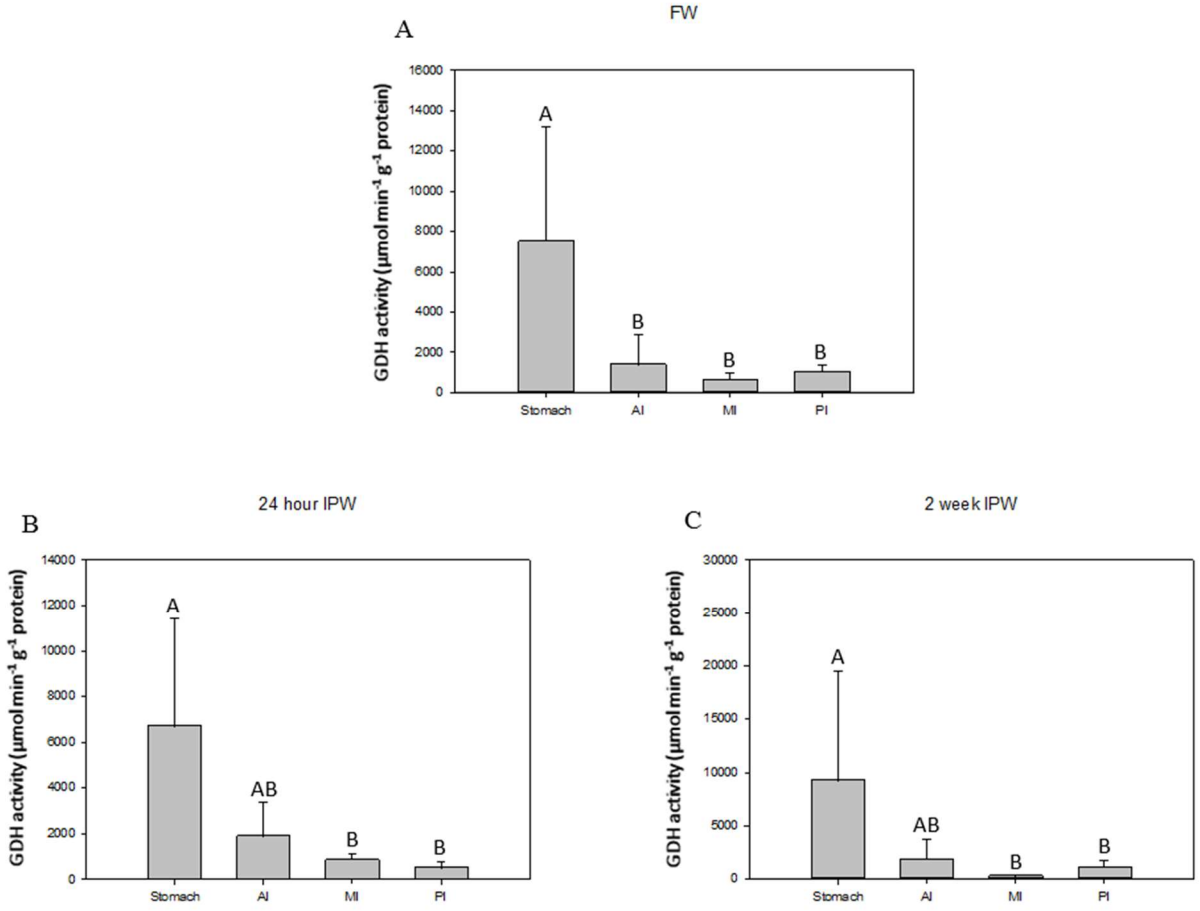

Figure 20. Glutamate dehydrogenase activity in the stomach, AI, MI and PI after A) FW (one-way repeated measures ANOVA, p= 0.009, n=5,6,5,6), B) 24 hour (one-way repeated measures ANOVA, p<0.001, n=5,6,6,5), and C) 2-week IPW exposure (one-way repeated measures ANOVA, p=0.002, n=5,7,5,7). Bars that share the same letter are not significantly different.

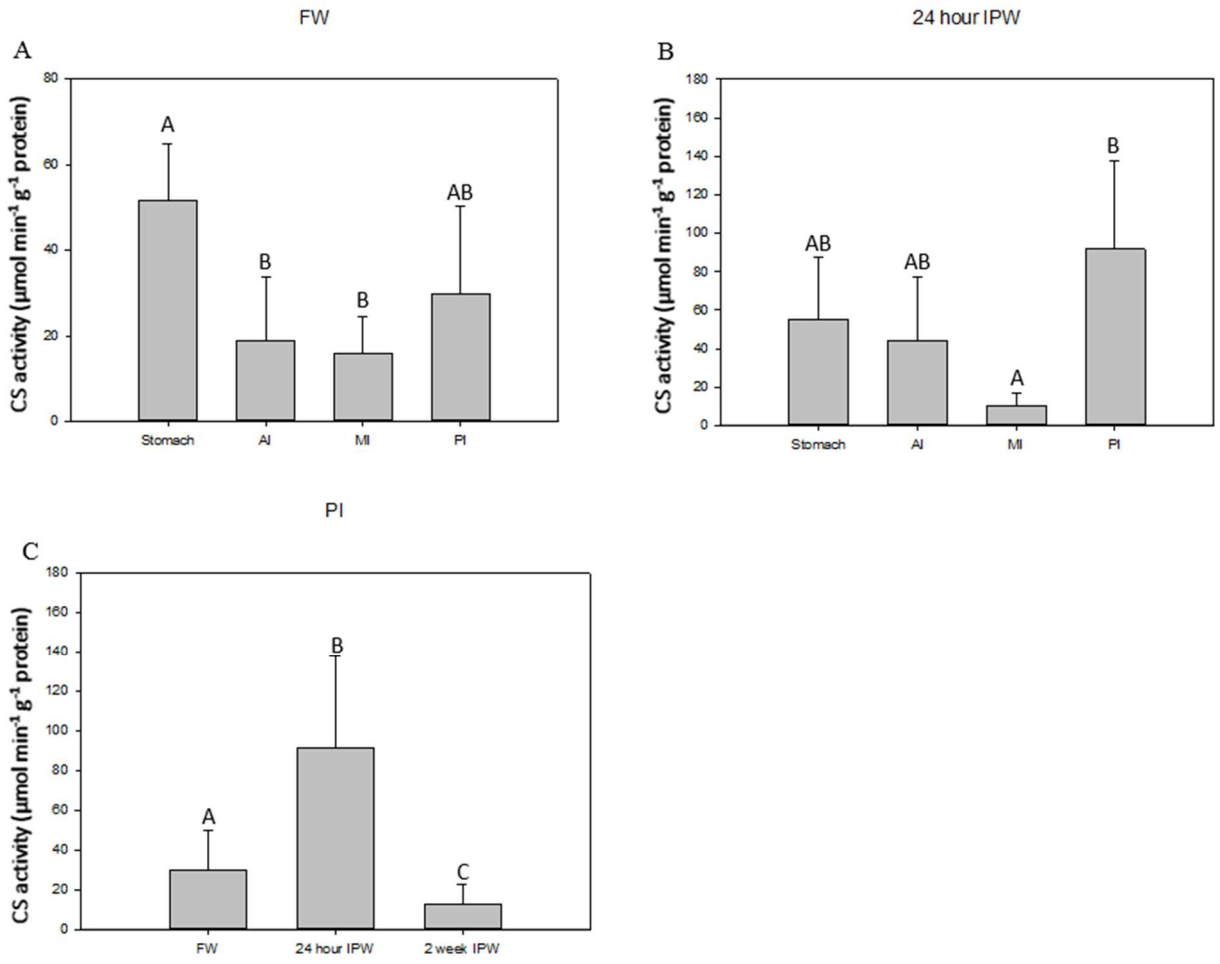

Figure 21. Citrate synthase activity in the stomach, AI, MI and PI of rainbow trout exposed A) FW (one-way repeated measures ANOVA, p=0.013, n=4,7,5,8), B) 24-hour IPW (one-way repeated measures ANOVA, p=0.011, n=5,5, 6,6) and C) in the PI with FW and IPW exposure (one-way ANOVA, p=0.001, n=8,6,5). Bars that share the same letter are not significantly different.

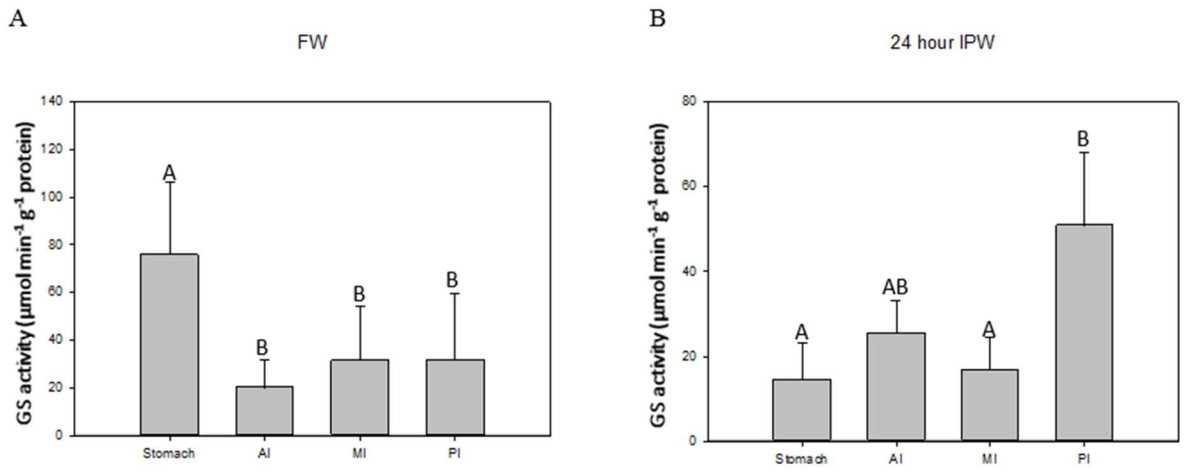

Figure 22. Glutamine synthetase activity in the stomach, AI (anterior), MI (middle) and PI (posterior intestine) after A) FW (one-way repeated measures ANOVA, p=0.011, n=5) and B) 24-IPW (one-way repeated measures ANOVA, p=0.002, n=5) exposure. Bars that share the same letter are not significantly different.

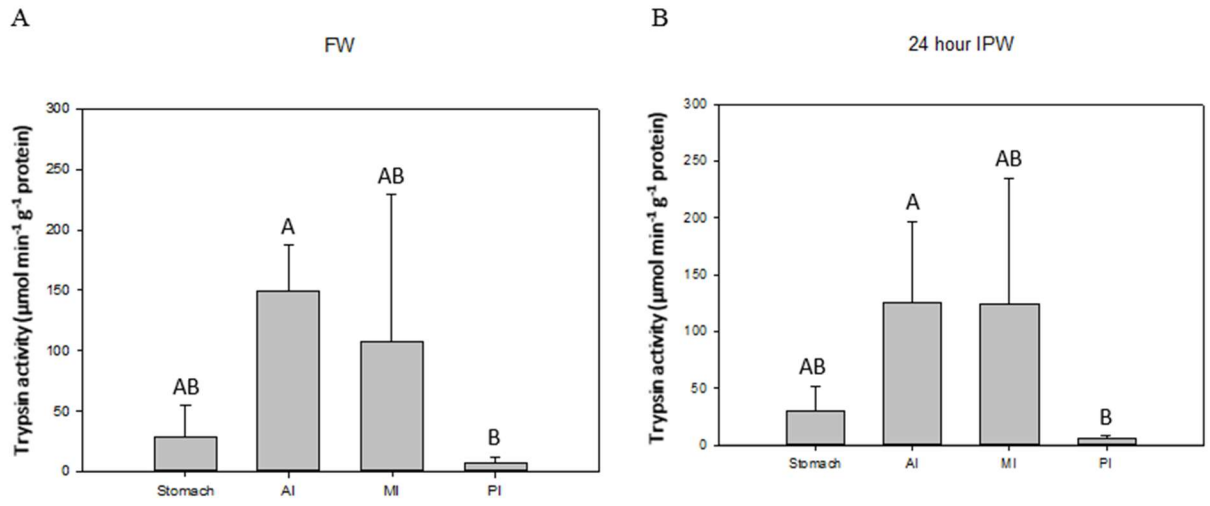

Figure 23. Trypsin activity in the stomach, AI (anterior), MI (middle) and PI (posterior intestine) of rainbow trout exposed to A) FW (one-way repeated measures ANOVA, $p=0.011$, $n=5$) and B) 24-hour IPW (one-way repeated measures ANOVA, $p<0.001$, $n=5$). Bars that share the same letter are not significantly different.

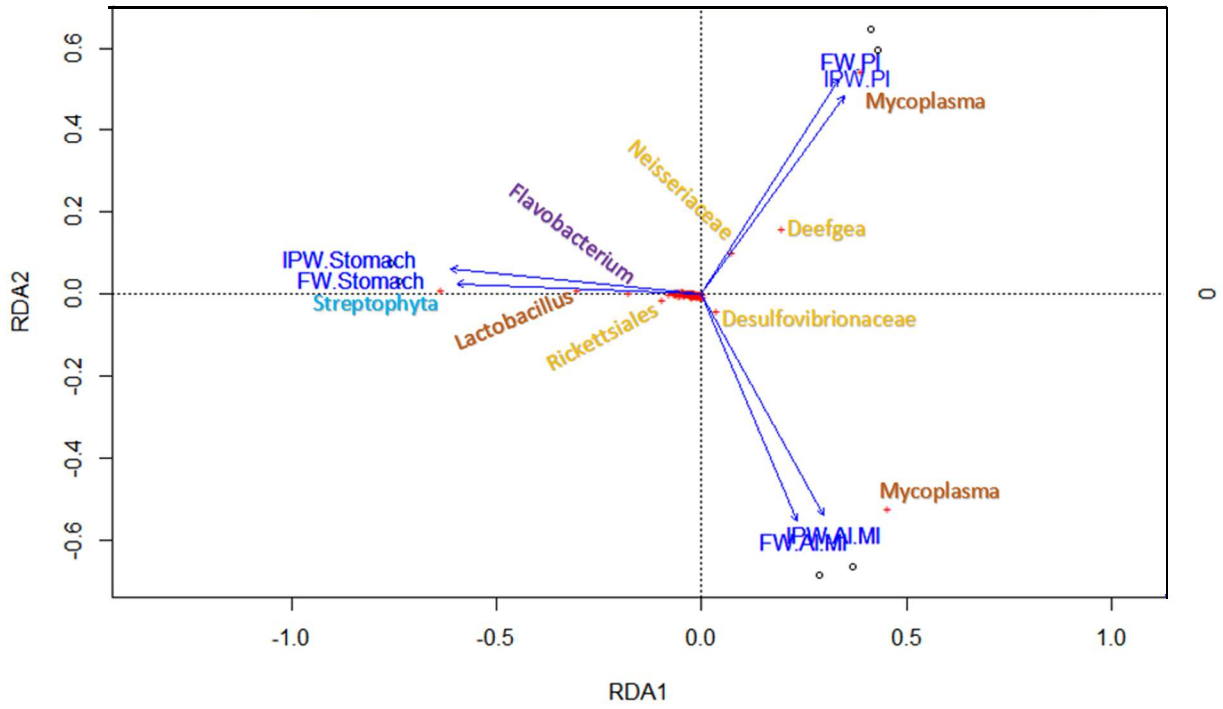

Figure 24. Multivariate redundancy analysis (RDA) depicting the variation of bacterial species abundance (represented by the red cross) in the freshwater (FW) and 75% ion-poor water (IPW) exposed stomach, AI (anterior), MI (middle) and PI (posterior intestine) zone samples (shown in dark blue). Bacterial taxa identities labelled near closest red cross: genus Lactobacillus and genus Mycoplasma (both of phylum Firmicutes shown in orange); order Streptophyta (of phylum Cyanobacteria shown in light blue); order Rickettsiales, genus family Neisseriaceae, order Desulfovibrionaceae and genus Deefgea (all of phylum Proteobacteria shown in yellow); genus Flavobacterium (of phylum Bacteroidetes shown in purple). Generated with R Studio.

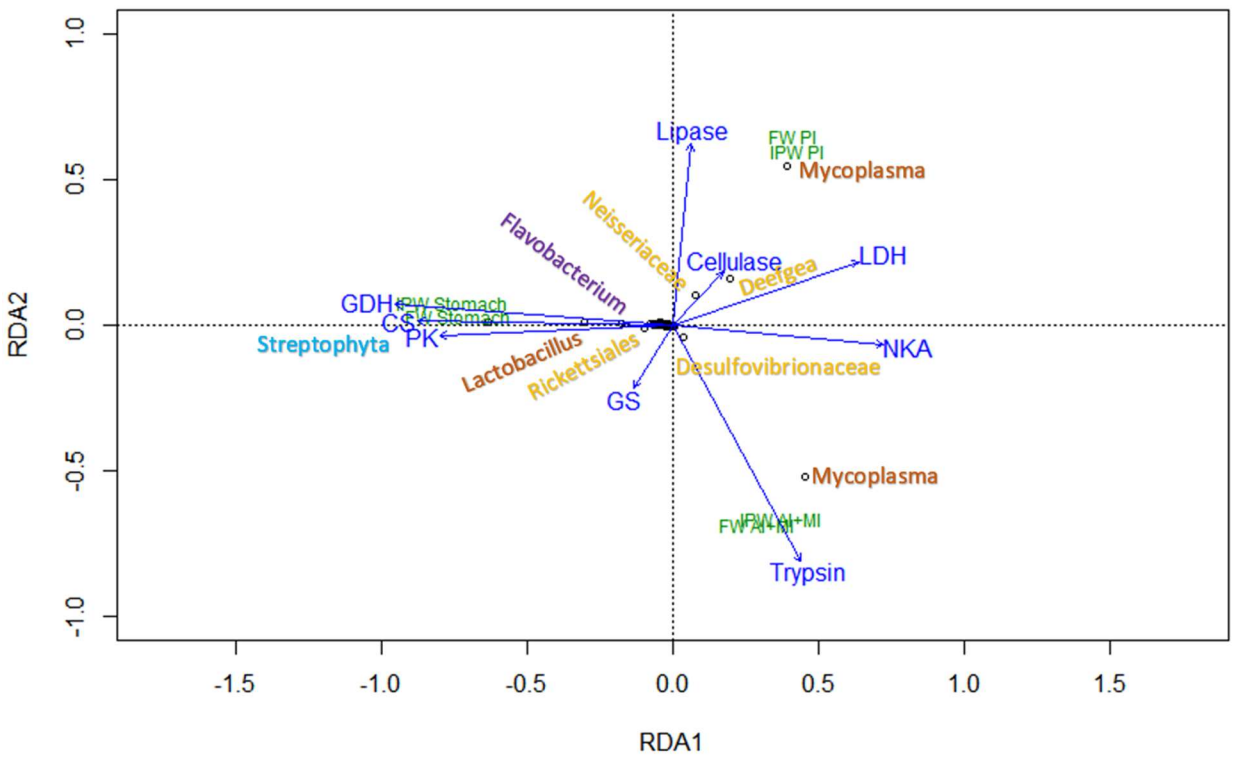

Figure 25. Multivariate RDA depicting the distinct separation and the correlation between the bacterial species abundance (represented by open circles) in the freshwater (FW) and 75% ion-poor water (IPW) stomach, AI (anterior), MI (middle) and PI (posterior intestine) zone samples (shown in green) and enzyme activities (shown in dark blue). NKA = sodium-potassium ATPase; LDH = lactate dehydrogenase; PK = pyruvate kinase; CS = citrate synthase; GDH = glutamate dehydrogenase; GS = glutamine synthetase. Bacterial taxa identities labelled near closest open circle: genus Lactobacillus and genus Mycoplasma (both of phylum Firmicutes shown in orange); order Streptophyta (of phylum Cyanobacteria shown in light blue); order Rickettsiales, genus family Neisseriaceae, order Desulfovibrionaceae and genus Deefgea (all of phylum Proteobacteria shown in yellow); genus Flavobacterium (of phylum Bacteroidetes shown in purple). Generated with R Studio.

Discussion

Using an ion-poor water experiment with rainbow trout, the effects of low salinity on the gut microbiome and zonation were explored to determine how metabolic and digestive processes respond to salinity challenge and how these differences indicate specialization to certain regions along the GIT. Freshwater and saltwater salinities have been reported to affect the bacterial populations (Luzopone and Knight 2007; Sullam et al. 2012), however it is not known if ion-poor water would impact the microbiome in a predictable manner. Additionally, the effect of ion-poor water on the diversity (richness and abundance) of bacterial communities along the GIT lumen was examined to see whether zonation patterns existed in the microbiome for the first time. It was expected that reducing the salinity of the surrounding water would greatly impact regions of the gut with low bacterial diversity, namely the posterior regions of the intestine because fewer taxa exist and thus changes to major taxa would be more evident in sections with less bacteria overall (Luzopone and Knight 2007). Furthermore, correlations with enzymatic activities were examined due to the newly established connection between the microbiome and enzymatic activities (Bairaigi et al. 2002; Turnbaugh et al. 2006; Francois et al. 2011; Liu et al. 2016; Nieuwdorp et al. 2016). I predicted to see corresponding alterations in enzyme activity as bacterial community structures were altered with ion-poor water.

9.1 Salinity and the gut microbiome

The bacterial diversity was highest in the stomach, followed by the PI and AI+MI samples, respectively as was hypothesized (Figure 3C, D; Figure 5). In the present study, decreased water salinity (IPW) conditions did not have a marked effect on the richness or abundance of the stomach, AI+MI and PI samples over the 2-week period. In the stomach, AI+MI and PI, the relative proportions of core gut bacteria remained mostly unchanged (Figure

3, Table 1). However, it appears decreased salinity slightly reduced the diversity of bacteria in the AI+MI and PI but not in the stomach in the Shannon plot (Figure 3C). Luzopone and Knight (2007) found that bacterial diversity decreased in non-saline environments when compared to saline environments which supports the results in the AI+MI and PI samples. The relative abundance of Tenericutes and Proteobacteria changed slightly with ion-poor water exposure in the AI+MI and PI samples. In the AI+MI samples the abundance increased from 2.11% to 6.09% and in the PI, it decreased from 25.7% to 13.7%. Tenericutes proportion in the AI+MI decreased from 97.0% to 93.8% and in the PI increased slightly from 74.2% to 86.3% (Figure 3, Table 1). Thus, the PI and to a lesser extent the AI+MI regions appeared to be more impacted by salinity challenge compared to the stomach as was hypothesized.

The ability of the gut to control the microbiome populations with salinity challenge has previously been explored. Schmidt et al. (2015) examined the gut microbiome of a euryhaline fish species with increased water salinity and monitored bacterial diversity in their water tanks. Fish core bacterial taxa are rare in the surrounding water environment and vice versa; in addition, gut bacterial abundance did not show any correlation in the abundance of corresponding bacteria in the water although the gut bacteria diversity was affected by changing salinity (Schmidt et al. 2015). They proposed that the bacterial community assembly in the gut was deterministic and not stochastic meaning that the host fish physiology affected the way bacterial taxa colonized and responding to external salinity changes more so than the direct effect of salinity on the gut. Unlike at higher water salinities, the physiological changes such as decreased drinking, reduced gill epithelial permeability to conserve ions in the fish host associated with lower salinities where ion availability is low internal hyperosmotic pressure is higher, may not produce a significant change in bacterial diversity in the GIT lumen (Chasiotis et al. 2011).

9.2 The effect of ion-poor water exposure on the stomach microbiome and enzyme activities

In the present study, the bacterial composition was more distinct in the stomach compared the intestinal samples as expected (Figure 5; Lesel and Peringer 1981; Bik et al. 2006). The IPW stomach had higher richness than the FW stomach (Figure 3A, C, D). The relative abundances of the core gut bacteria were not greatly impact with IPW treatment (Figure 3, Table 1). This was not expected as it has been previously shown that diversity decreases with reduced salinity likely due to reduced ion availability (Luzopone and Knight 2007). Regulatory mechanisms within the gut may maintain core gut bacteria abundances even when the fish is undergoing other physiological changes to reduced salinity challenge such as decreased epithelial permeability (Chasiotis et al. 2011). The stable core gut microbiome may serve to increase host survival when environmental water salinity is reduced, and the availability of dietary ions alone supplements the host's daily requirements for optimal function; dietary nutrient extraction by the microbiome and its contribution to host physiology can be maintained.

The stomach samples were highly and significantly correlated with CS, PK, GDH (significantly) and GS (significantly) activities; in addition, a variety of bacteria including *Streptophyta* of phylum Cyanobacteria, *Lactobacillus* of phylum Firmicutes, *Flavobacterium* of phylum Bacteroidetes and *Rickettsiales* of phylum Proteobacteria were all in high abundance (Figure 9A, B; Figure 8D, E, F; Figure 13). PK activity has previously been found to increase in the intestine with increased salinity. Jarvis and Ballantyne (2003) exposed junvenile shortnose sturgeon (*A. brevirostrum*) to 0‰ and 20‰ salinity and observed an increase in PK from 15.6±1.2 to 17.3±1.2 μmol $min^{-1}g^{-1}$ tissue in the intestine. The increased activity in PK may be associated with an increase in the activity of NKA at higher salinity as excess ions are pumped out of the organism (Bath and Eddy 1979; Flores and Shrimpton 2012). In addition, CS activity

increased by 1.1% in the gills of juvenile coho salmon (*Oncorhynchus kisutch)* over a one-day period and then remained consistent over a 13-day period; increased CS activity was also accompanied by increased NKA activity in the gills at higher salinities as metabolic demand increases (Shrimpton et al. 1994). High NKA activity requires high levels of ATP; increased cellular respiration through an increase in the activities PK and CS would serve to increase ATP production. However, maximal NKA activity was not associated with these regions indicating that there are other processes likely influencing the increased activities of these enzymes. *Lactobacillus* is involved in sugar fermentation and lactic acid production, a process which requires ATP, and decreases the permeability of the gut epithelia by inducing increased rigidity in tight junction proteins (Ratten et al. 1997; Lutgendorff et al. 2008; Sommer and Backhed 2013). This reduced permeability might serve to reduce the passive transport loss of ions from the body in IPW (Bath and Eddy 1979). GDH and GS activity might be significantly elevated in this region to facilitate cell volume regulation by the production of free amino acids as osmolytes and local detoxification of toxic ammonia, a by-product of protein digestion, in the stomach lumen (Figure 10D, E, F; Wicks and Randall 2002; Wright et al. 2007; Rubino et al. 2014).

As was mentioned in section 5.3, *Flavobacterium* have been associated with cold-water disease in rainbow trout (Madsen and Dalsgaard 1999; LaFrentz et al. 2003). Evidence suggests Proteobacteria such as *Rickettsiales* modulates the populations of other bacteria including pathogens (Snyder et al. 2002; Qi et al. 2009; Cao et al. 2012). It is possible that *Rickettsiales* may prevent *Flavobacterium* from proliferating in the gut and causing disease.

Streptophyta bacteria, associated with plant material, may have been ingested with the fish feed as was previously discussed in section 5.3. It may be possible that plant fermentation by

Bacteroidetes, which is in high abundance, may be occurring at a high rate in this region (Figure 3). However maximal cellulase activity was not associated with the stomach (Figure 13).

9.3 The effect of ion-poor water exposure on the anterior and middle intestine microbiome and enzyme activities

As mentioned earlier, the IPW treatment had a negligible effect on the bacterial diversity of the AI+MI region as the bacterial composition remained relatively unchanged. The intestinal samples were the least diverse in terms of bacterial compositions (Figure 3; Table 1; Figure 4; Figure 5). The AI+MI samples were composed primarily of Tenericutes bacteria (FW=97.01%; IPW=93.78%) with Proteobacteria being the second most abundance phyla (Table 1). Elevated Trypsin (significantly), GS (elevated, though not significant) and NKA (significantly) activity were highly associated with this region as was *Mycoplasma* (Firmicutes) and *Desulfovibrionaeceae* (Proteobacteria) to a lesser extent (Figure 11; Figure 10C; Figure 6D; Figure 13). Firmicutes/Tenericutes bacteria, which appear in high abundance in this region, are highly associated with protein digestion such as is facilitated through trypsin; increased GS activity may then be employed to detoxify ammonia produced through protein degradation (Semova et al. 2014; Carmody and Turnbaugh 2012; Wicks and Randall 2002; Wright et al. 2007; Rubino et al. 2014). NKA activity was not previously observed to be affected by IPW treatment which indicates that the observed increase is due to other factors; increased activity of NKA indicates either an increased transport of substances across the epithelia or ion-balance possibly linked to other physiological processes related to IPW adaptation (Flores and Shrimpton 2012; Jampol 1970; McCormick 1993).

9.4 The effect of ion-poor water exposure on the posterior intestine microbiome and enzyme activities

The PI region had the second most diverse region of the gut after the stomach but was more similar to the AI+MI region than the stomach (Figure 2; Table 1; Figure 3C; Figure 5). This region was slightly affected by the IPW treatment where the proportion of Tenericutes bacteria slightly increased and Proteobacteria decreased as was discussed in section 9.1 (Figure 2; Table 1). The PI region was highly associated with lipase and cellulase (although no significant differences were detected in the enzyme assays) as well as LDH activity as well as with *Mycoplasma* (Firmicutes), *Deefgea* (Proteobacteria) and *Neisseriaceae* (Proteobacteria). The high proportion of Firmicutes may be related to the increase in lipase and cellulase activity, enzymes which have previously been associated with this bacterial phylum (Semova et al. 2014; Carmody and Turnbaugh 2012; Li et al. 2015). *Mycoplasma* produce lactic and acetic acid; these bacteria have previously been associated with the microbiome of salmonids (Freundt and Razin 1958; Holben et al. 2002). *Deefgea* are closely related to *Neisseriaceae* and are known to oxidize and ferment glucose in the gut of fish (Jung and Jung-Schroers 2011). This carbohydrate degradation and production of lactic acid through anaerobic respiration may be related to the increased LDH activity observed in this region. The hypothesis that the PI region of the gut would be the most affected by salinity was incorrect as enzyme activity changed in different regions of the gut with IPW treatment.

9.5 Conclusions

Regionalized microbiome and enzyme activity were identified in the gut where the stomach had the most diverse bacterial composition followed by the PI and AI+MI. Although no changes were observed in the regional bacterial populations, changes in enzyme activity were identified along the GIT with the results of the enzyme assays indicating that IPW or natural fluctuations in GIT physiology affected the endogenous enzyme activity more so than that of the

bacteria. Most notably, NKA activity was found to be depressed after 2 weeks IPW water exposure in the MI (Figure 6E) which did not correspond to our hypothesis as NKA activity has previously been found to be unaffected by IPW treatment in the gills of rainbow trout (Flores and Shrimpton 2012). This perhaps host-driven change in activity and its region-specific change indicate that the bacteria are less important for function than zonation. In comparing the results of the gill in the Flores and Shrimpton (2012) study to the present findings, changes in enzyme activity and responses are also tissue specific. This region-specific activity was also not highly correlated with LDH and PK activity as previously found (Le Francois and Blier 2003; Le Francois et al. 2004). Overall, these enzyme data indicate that complex mechanisms along the GIT may be influenced by changes in gut physiology with IPW salinity challenge and that the microbiome can be controlled by the intestinal environment even when there are changes in the external environment (Schmidt et al. 2015). These findings also further emphasize the importance of considering zonation in the study of the GIT, as the zone-specific responses would otherwise be obscured if the GIT was considered as a whole.

Chapter 4: Comparison of gut microbiome and enzyme activity zonation responses to alterations in temperature and ion-poor water salinity challenge

10.1 Overview

Temperature and salinity have previously been found to separately affect both the microbiome and enzyme activity in the gut. Additionally, several studies have shown evidence for zonation regarding the microbiome as well as enzyme activity; however, few studies have provided a more comprehensive survey of the interplay between the microbiome and enzyme activity with respect to zonation. The objective of this thesis was to explore functional zonation by manipulating two external environmental factors, temperature and salinity, to observe zonation patterns in the bacterial communities, and corresponding digestive and metabolic enzyme activities in the GIT. Since temperature and salinity have been shown to affect the microbiome and enzyme activity, and morphological zonation has been established, it was hypothesized that there would be a region-specific response along the GIT zones with respect to temperature and salinity manipulation. The zonation patterns and responses to environmental manipulation investigated in the present study will contribute to our understanding of the complex role of the gut in fish physiology. Additionally, this research is beneficial to the aquaculture industry; knowledge of GIT microbiome and enzyme regional profiles can be used to formulate fish feed and optimize fish husbandry for increased growth and improved health. Finally, with climate change mean temperatures around the world are expected to increase by 1.8 in 4.0°C over the next 100 years (Solomon et al. 2007). Rising water temperatures will cause fish populations to migrate to habitats that are more conducive to their optimal thermal ranges which will also expose them to different habitats, diets and water salinities. Understanding the relationship between GIT bacteria, enzyme function and the potential impacts on fish physiology

can allow scientists and conservationists to create plans to mitigate the negative effects of these changes on fish populations worldwide.

For the first time, I have shown that zonation is more indicative of bacterial communities along the gut than environmental stressors such as temperature and salinity. I have also shown that temperature impacts the microbiome of all section of the gut more so than reduced salinity. My results also confirm previous observations of zonation in the microbiome and enzyme activity and provides specific correlations between bacteria species and enzyme activities. The evidence from my experiments suggest a synergistic relationship between the microbiome and enzyme activity.

10.2 Zonation patterns

Zonation of the bacterial communities along the gut is more supported than differences with temperature or salinity challenge. This was evident in the weighted bootstrap trees (which compared bacterial identity and abundances between samples) where the stomach, AI+MI and PI samples cluster more closely to one another regardless of environmental stressor (Figure 4 and Figure 16). Bacterial zonation patterns were evident in the control samples from both experiments indicating that the rainbow trout core gut microbiome is consistent. The core gut microbiome retained similar ratios in the control CW (6°-12°C), FW GIT zone samples from both the temperature and salinity experiments (Table 1, Figure 2 vs. Table 2, Figure 14). It can be postulated that morphological and/or histochemical differences in co-ordinance with other complex physiological mechanisms may control bacterial community assembly at each region.

The stomach was the most diverse region of the gut followed by the AI+MI and PI in the CW controls (Figure 3 vs. Figure 15). Firmicutes/Tenericutes comprised majority of the bacterial

community in the control stomachs followed by Proteobacteria and Bacteroidetes as this phylum was in the AI+MI and PI. CS and PK activity were weakly correlated with the control stomach in the temperature experiment but strongly correlated with the control stomach in the IPW experiment. These consistent correlations indicate the stomach likely has a significant number of aerobic bacteria utilizing these pathways for energy production (Lesel and Peringer 1981). Further study of other types of metabolic and digestive enzymes may elucidate specific connections between this metagenome and function (Bik et al. 2006).

Though the core bacterial phyla composition in the AI+MI regions were similar in both controls, different bacteria species were associated with the AI+MI samples in the two experiments (Figure 13 vs. Figure 25). Differences in the GIT bacterial communities of between individuals has previously been documented in fish and mammals (e.g. Ratten et al. 2017; Ley et al. 2006; Walker et al. 2011; Yan et al. 2012). These variations are thought to be due to host-specific gut conditions and health, random colonization in bacterial community assembly and competition between bacterial species (Schmidt et al. 2015). To further explore this phenomenon, an experiment in which the GIT bacterial communities of individuals in each treatment are explored would allow for the measurement of the degree of variation between individuals to determine whether differences in bacterial species impact enzyme activity and whether bacterial communities are significantly different between individuals and treatments. Maximal trypsin activity was highly correlated with the control AI+MI sample in both experiments while PK, CS and GDH activity were closely correlated with the AI+MI in the temperature experiment and NKA and GS were more closely related to the AI+MI the IPW experiment (Figure 13 vs. Figure 25). The bacterial community and activity profile here suggests protein digestion becomes more important in this region; high levels of Firmicutes, associated

with carnivorous diets, and trypsin activity as well as evidence of ammonia detoxification indicate this function.

Bacterial compositions were slightly different in the PI controls where the temperature control contained 88% Firmicutes/Tenericutes compared to 75% in the IPW control, Proteobacteria comprised 10% of the temperature control and 25% of the IPW control; Bacteroidetes comprised <1% of both samples (Table 1, Figure 2 vs. Table 2, Figure 14). Thus, between the AI+MI and PI regions, Firmicutes/Tenericutes populations are reduced and Proteobacteria elevated marking a distinct zonation in the intestinal microbiome. Cellulase activity was also correlated with this region in both experiments though more strongly in the IPW experiment indicating the PI's importance in cellulose degradation (Figure 13 vs. Figure 25). Elevated LDH and lipase activity were identified in the IPW control PI (Figure 25). Firmicutes/Tenericutes bacteria is likely contributing to this cellulase and lipase activity in this region and may be enhanced by Proteobacteria through some process of modulation. In contrast, the temperature control PI was also associated with maximal GDH activity indicating local ammonia detoxification in this region likely a by-product of protein digestion in the more anterior regions of the gut (Figure 25).

Overall, the stomach, AI+MI and PI regions in the controls exhibited distinct bacterial compositions and each section was associated with enzyme activity profile that was associated with certain types of digestive processes but not necessarily with any particular metabolic enzyme activity. Nutrient assimilation may be manipulated by altering the bacteria but altering the cellular responses and optimizing cellular metabolism (and by extension whole animal metabolism) may be targeted through host manipulation not bacterial influence.

10.3 Environmental stressors: Temperature and ion-poor water

Temperature had a more profound effect on the gut microbiome than IPW salinity challenge (Table 1, Figure 2 vs. Table 2, Figure 14). Fish exposed to environmental temperature fluctuations or seasonal temperature changes would have microbiomes and enzymatic activity that was more impacted than fish in freshwater environments experiencing transient changes in salinity. Based on the results of the temperature experiment, it seems that increased temperature increases digestive and metabolic processes in some regions of the gut such as trypsin, lipase, PK, and CS in the AI+MI and GDH in the PI. Although the bacterial composition was not greatly affected by IPW salinity challenge, a significant spike in the activity of enzymes such as NKA and CS were observed at 24-hour IPW exposure, however, these activities returned to FW treatment levels by 2-week IPW exposure (Figure 18B, Figure 21C). This suggests a perfect compensation response to IPW challenge in which acclimation occurs following metabolic adjustments to decreased water ion availability.

10.4 Exploring zonation and the effect of environmental stressors

Temperature most impacted the ratio of the core gut bacteria - particularly in the AI+MI but also in the PI. The increased bacterial evenness in the AI+MI with WW treatment was correlated with increased lipase activity (Figure 14, Figure 25). It appears that the AI+MI region may become specialized for increase lipase activity in WW fish potentially associated with the production of short-chain fatty acids (SCFA) used as an energy source for enterocytes (Lencki et al. 1998); this increased energy production is likely a result of increased metabolic processes associated with higher temperatures in organisms (Horn 1997; Clements and Raubenheimer 2005; Wilson and Castro 2010; Carrie and Schulte 2014). With climate change, elevated environmental temperature will increase the metabolic demand of individuals; lipase activity in the AI+MI region of the gut will become more important in order to provide the fish with energy

to maintain homeostasis. Increased Proteobacteria may also facilitate trypsin activity required for increased protein digestion in the AI+MI although trypsin activity was only associated with CW AI+MI in this experiment (Figure 25).

The PI became highly associated with NKA and LDH activity with WW treatment, while in the control FW PI of the IPW experiment, NKA and LDH association with this region persisted (Figure 13 vs. Figure 25). GS activity in the PI appears to become more important in the PI and is likely associated with increased local ammonia detoxification in the intestinal lumen following increased protein digestion in the more anterior portion of the intestinal region. It is noted that the activity of GDH, another enzyme highly associated with local ammonia detoxification in the gut lumen, is variably associated with the stomach and AI+MI regions in the controls from the temperature and IPW experiments (Figure 13 vs. Figure 25). This is perhaps due to a more complex mechanism of ammonia detoxification along the gut or perhaps the participation of GDH and GS in more complex processes related to the microbiome and native physiology of the gut. Nonetheless, the PI appears to be associated with increased cellulase activity regardless of treatment indicating its importance in plant digestion. Rainbow trout are carnivores and thus would not normally feed on plant material, the origin of this activity is likely due to enzymes in the commercial fish feed they were fed during the experiment. Thus, our hypothesis that temperature and salinity would affect the gut bacteria composition and enzyme activity along the GIT was partially supported; temperature seemed to be more impactful than decreased salinity.

Overall, the results of this study indicate the microbial zonation is present in along the GIT of the rainbow trout and that it is more affected by temperature than decreased salinity. Clear demarcations of digestive processes were observed in the AI+MI, which was associated

with protein and lipid digestion, and the PI, which appeared to be more associated with plant material digestion. The diversity of the stomach was correlated with varying activities of metabolic enzymes between the two experiments indicating the stomachs complex role in gut physiology. Metabolic physiology was variable across the gut regardless of treatment for the most part except with regards to the activities of CS, which shows maximal enzyme activity in the stomach, and GS, which was highly associated with PI. Thus, our hypothesis that functional zonation is present along the GIT of the rainbow trout is supported by the evidence of this investigation. Our research shows that there is incredible diversity along the GIT which may be missed if the GIT is considered as one whole organ. It is important to consider these differences in the study of the GIT, it's function and contribution to overall physiology.

Perspective and future directions

Fish are currently used in research of the microbiome because it is easy to manipulate and sample their external and internal microflora (Rawls et al. 2006; Lowrey 2014; Schmidt et al. 2015). The rainbow trout make an excellent model for studying the effects of environmental stressors like temperature and salinity due to their eurythermal and euryhaline nature. In other studies, comparisons of species adapted to more stable environments (i.e. stenothermal temperate vs. Antarctic fish or stenohaline marine versus freshwater fish) often results in comparisons of species across diets and taxonomies (Schmidt et al. 2015; e.g. Givens 2014, Sullam et al. 2012). These types of studies often neglect to consider species-specific differences in native bacterial community assembly and physiological adaptations of endogenous enzymes to the host in their comparisons of the effects of environmental stressors. Using a fish like the rainbow trout as a model organism allows for researchers to focus on examining the mechanisms underlying observed changes which would then serve to aid in understanding differences between species.

This novel study shows evidence for the contribution of the microbiome to functional zonation in the gut of the rainbow trout. Bacterial communities were identified to exhibit distinct compositions along the gut. Firmicutes, bacteria that are highly associated with carnivorous fish microbiomes, made up most of the bacterial composition in all sections studied though were found in slightly differing abundances in the stomach, AI+MI and PI. Accompanying these differences were varying levels of other types of core (Proteobacteria and Bacteroidetes) and non-core gut bacteria. Enzyme activity appeared to be influenced by the presence of certain bacterial taxa as bacterial phyla were indicative of the activity digestive enzymes in many cases though clear relationships between the bacteria and metabolic enzyme activity were not as distinguishable. Future studies could include a larger survey of enzyme activity profiles and other biochemical assays to identify the effects of bacterial populations on the gut lumen.

Some fish, such as Cyprinids which include goldfish, lack a morphological stomach (Junger et al. 1989). Microbiome characterization of their gut might reveal patterns which indicate stomach-like activity in digestion and absorption of dietary materials along the GIT. Thus, the microbiome can be used as a valuable tool for understanding functional zonation.

The stomach and intestine samples were analyzed in the enzyme assays and bacterial analysis as whole homogenates and the contributions of different cell types were not considered. Subsequent research should examine the individual contribution of cell types such as enterocytes, smooth muscle, and bacteria to regional function to determine which cell types are more influential and characterize GIT zones as well as the effect of environmental stress on different cell types. A future experiment could separate these cell types and assay their enzyme activity separately to see how each cell type responds to environmental stress and how these cell types might work cohesively to contribute to function.

This study focused primarily on determining key correlations between major bacterial taxa and enzyme activity. The next step would be determining causative relationships between bacteria and functional zonation in the GIT. One of the major challenges in the study of the mechanistic properties underlying the host and microbiome relationship is the fact that their interactions are incredibly complex and dynamic (Sun et al. 2014). Measuring enzyme activities and then inferring a contribution by the bacteria to the enzyme function based on previous data was a limitation to this study. Other studies have narrowed the scope of their study to one or few functions and designed their experiments to measure changes in host properties thought to be affected by certain bacteria. For example, Fei and Zhao (2013) explored causal relationships between bacteria which produced endotoxins and obesity and insulin resistance in mice by monitoring changes in the parameters such as permeability of the gut, serum endotoxin and inflammatory biomarkers with subcutaneous infusion of endotoxins previously purified from *E. coli*. In studies by Koeth et al. (2013) and Hartiala et al. (2014), *Bacteroidetes* in the GIT have been linked to atherosclerosis through the promotion of trimethylamine oxide, a proinflammatory agent, produced it its metabolism of dietary carnithine and phosphatidylcholine. Future studies can use the approaches in these studies and focus on the effects of bacteria on specific pathways that influence host physiology and health to develop a better understanding of causative relationships with the host.

Study of the gut microbiome is an exciting field of research and understanding how zonation in the microbiome influences host health is creating a change in thinking about gut physiology. In human health, the gut microbiome has been implicated in nutrition, neurobiology, cancer, immunology, and a variety of diseases (Shin et al. 2015; Distefano et al. 2015). Knowledge of the chemical associations between the microbiome and the gut in health and

disease have aided with our understanding of how drug therapies might exert clinical effects (Distefano et al. 2015). Further investigation of regional differences in these associations along the gut would benefit the development of targeted drug therapies for treatment of diseases and disorders.

References

Abaurrea-Equisoain MA, Ostos-Garrido MV. 1996. Cell types in the esophageal epithelium of *Anguilla anguilla* (Pisces, Teleostei). Cytochemical and ultrastructural characteristics. Micron. 27:419–429.

Aho E, Vornanen M. 2001. Cold acclimation increases basal heart rate but decreases its thermal tolerance in rainbow trout (*Oncorhynchus mykiss*). J. Comp. Physiol. B. 171:173–179. doi:10.1007/s003600000171.

Al-Hisnawi A, Ringo E, Davies SJ, Waines P, Bradley G, Merrifield DL. 2015. First report on the autochthonous gut microbiota of brown trout (*Salmo trutta Linnaeus*). Aquac. Res. 46:2962–2971. doi:10.1111/are.12451.

Backhed F, Ding H, Wang T, Hooper LV, Koh GY, Nagy A, Semenkovich CF, Gordon JI. 2004. The gut microbiota as an environmental factor that regulates fat storage. PNAS. 101:15718-15723.

Bairagi A, Ghosh KS, Kumar S, Ray AK. 2002. Enzyme producing bacterial flora isolated from fish digestive tracts. Aquaculture. 10: 109-121.

Baker GC, Smith JJ, Cowan DA. 2003. Review and re-analysis of domain-specific 16S primers. J. Microbiol. Methods 55:541–555.

Baker-Austin C, Stockley L, Rangdale R, Martinez-Urtaza J. 2010. Environmental occurrence and clinical impact of *Vibrio vulnificus* and *Vibrio parahaemolyticus*. 2:7–18. doi:10.1111/j.1758-2229.2009.00096.x.

Baldwin J. 1971. Adaptation of enzymes to temperature: acetylcholinesterases in the central nervous system of fishes. Comp. Biochem. Physiol. Part B Biochem. 40:181–187. doi:10.1016/0305-0491(71)90074-5.

Ballantyne JS. 2001. Amino acid metabolism. Fish Physiol. 20:77–107.

Bath RN, Eddy FB. 1979. Salt and water balance in rainbow trout (*Salmo gairdneri*) rapidly transferred from fresh water to sea water. J. Exp. Biol. 83:193–202.

Bauermeister AEM, Pirie BJS, Sargent JR. 1979. An electron microscopic study of lipid absorption in the pyloric caeca of rainbow trout (*Salmo gairdnerii*) fed wax ester—rich zooplankton. Cell Tissue Res. 200:475–486.

Belanger F, Blier PU, Dutil JD. 2002. Digestive capacity and compensatory growth in Atlantic cod (*Gadus morhua*). Fish Physiol. Biochem. 26:121–128. doi:10.1023/A:1025461108348.

Bik EM, Eckburg PB, Gill SR, Nelson KE, Purdom EA, Francois F, Perez-Perez G, Blaser MJ, Relman DA. 2006. Molecular analysis of the bacterial microbiota in the human stomach. Proc. Natl. Acad. Sci. U. S. A. 103:732–7. doi:10.1073/pnas.0506655103.

Blier PU, Lemieux H. 2001. The impact of the thermal sensitivity of cytochrome c oxidase on the respiration rate of Arctic charr red muscle mitochondria. J. Comp. Physiol. B Biochem. Syst. Environ. Physiol. 171:247–253.

Bogé G, Lopez L, Peres G. 1988. An in vivo study of the role of pyloric caeca in water absorption in rainbow trout (*Salmo gairdneri*). Comp. Biochem. Physiol. Part A Physiol. 91:9–13.

Bonga SEW, Van der Meij JCA. 1981. Effect of ambient osmolarity and calcium on prolactin cell activity and osmotic water permeability of the gills in the teleost *Sarotherodon mossambicus*. Gen. Comp. Endocrinol. 43:432–442.

Borlongan LG. 1990. Studies on the digestive lipases of milkfish, *Chanos chanos*. Aquaculture. 89(3-4): 315-325.

Britain G, Hochachka W. 1968. The effect of temperature on catalytic and regulatory functions of pyruvate kinases of the rainbow trout and the Antarctic fish *Trematomus bernacchii*. 110:395–400.

Bucking C, Edwards SL, Tickle P, Smith CP, McDonald MD, Walsh PJ. 2013. Immunohistochemical localization of urea and ammonia transporters in two confamilial fish species, the ureotelic gulf toadfish (*Opsanus beta*) and the ammoniotelic plainfin midshipman (*Porichthys notatus*). Cell Tissue Res. 352:623–637.

Bucking C, LeMoine CMR, Craig PM, Walsh PJ. 2013. Nitrogen metabolism of the intestine during digestion in a teleost fish, the plainfin midshipman (*Porichthys notatus*). J. Exp. Biol. 216:2821–32. doi:10.1242/jeb.081562.

Bucking C, Wood CM. 2012. Digestion of a single meal affects gene expression of ion and ammonia transporters and glutamine synthetase activity in the gastrointestinal tract of freshwater rainbow trout. 182:341–350. doi:10.1007/s00360-011-0622-y.

Buddington RK, Diamond JM. 1986. Aristotle revisited: the function of pyloric caeca in fish. Proc. Natl. Acad. Sci. U. S. A. 83:8012–8014. doi:10.1073/pnas.83.20.8012.

Bunik V, Atiukhov A, Aleshin V, Mkrtchyan G. 2016. Multiple forms of glutamate dehydrogenase in animals: structural determinants and physiological implications. Biology (Basel). 5:1–30. doi:10.3390/biology5040053.

Cao H, He S, Wang H, Hou S, Lu L, Yang X. 2012. Bdellovibrios, potential biocontrol bacteria against pathogenic *Aeromonas hydrophila*. Vet. Microbiol. 154:413–418. doi:10.1016/j.vetmic.2011.07.032.

Caporaso JG, Bittinger K, Bushman FD, DeSantis TZ, Andersen GL, Knight R. 2009. PyNAST: a flexible tool for aligning sequences to a template alignment. Bioinformatics 26:266–267.

Caporaso JG, Kuczynski J, Stombaugh J, Bittinger K, Bushman FD, Costello EK, Fierer N, Peña AG, Goodrich K, Gordon JI, et al. 2010. QIIME allows analysis of high-throughput community sequencing data. Nat. Methods 7:335–336. doi:10.1038/nmeth.f.303.QIIME

Caporaso JG, Lauber CL, Walters WA, Berg-Lyons D, Lozupone CA, Turnbaugh PJ, Fierer N, Knight R. 2011. Global patterns of 16S rRNA diversity at a depth of millions of sequences per sample. Proc. Natl. Acad. Sci. 108:4516–4522. doi:10.1073/pnas.1000080107.

Carmody RN, Turnbaugh PJ. 2012. Previews gut microbes make for fattier fish. Cell Host Microbe 12:259–261. doi:10.1016/j.chom.2012.08.006.

Chamberlin ME, Glemet HC, Ballantyne JS. 1991. Glutamine metabolism in a holostean (*Amia calva*) and teleost fish (*Salvelinus namaycush*). Am. J. Physiol. 260:R159–R166.

Ciardiello MA, Camardella L, Carratore V, di Prisco G. 2000. l-Glutamate dehydrogenase from the Antarctic fish *Chaenocephalus aceratus*. Biochim. Biophys. Acta - Protein Struct. Mol. Enzymol. 1543:11–23. doi:10.1016/S0167-4838(00)00186-2.

Clark TD, Jeffries KM, Hinch SG, Farrell AP. 2011. Exceptional aerobic scope and cardiovascular performance of pink salmon (*Oncorhynchus gorbuscha*) may underlie resilience in a warming climate. J. Exp. Biol. 214:3074–3081.

Clements KD, Raubenheimer D. 2005. Feeding and nutrition. In: Evans DH, Claiborne JB, editors. The Physiology of Fishes. 3rd ed. Boca Raton: CRC Press. p. 47–82.

Coppes ZL, Somero GN. 1990. Temperature-adaptive differences between the M4 lactate dehydrogenases of stenothermal and eurythermal sciaenid fishes. J. Exp. Zool. 254:127–131. doi:10.1002/jez.1402540203.

Corbitt NM. 2011. The gut microbiota and the liver: collaborators in host immunity and metabolism [dissertation]. University of Pittsburgh. 133 p.

Crockett E, Sidell B. 1990. Some of energy some metabolism are pathways in Antarctic cold fishes adapted. Physiol. Zool. 63: 472-488.

Crowder III AL, Barker R, Swenson CA. 1973. Ultraviolet difference spectroscopic studies of the binding of ligands to rabbit muscle aldolase. Biochemistry 12:2078–2083.

Currie S, Schulte PM. 2014. Thermal stress. In: Evans DH, Claiborne JB, editors. The Physiology of Fishes. 4th ed. Boca Raton: CRC Press. p. 257–287.

Davison IR, Davison JO. 1987. The effect of growth temperature on enzyme activities in the brown alga *Laminaria saccharina*. Brit Phycol J. 22:77-87. doi:10.1080/00071618700650101.

De Silva S, Anderson T. 1994. Fish Nutrition in Aquaculture. Vol. 1. Aquaculture Series. Springer Netherlands.

Denison R, and Koehn DA. 1977. Cellulase activity of *Poronia oedipus*. Mycologia 69: 592-603.

DePaola A, Kaysner CA, Bowers J, Cook DW. 2000. Environmental investigations of *Vibrio parahaemolyticus* in oysters after outbreaks in Washington, Texas, and New York (1997 and 1998). Appl. Environ. Microbiol. 66:4649–4654.

Derrien M, van Passel MWJ, van de Bovenkamp JHB, Schipper R, de Vos W, Dekker J. 2010. Mucin-bacterial interactions in the human oral cavity and digestive tract. 1: 254-268. doi:10.4161/gmic.1.4.12778.

Distefano MD. 2015. NIH Public Access. 17: 213–223. doi:10.1007/978-1-62703-673-3.

Dutil J, Jabouin C, Larocque R, Desrosiers G, Blier PU. 2008. Atlantic cod (*Gadus morhua*) from cold and warm environments differ in their maximum growth capacity at low temperatures. 2591:2579–2591. doi:10.1139/F08-159.

Eddy F. 1975. The effect of calcium on gill potentials and on sodium and chloride fluxes in the goldfish, *Carassius auratus*. J. Comp. Physiol. B Biochem. Syst. Environ. Physiol. 96:131–142.

Edgar RC, Haas BJ, Clemente JC, Quince C, Knight R. 2011. UCHIME improves sensitivity and speed of chimera detection. Bioinformatics 27:2194–2200. doi:10.1093/bioinformatics/btr381.

Edgar RC. 2010. Search and clustering orders of magnitude faster than BLAST. Bioinformatics 26:2460–2461. doi:10.1093/bioinformatics/btq461.

Elliott T. 2003. Metabolic zonation in teleost gastrointestinal tract: effect of fasting and cortisol in tilapia metabolic zonation in teleost gastrointestinal tract. 175: 409-418. doi:10.1007/s00360-003-0349-5.

Ellis LM, Bloomfield Victor A, Woodward CK. 1975. Hydrogen-tritium exchange kinetics of soybean trypsin inhibitor (Kunitz). Solvent accessibility in the folded conformation. Biochemistry 14:3413–3419.

Esteve C. 1995. Numerical taxonomy of Aeromonadaceae and Vibrionaceae associated with reared fish and surrounding fresh and brackish water. Syst. Appl. Microbiol. 18:391–402. doi:10.1016/S0723-2020(11)80432-7.

Ezeasor DN, Stokoe WM. 1980. Scanning electron microscopic study of the gut mucosa of the rainbow trout *Salmo gairdneri Richardson*. J. Fish Biol. 17:529–539.

Falcon LI, Magallon S, Castillo A. 2010. Dating the cyanobacterial ancestor of the chloroplast. ISME J. 4:777–783. doi:10.1038/ismej.2010.2.

Fange R, Grove D. 1979. Digestion. In: Hoar WS, Randall DJ, Brett JR, editors. Fish Physiology, Volume 8. United Kingdom: Academic Press Inc. p. 162–241.

FAO (Food and Agriculture Organization of the United Nations). 2016. The state of world fisheries and aquaculture 2016. Contributing to food security and nutrition for all. Rome. p. 200.

Farkas J, Christian P, Gallego-Urrea JA, Roos N, Hassellöv M, Tollefsen KE, Thomas K V. 2011. Uptake and effects of manufactured silver nanoparticles in rainbow trout (*Oncorhynchus mykiss*) gill cells. Aquat. Toxicol. 101:117–25. doi:10.1016/j.aquatox.2010.09.010. [accessed 2015 Oct 26]. http://www.sciencedirect.com/science/article/pii/S0166445X10003772.

Fei N, and Zhao L. 2013. An opportunistic pathogen isolated from the gut of an obese human causes obesity in germfree mice. ISME. 7: 880-884.

Flores AM, Mark Shrimpton J. 2012. Differential physiological and endocrine responses of rainbow trout, Oncorhynchus mykiss, transferred from fresh water to ion-poor or salt water. Gen. Comp. Endocrinol. 175: 244–250. doi:10.1016/j.ygcen.2011.11.002.

Freundt E, Razin S. 1958. Genus Mycoplasma. In: Krieg N, Holt J, editors. Bergey's manual of systematic bacteriology. Baltimore: Williams and Wilkins. p. 742–770.

Fuentes J, Soengas JL, Rey P, Rebolledo E. 1997. Progressive transfer to seawater enhances intestinal and branchial Na+-K+-ATPase activity in non-anadromous rainbow trout. Aquac. Int. 5:217–227. doi:10.1023/A:1018387317893.

Furne M, Sanz A. 2005. Digestive enzyme activities in Adriatic sturgeon *Acipenser naccarii* and rainbow trout *Oncorhynchus mykiss*. A comparative study. Aquaculture. 250:391–398. doi:10.1016/j.aquaculture.2005.05.017.(Farkas et al. 2011)c

Galloway BJ, Kieffer JD. 2003. The effects of an acute temperature change on the metabolic recovery from exhaustive exercise in juvenile Atlantic salmon (*Salmo salar*). Physiol. Biochem. Zool. 76:652–662.

German DP, Nagle BC, Villeda JM, Ruiz AM, Thomson AW, Balderas SC, Evans DH. 2010. Evolution of herbivory in a carnivorous clade of minnows (Teleostei: Cyprinidae): effects on gut size and digestive physiology. Physiol. Biochem. Zool. 83:0–0. doi:10.1086/648510.

German DP, Neuberger DT, Callahan MN, Lizardo NR, Evans DH. 2010. Feast to famine: The effects of food quality and quantity on the gut structure and function of a detritivorous catfish (Teleostei: Loricariidae). Comp. Biochem. Physiol. - A Mol. Integr. Physiol. 155:281–293. doi:10.1016/j.cbpa.2009.10.018.

Givens CE. 2014. A fish tale: comparison of the gut microbiome of 15 fish species and the influence of diet and temperature on its composition [dissertation]. University of Georgia. p. 229.

Guderley H, Leroy PH. 2001. Thermal acclimation, growth, and burst swimming of threespine stickleback: enzymatic correlates and influence of photoperiod. Physiol. Biochem. Zool. 74:66–74.

Haider, D, Sauer G. 1977. Enzyme activities in the serum of rainbow trout, *Salmo gairdneri Richardson;* the effects of water temperature. J Fish. Biol. 11:605–612.

Harder W. 1975. Anatomy of fishes, part I: text. Ed. Stuttgart, Schweizerbartsche Verlagsbuchhandlung. Germany: Publikations-Service. p. 128-180.

Hartiala J, Bennett B, Tang W, et al. 2014. Comparative genome-wide association studies in mice and humans for trimethylamine N-Oxide, a proatherogenic metabolite of choline and L-carnitine. Arterioscler. Thromb. Vasc. Biol. 34: 1307-1313.

Hazel JR, Prosser CL. 1974. Molecular mechanisms of temperature compensation in poikilotherms. Physiol. Rev. 54:620–677.

Holben W, Williams P, Saarinen M, Sarkilahti L, Apajalahti J. 2002. Phylogenetic analysis of intestinal microflora indicates a novel mycoplasma phylotype in farmed and wild salmon. Microb. Ecol. 44:175–185. doi:10.1007/s00248-002-1011-6.

Horn MH. 1997. Feeding and digestion. In: Evans DH, Claiborne JB, editors. The physiology of fishes. 2nd ed. Boca Raton: CRC Press. p. 43–63.

Huber I, Spanggaard B, Appel KF, Rossen L, Nielsen T, Gram L. 2004. Phylogenetic analysis and in situ identification of the intestinal microbial community of rainbow trout (*Oncorhynchus mykiss, Walbaum*). J. Appl. Microbiol. 96:117–132.

Humbert W, Kirsch R, Meister MF. 1984. Scanning electron microscopic study of the oesophageal mucous layer in the eel, *Anguilla anguilla L*. J. Fish Biol. 25:117–122. doi:10.1111/j.1095-8649.1984.tb04856.x.

Iwai T. 1968. Fine structure and absorption patterns of intestinal epithelial cells in rainbow trout alevins. Cell. Tissue. Res. 91:366–379. doi:10.1007/BF00440764.

Jarvis PL, Ballantyne JS. 2003. Metabolic responses to salinity acclimation in juvenile shortnose sturgeon *Acipenser brevirostrum*. Aquaculture. 219:891–909. doi:10.1016/S0044-8486(03)00063-2.

Jung A, Jung-Schroers V. 2011. Detection of *Deefgea chitinilytica* in freshwater ornamental fish. Lett. Appl. Microbiol. 52:497–500. doi:10.1111/j.1472-765X.2011.03030.x.

Kapoor BG, Smit H, Verighina IA. 1976. The alimentary canal and digestion in teleosts. Adv. Mar. Biol. 13:109–239.

Karlsson A, Eliason EJ, Mydland LT, Farrell AP, Kiessling A. 2006. Postprandial changes in plasma free amino acid levels obtained simultaneously from the hepatic portal vein and the dorsal aorta in rainbow trout (*Oncorhynchus mykiss*). J. Exp. Biol. 209:4885–4894.

Keen AN, Gamperl AK. 2012. Blood oxygenation and cardiorespiratory function in steelhead trout (*Oncorhynchus mykiss*) challenged with an acute temperature increase and zatebradine-induced bradycardia. J. Therm. Biol. 37:201–210.

Kelly B, O'Neill LA. 2015. Metabolic reprogramming in macrophages and dendritic cells in innate immunity. Cell Res. 25:771–784. doi:10.1038/cr.2015.68.

Kessel MAHJ Van, Dutilh BE, Neveling K, Kwint MP, Veltman JA, Flik G, Jetten MSM, Klaren PHM, Jm H, Camp O Den. 2011. Pyrosequencing of 16S rRNA gene amplicons to study the microbiota in the gastrointestinal tract of carp (*Cyprinus carpio L.*). 1:1–9.

Khoruts A, Dicksved J, Jansson JK, Sadowsky MJ. 2010. Changes in the composition of the human fecal microbiome after bacteriotherapy for recurrent *Clostridium difficile*-associated diarrhea. J. Clin. Gastroenterol. 44:354–360.

Kieffer JD, Wakefield AM. 2009. Oxygen consumption, ammonia excretion and protein use in response to thermal changes in juvenile Atlantic salmon *Salmo salar*. J. Fish Biol. 74:591–603.

Kim D, Brunt J, Austin B. 2007. Microbial diversity of intestinal contents and mucus in rainbow trout (*Oncorhynchus mykiss*). 102:1654–1664. doi:10.1111/j.1365-2672.2006.03185.x.

Koeth R, Wang Z, Levison B, et al. 2013. Intestinal microbiota metabolism of L-carnitine, a nutrient in red meat, promotes atherosclerosis. Nat. Med. 19: 576-585.

Koshland BDE, Neet KE. 1968. The catalytic and regulatory properties of enzymes. Annu Rev Biochem. 37: 359-411.

Kristjbnsson MM. 1991. Purification and characterization of trypsin from the pyloric caeca of rainbow trout (*Oncorhynchus mykiss*). J Agr. Food. Chem. 1738–1742.

Kuczynski J, Stombaugh J, Anton Walters W, Gonzalez A, Caporaso G, Knight R. 2012. Using QIIME to analyze 16S rRNA gene sequences from microbial communities. Curr. Protoc. Microbiol. 1–30. doi:10.1002/9780471729259.mc01e05s27.Using.

Kultz D. 2015. Review: Physiological mechanisms used by fish to cope with salinity stress. J. Exp. Biol. 218:1907–14. doi:10.1242/jeb.118695..

Kwong R, Kumai Y, Perry S. 2013. Evidence for a role of tight junctions in regulating sodium permeability in zebrafish (*Danio rerio*) acclimated to ion-poor water. J. Comp. Physiol. B Biochem. Syst. Environ. Physiol. 183:203–213. doi:10.1007/s00360-012-0700-9.

LaFrentz B, LaPatra S. 2003. Passive immunization of rainbow trout, *Oncorhynchus mykiss* (Walbaum), against Flavobacterium psychrophilum, the causative agent of bacterial coldwater disease. Fish Dis. 26:377–384. doi:10.1046/j.1365-2761.2003.00468.x.

Langdon JS, Thorpe JE. 1985. The ontogeny of smoltification: developmental patterns of gill Na^+ K^+-ATPase, SDH, and chloride cells in juvenile Atlantic salmon, *Salmo salar L*. Aquaculture 45:83–95.

Lauff M, Hofer R. 1984. Proteolytic enzymes in fish development importance of dietary enzymes and the importance of dietary enzymes. 37:335–346

Le Francois NR, Blier PU. 2003. The early ontogeny of digestive and metabolic enzyme activities in two commercial strains of Arctic charr (*Salvelinus alpinus L*.). J. Exp. Zool. Part A Ecol. Genet. Physiol. 299:151–160.

Le Francois NR, Lamarre SG, Blier PU. 2004. Tolerance, growth and haloplasticity of the Atlantic wolffish (*Anarhichas lupus*) exposed to various salinities. Aquaculture 236: 659–675. doi:10.1016/j.aquaculture.2004.02.021.

Lencki RW, Smink N, Snelting H, Arul J. 1998. Increasing short-chain fatty acid yield during lipase hydrolysis of a butterfat fraction with periodic aqueous extraction. J. Am. Oil Chem. Soc. 75:1195–1200. doi:10.1007/s11746-998-0311-5.

Lesel R, Fromageot C, M L. 1986. Cellulose digestibility in grass carp, *Ctenopharyngodon idella* and in goldfish, *Carassius auratus*. Aquaculture. 54:11–17.

Lesel R, Peringer P. 1981. Influence of temperature on the bacterial microflora in *Salmo gairdneri Richardson*. Archiv. fur. hydrobiologie. 93: 109-120.

Lesel R. 1991. Does a digestive active bacterial flora exist in fish? Colloq. l'INRA (France).

Ley RE, Hamady M, Lozupone C, Turnbaugh PJ, Ramey RR, Bircher JS, Schlegel ML, Tucker TA, Schrenzel MD, Knight R, et al. 2008. Evolution of mammals and their gut microbes. 320: 1647-1651.

Li T, Long M, Gatesoupe F. 2015. Comparative analysis of the intestinal bacterial communities in different species of carp by pyrosequencing. Microb. Ecol. 69:25–36. doi:10.1007/s00248-014-0480-8.

Licht P. 1967. Thermal adaptation in the enzymes of lizards in relation to preferred body temperatures. Mol. Mech. Temp. Adapt. Am. Assoc. Adv. Sci. Washington, DC. p. 131–145.

Liu H, Guo X, Gooneratne R, Lai R, Zeng C, Zhan F. 2016. The gut microbiome and degradation enzyme activity of wild freshwater fishes influenced by their trophic levels. Nat. Publ. Gr.:1–12. doi:10.1038/srep24340.

Locasale JW, Cantley LC. 2011. Metabolic flux and the regulation of mammalian cell growth. Cell Metab. 14:443–451. doi:10.1016/j.cmet.2011.07.014

Low PS, Somero GN. 1976. Adaptation of muscle pyruvate kinases to environmental temperatures and pressures. J. Exp. Zool. 198:1–11. doi:10.1002/jez.1401980102.

Lowrey LT. 2014. The microbiome of rainbow trout (*Oncorhynchus mykiss*) [thesis]. The University of New Mexico. p. 80.

Lozupone CA, Knight R. 2007. Global patterns in bacterial diversity. P Natl. Acad. Sci. 104:11436-11440.

Lutgendorff F, Akkermans L, Soderholm JD. 2008. The role of microbiota and probiotics in stress-induced gastrointestinal damage. Curr. Mol. Med. 8:282–298.

Macpherson AJ, Harris NL. 2004. Interactions between commensal intestinal bacteria and the immune system. Nat Rev Immunol 4:478–485.

Madsen L, Dalsgaard I. 1999. Reproducible methods for experimental infection with *Flavobacterium psychrophilum* in rainbow trout *Oncorhynchus mykiss*. Dis. Aquat. Organ. 36:169–176. doi:10.3354/dao036169.

Maetz J. 1974. Aspects of adaptation to hypo-osmotic and hyper-osmotic environments. Biochem. Biophys. Perspect. Mar. Biol. 1:1–167.

Magasanik B. 1977. Regulation of bacterial nitrogen assimilation by glutamine synthetase. Trends Biochem. Sci. 2:9–12.

McCormick S. 1993. Methods for nonlethal gill biopsy and measurement of Na^+-K^+-ATPase activity. Can. J Fish. Aquat. Sci. 50: 656-658.

McCormick SD, Saunders RL, MacIntyre AD. 1989. The effect of salinity and ration level on growth rate and conversion efficiency of Atlantic salmon (*Salmo salar*) smolts. Aquaculture 82:173–180.

McDonald D, Rogano M. 1986. Ion regulation by the rainbow trout, *Salmo gairdneri*, in ion-poor water. Physiol. Zool. 59:318–331.

Mcfall-Ngai MJ. 1998. The development of cooperative associations between animals and bacteria: establishing détente among domains. Oxford University Press. 38: 593–608.

Metz JR, Burg EH Van Den, Bonga SEW, Flik G. 2003. Regulation of branchial Na^+/ K^+-ATPase in common carp *Cyprinus carpio L*. acclimated to different temperatures. 206:2273–2280. doi:10.1242/jeb.00421.

Mommsen TP, Busby ER, Von Schalburg KR, Evans JC, Osachoff HL, Elliott ME. 2003b. Glutamine synthetase in tilapia gastrointestinal tract: zonation, cDNA and induction by cortisol. J. Comp. Physiol. B Biochem. Syst. Environ. Physiol. 173:419–427. doi:10.1007/s00360-003-0350-z.

Mommsen TP, Osachoff HL, Elliott ME. 2003a. Metabolic zonation in teleost gastrointestinal tract. J. Comp. Physiol. B Biochem. Syst. Environ. Physiol. 173:409–418. doi:10.1007/s00360-003-0349-5.

Murai T, Ogata H, Hirasawa Y, Akiyama T, Nose T. 1987. Portal absorption and hepatic uptake of amino acids in rainbow trout [*Onchorhynchus masou*] force-fed complete diets containing casein or crystalline amino acids. Bull. Japanese Soc. Sci. Fish. 53: 1847-1859. (Uematsu et al. 1992)

Murray AL, Pascho RJ, Alcorn SW, Fairgrieve WT, Shearer KD, Roley D. 2003. Effects of various feed supplements containing fish protein hydrolysate or fish processing by-products on the innate immune functions of juvenile coho salmon (*Oncorhynchus kisutch*). Aquaculture 220: 643–653.

Mutchmor J. 1967. Temperature adaptation in insects. In: Prosser C, editor. Molecular Mechanisms of Temperature Adaptation. AAAS Publications. p. 165–176.

Navarrete P, Magne F, Mardones P, Riveros M, Opazo R, Suau A, Pochart P, Romero J. 2009. Molecular analysis of intestinal microbiota of rainbow trout (*Oncorhynchus mykiss*). FEMS Microbiol. Ecol. 71:148–156.

Nayak SK. 2010. Role of gastrointestinal microbiota in fish. Aquacult. Res. 41:1553–1573. doi:10.1111/j.1365-2109.2010.02546.x.

Noaillac-Depeyre J, Gas N. 1976. Electron microscopic study on gut epithelium of the tench (*Tinca tinca L*.) with respect to its absorptive functions. Tissue cell. 8:511–530.

Oduleye SO. 1975. The effects of calcium on water balance of the brown trout *Salmo trutta. J*. Exp. Biol. 63:343–356.

Ogasawara T, Hirano T. 1984. Changes in osmotic water permeability of the eel gills during seawater and freshwater adaptation. J. Comp. Physiol. B Biochem. Syst. Environ. Physiol. 154:3–11.

Ogawa T. 1975. Thermal influence on palmer swearing and mental influence on generalized sweating in man. Jpn. J. Physiol. 25:525–536. doi:10.2170/jjphysiol.25.525.

Oksanen J, Blanchet FG, Friendly M, Kindt R, Legendre P, Mcglinn D, Minchin PR, O'Hara RB, Simpson GL, Solymos P. 2015. Vegan: Community Ecology Package. R Packag. version 2.3-2: https://CRAN.R-project.org/package=vegan.

Olsen RE, Ringø E. 1997. Lipid digestibility in fish: a review. Recent Res. Dev. Lipid Res 1:199–265.

Owen TG, Wiggs AJ. 1971. Thermal compensation in the stomach of the brook trout (*Salvelinus fontinalis Mitchill*). Comp. Biochem. Physiol. - Part B Biochem. 40:465–473. doi:10.1016/0305-0491(71)90231-8.

Ozernyuk ND, Klyachko OS, Polosukhina S. 1994. Acclimation temperature affects the functional and structural properties of lactate dehydrogenase from fish (*Misgurnus fossilis*) skeletal muscles. 107:141–145.

Paola ADE, Kaysner CA, Bowers J, Cook DW, Ray B, Wiles K, DePaola A, Cook D, Kaysner C, Puhr N. 2000. Environmental investigations of *Vibrio parahaemolyticus* in oysters after outbreaks in Washington, Texas, and New York (1997 and 1998). Appl. Environ. Microb. 66: 4649–4654.

Peh WYX, Chew SF, Ching BY, Loong AM, Ip YK. 2010. Roles of intestinal glutamate dehydrogenase and glutamine synthetase in environmental ammonia detoxification in the euryhaline four-eyed sleeper, *Bostrychus sinensis*. Aquat. Toxicol. 98: 91–98. doi:10.1016/j.aquatox.2010.01.018.

Perez T, Balcazar JL, Halaihel N, Vendrell D, Blas I De, Jl M. 2010. Host – microbiota interactions within the fish intestinal ecosystem. Mucosal Immunol. 1–6. doi:10.1038/mi.2010.12.

Perry SF, Walsh PJ. 1989. Metabolism of isolated fish gill cells: contribution of epithelial chloride cells. J. Exp. Biol. 144:507–520.

Potts WTW, Fleming WR. 1970. The effects of prolactin and divalent ions on the permeability to water of *Fundulus kansae*. J. Exp. Biol. 53:317–327.

Precht H. 1958. Concepts of temperature adaptation of unchanging reaction systems of cold-blooded animals. Physiol. Adapt. 50–78.

Price MN, Dehal PS, Arkin AP. 2009. Fasttree: Computing large minimum evolution trees with profiles instead of a distance matrix. Mol. Biol. Evol. 26:1641–1650. doi:10.1093/molbev/msp077.

Prosser CL. 1969. Principles and general concepts of adaptation. Environ. Res. 2:404–416.

Qi Z, Zhang X-H, Boon N, Bossier P. 2009. Probiotics in aquaculture of China—current state, problems, and prospect. Aquaculture. 290:15–21.

Rachman MA, Furutani Y, Nakashimada Y, Kakizono T, Nishio N. 1997. Enhanced hydrogen production in altered mixed acid fermentation of glucose by *Enterobacter aerogenes*. J. Ferment. Bioeng. 83: 358–363. doi:10.1016/S0922-338X(97)80142-0.

Randall D, Burggren WW, French K, and Eckert R. 2002. Eckert animal physiology. MacMillan: New York.

Rasmussen RA, Rasmussen LE. 1967. Some observations on the protein and enzyme levels and fractions in normal and stressed elasmobranchs. Trans. N. Y. Acad. Sci. 29:397–413.

Ratten J, Beyer M, Hasler M, Laroche J, Schulz C. 2017. The malleable gut microbiome of juvenile rainbow trout (*Oncorhynchus mykiss*): diet-dependent shifts of bacterial community structures. PLoS One. 12:1–21.

Ray A, Ghosh K, Ringo E. 2012. Enzyme-producing bacteria isolated from fish gut: a review. Aquac. Nutr. 18. doi:10.1111/j.1365-2095.2012.00943.x.

Read KRH. 1967. Thermostability of proteins in poikilotherms. In: Prosser CL, editor. Molecular Mechanisms of Temperature Adaptation. AAAS Publications. p. 93-106.

Refstie S, Sahlström S, Bråthen E, Baeverfjord G, Krogedal P. 2005. Lactic acid fermentation eliminates indigestible carbohydrates and antinutritional factors in soybean meal for Atlantic salmon (*Salmo salar*). Aquaculture. 246:331–345. doi:10.1016/j.aquaculture.2005.01.001.

Rodnick KJ, Gamperl AK, Lizars KR, Bennett MT, Rausch RN, Keeley ER. 2004. Thermal tolerance and metabolic physiology among redband trout populations in south-eastern Oregon. J. Fish Biol. 64:310–335.

Rombout J, Lamers CHJ, Helfrich MH, Dekker A, Taverne-Thiele JJ. 1985. Uptake and transport of intact macromolecules in the intestinal epithelium of carp (*Cyprinus carpio L.*) and the possible immunological implications. Cell Tissue Res. 239:519–530.

Rubino JG, Zimmer AM, Wood CM. 2014. An in vitro analysis of intestinal ammonia handling in fasted and fed freshwater rainbow trout (*Oncorhynchus mykiss*). 184:91–105. doi:10.1007/s00360-013-0781-0.

Saha S, Roy R, Sen S, and Ray AK. 2006. Characterization of cellulase-producing bacteria from the digestive tract of tilapia, *Oreochromis mossambica* (Peters) and grass carp, *Ctenopharyngodon idella* (Valenciennes). Aquacult. Res. 37: 380-388.

Schmidt VT, Smith KF, Melvin DW, Amaral-Zettler LA. 2015. Community assembly of a euryhaline fish microbiome during salinity acclimation. Mol. Ecol. 24:2537–2550. doi:10.1111/mec.13177.

Schulte PM, Healy TM, Fangue NA. 2011. Thermal performance curves, phenotypic plasticity, and the time scales of temperature exposure. Integr. Comp. Biol. 51:691–702.

Scott GR, Schulte PM, Wood CM. 2006. Plasticity of osmoregulatory function in the killifish intestine: drinking rates, salt and water transport, and gene expression after freshwater transfer. J. Exp. Biol. 209:4040–4050. doi:10.1242/jeb.02462.

Seebacher F, Brand MD, Else PL, Guderley H, Hulbert AJ, Moyes CD. 2010. Plasticity of oxidative metabolism in variable climates: molecular mechanisms. Physiol. Biochem. Zool. 83:721–732.

Sekirov I, Russell SL, Antunes LCM, Finlay BB. 2010. Gut microbiota in health and disease. Physiol. Rev. 90:859–904. doi:10.1152/physrev.00045.2009.

Semova I, Carten JD, Stombaugh J, Mackey LC, Knight R, Farber SA. 2012. Article microbiota regulate intestinal absorption and metabolism of fatty acids in the zebrafish. Cell Host Microbe 12:277–288. doi:10.1016/j.chom.2012.08.003.

Shcherbina MA, Kazlawlene OP. 1971. The reaction of the medium and the rate of absorption of nutrients in the intestine of carp. J. Ichthyol. 11:81–85.

Shehadeh ZH, Gordon MS. 1969. The role of the intestine in salinity adaptation of the rainbow trout, *Salmo gairdneri*. Comp. Biochem. Physiol. 30:397–418. doi:10.1016/0010-406X(69)92011-8.

Shephard KL. 1994. Functions for fish mucus. Rev. Fish Biol. Fish. 4:401–429. doi:10.1007/BF00042888.

Shin N, Whon TW, Bae J. 2015. Proteobacteria : microbial signature of dysbiosis in gut microbiota. Trends Biotechnol. 33:496–503. doi:10.1016/j.tibtech.2015.06.011.

Shrimpton JM, Bernier NJ, Randall DJ. 1994. Changes in cortisol dynamics in wild and hatchery-reared juvenile coho salmon (*Oncorhynchus kisutch*) during smoltification. Can. J. Fish. Aquat. Sci. 51:2179–2187.

Sire M-F, Lutton C, Vernier J-M. 1981. New views on intestinal absorption of lipids in teleostean fishes: an ultrastructural and biochemical study in the rainbow trout. J. Lipid Res. 22:81–94.

Smit H. 1967. Influence of temperature on the rate of gastric juice secretion in the brown bullhead, Ictalurus nebulosus. Comp. Biochem. Physiol. 21:125–132.

Smith MW, Ellory JC. 1971. Temperature-induced changes in sodium transport and NKA activity in the intestine of goldfish (*Carassius auratus L.*). Comp. Biochem. Physiol. 39:209–218.

Smith MW. 1970. Selective regulation of amino acid transport by the intestine of goldfish (*Carassius auratus L.*). Comp. Biochem. Physiol. 35:387–401.

Snyder AR, Williams HN, Baer ML, Walker KE, Stine OC. 2002. 16S rDNA sequence analysis of environmental Bdellovibrio-and-like organisms (BALO) reveals extensive diversity. Int. J. Syst. Evol. Microbiol. 52:2089–2094

Soengas JL, Barciela P, Aldegunde M, Andres D. 1995. Gill carbohydrate metabolism of rainbow trout is modified during gradual adaptation to sea water. J. Fish Biol. 46:845–856.

Solomon S. 2007. Climate change 2007-the physical science basis: working group I contribution to the fourth assessment report of the IPCC. Cambridge University Press.

Somero GN, Bernard C, Bohr C, Krogh A. 2011. Comparative physiology: a "crystal ball" for predicting consequences of global change. Am. J Physiol. 301: R1-14. doi:10.1152/ajpregu.00719.2010.

Somero GN. 1975. Temperature as a selective factor in protein evolution: the adaptational strategy of "compromise." J. Exp. Zool. Part A Ecol. Genet. Physiol. 194:175–188.

Somero, GN, Hochachka PW. 1968. The adaptation of enzymes to temperature. 27: 659-664.

Sommer F, Bäckhed F. 2013. The gut microbiota - masters of host development and physiology. Nat. Publ. Gr. 11:227–238. doi:10.1038/nrmicro2974.

Spanggaard B, Huber I, Nielsen J, Nielsen T, Appel KF, Gram L. 2000. The microflora of rainbow trout intestine: a comparison of traditional and molecular identification. Aquaculture 182:1–15.

Steinhausen MF, Sandblom E, Eliason EJ, Verhille C, Farrell AP. 2008. The effect of acute temperature increases on the cardiorespiratory performance of resting and swimming sockeye salmon (*Oncorhynchus nerka*). J. Exp. Biol. 211:3915–3926.

Stevens CE, Hume ID. 2004. Comparative physiology of the vertebrate digestive system. Cambridge University Press.

Stevens D. 1982. The effect of acclimation temperature, assay temperature, and ration on the specific activity of trypsin and chymotrypsin. Comp Biochem. Physiol. B Biochem. Mol. Biol. 73: 631-634. doi:10.1016/0305-0491(82)90087-6.

Stevens ED, Sutterlin AM. 1976. Heat transfer between fish and ambient water. J. Exp. Biol. 65:131–145.

Stickney, RR; and Shumway S. 1974. Occurrence of cellulase activity in the stomachs of fishes. J Fish. Biol. 6:779–790.

Stone DAJ, Allan GL, Anderson AJ. 2003. Carbohydrate utilization by juvenile silver perch, *Bidyanus bidyanus* (Mitchell). III. The protein-sparing effect of wheat starch-based carbohydrates. Aquac. Res. 34:123–134.

Stroband HWJ, Van Der Veen FH. 1981. Localization of protein absorption during transport of food in the intestine of the grasscarp, *Ctenopharyngodon idella* (Val.). J. Exp. Zool. Part A Ecol. Genet. Physiol. 218:149–156.

Stroband HWJ. 1977. Growth and diet dependant structural adaptations of the digestive tract in juvenile grass carp (*Ctenopharyngodon idella*, Val.). J. Fish Biol. 11:167–174. doi:10.1111/j.1095-8649.1977.tb04110.x.

Sullam KE, Essinger SD, Lozupone CA, Connor MPO. 2012. Environmental and ecological factors that shape the gut bacterial communities of fish: a meta-analysis. Mol. Ecol. 21: 3363-3378.

Sullivan MX. 1907. The physiology of the digestive tract of elasmobranchs. Bull. Bur. Fish. 27:1–27.

Sun J, and Chang E. 2014. Exploring gut microbes in human health and disease: pushing the envelope. Genes. Diseas. 1: 132-139.

Tantillo GM, Fontanarosa M, Di Pinto A, Musti M. 2004. Updated perspectives on emerging Vibrios associated with human infections. Lett. Appl. Microbiol. 39:117–126.

Taylor J, Cooper C, Mommsen T. 2011. Implications of GI function for gas exchange, acid-base balance, and nitrogen metabolism. In: Grosell M, Farrell A, Brauner C, editors. The multifunctional gut of fish. 1st ed. Boca Raton: Academic Press. p. 216–248.

Taylor S, Egginton S, Taylor E. 1996. Seasonal temperature acclimatisation of rainbow trout: cardiovascular and morphometric influences on maximal sustainable exercise level. J. Exp. Biol. 199:835–845.

Thibault M, Blier PU, Guderley H. 1997. Seasonal variation of muscle metabolic organization in rainbow trout (Oncorhynchus mykiss). Fish Physiol. Biochem. 16:139–155.

Threader RW, Houston AH. 1983. Heat tolerance and resistance in juvenile rainbow trout acclimated to diurnally cycling temperatures. Comp. Biochem. Physiol. Part A Physiol. 75:153–155.

Tok CY, Chew SF, Peh WYX, Loong AM, Wong WP, Ip YK. 2009. Glutamine accumulation and up-regulation of glutamine synthetase activity in the swamp eel, *Monopterus albus* (Zuiew), exposed to brackish water. J. Exp. Biol. 212:1248–58. doi:10.1242/jeb.025395.

Torrissen KR. 1984. Characterization of proteases in the digestive tract of Atlantic salmon (*Salmo salar*) in comparison with rainbow trout (*Salmo gairdneri*). :669–674.

Trosvik P, de Muinck EJ. 2015. Ecology of bacteria in the human gastrointestinal tract—identification of keystone and foundation taxa. Microbiome 3:44. doi:10.1186/s40168-015-0107-4.

Turnbaugh PJ, Ley RE, Mahowald MA, Magrini V, Mardis ER, Gordon JI. 2006. An obesity-associated gut microbiome with increased capacity for energy harvest. Nature. 444:1027–1031. doi:10.1038/nature05414.

Ubeda C, Taur Y, Jenq RR, Equinda MJ, Son T, Samstein M, Viale A, Socci ND, Brink MRM Van Den, Kamboj M, et al. 2010. Vancomycin-resistant Enterococcus domination of intestinal

microbiota is enabled by antibiotic treatment in mice and precedes bloodstream invasion in humans. J Clin. Invest. 120:4332–4341. doi:10.1172/JCI43918DS1.

Uematsu K, Kitano M, Morita M, Iijima N. 1992. Presence and ontogeny of intestinal and pancreatic phospholipase A 2-like proteins in the red sea bream, Pagrus major. An immunocytochemical study. Fish Physiol. Biochem. 9:427–438.

Van Den Burg EH, Peeters RR, Verhoye M, Meek J, Flik G, Van der Linden A. 2005. Brain responses to ambient temperature fluctuations in fish: reduction of blood volume and initiation of a whole-body stress response. J. Neurophysiol. 93:2849–2855.

Veillette PA, White RJ, Specker JL, Young G. 2005. Osmoregulatory physiology of pyloric ceca: regulated and adaptive changes in chinook salmon. J. Exp. Zool. Part A Ecol. Genet. Physiol. 303:608–613.

Vergauwen L, Benoot D, Blust R, Knapen D. 2010. Long-term warm or cold acclimation elicits a specific transcriptional response and affects energy metabolism in zebrafish. Comp. Biochem. Physiol. Part A Mol. Integr. Physiol. 157:149–157.

Walsh P. 1995. Subcellular localization and biochemical properties of the enzymes of carbamoyl phosphate and urea synthesis in the batrachoidid fishes *Opsanus beta, Opsanus tau* and *Porichthys notatus*. J. Exp. Biol. 198: 755-766.

Walsh PJ, Blackwelder P, Gill KA, Danulat E, Mommsen TP. 1991. Carbonate deposits in marine fish intestines: a new source of biomineralization. Limnol. Oceanogr. 36:1227–1232. doi:10.4319/lo.1991.36.6.1227.

Watanabe K, Kodama Y, Harayama S. 2001. Design and evaluation of PCR primers to amplify bacterial 16S ribosomal DNA fragments used for community fingerprinting. J. Microbiol. Methods 44:253–262.

Wicks BJ, Randall DJ. 2002. The effect of sub-lethal ammonia exposure on fed and unfed rainbow trout: the role of glutamine in regulation of ammonia. Comp. Biochem. Physiol. Part A Mol. Integr. Physiol. 132:275–285.

Wilson JM, Castro LFC. 2010. Morphological diversity of the gastrointestinal tract in fishes. In: Grosell M, Farrel AP, Brauner CJ, editors. The multifunctional gut of fish. 1st ed. Oxford: Elsevier Inc. p. 1015–1029.

Windisch HS, Kathover R, Portner H-O, Frickenhaus S, Lucassen M. 2011. Thermal acclimation in Antarctic fish: transcriptomic profiling of metabolic pathways. Am. J. Physiol. Integr. Comp. Physiol. 301: R1453–R1466.

Woodward CK, Ellis LM. 1974. Dynamic solvent accessibility in the soybean trypsin inhibitor-trypsin complex. J Mol. Biol. 111:3419–3423.

Woodward CK, Ellis LM. 1975. Hydrogen exchange kinetics changes upon formation of the soybean trypsin inhibitor-trypsin complex. Biochemistry. 14:3419–3423.

Wright PA, Wood CM. 2009. A new paradigm for ammonia excretion in aquatic animals: role of Rhesus (Rh) glycoproteins. J. Exp. Biol. 212:2303–2312.

Wright PA. 1995. Nitrogen excretion in fish: three end products, many physiological roles. J. Exp. Biol. 198: 273-281.

Xia JH, Lin G, Fu GH, Wan ZY, Lee M, Wang L, Liu XJ, Yue GH. 2014. The intestinal microbiome of fish under starvation. BMC Genomics. 15: 266.

Yamamoto T. 1966. An electron microscope study of the columnar epithelial cell in the intestine of fresh water teleosts: Goldfish (*Carassius cauratus*) and rainbow trout (*Salmo irideus*). Cell Tissue Res. 72:66–87.

Yamamoto, M., and Hirano T. 1978. Morphological changes in the esophageal epithelium of the eel, *Anguilla japonica*, during adaptation to seawater. Cell Tissue Res 192:25–38.

Yancey PH, Somero GN. 1978. Temperature dependence of intracellular pH: Its role in the conservation of pyruvate apparent K_m values of vertebrate lactate dehydrogenases. J. Comp. Physiol. B 125:129–134. doi:10.1007/BF00686748.

Zarkasi KZ, Taylor RS, Abell GCJ, Tamplin ML, Glencross BD, Bowman JP. 2016. Atlantic salmon (*Salmo salar L.*) gastrointestinal microbial community dynamics in relation to digesta properties and diet. Microb. Ecol. 71:589–603. doi:10.1007/s00248-015-0728-y.

Zaugg, Mclain LR. 1975. Influence of water temperature on gill sodium, potassium-stimulated ATPase activity in juvenile coho salmon (*Oncorhynchus kisutch*). Comp. Biochem. Phys A. 54:5–7.

Appendix A: Command Scripts for QIIME

1. Validate_mapping_file.py: The validity of the barcode, linker-primer, and reverse-primer fields were checked to ensure correct IUPAC DNA characters and non-degenerate barcode sequence characters. Invalid alphanumeric characters, duplicate barcodes, valid header characters were flagged, and barcodes were checked for similar length for use in downstream processing.

2. Split_libraries.py: Barcode and linker-primer sequences were removed, and quality filtering was performed for the total sequences. Sequences with incorrect primer sequence or no corresponding barcode were removed. New barcodes were assigned to the filtered reads from each sample.

3. Pick_otus.py: A closed-reference Operational taxonomic units (OTUs) picking protocol was used to pick OTUs based on a 97% sequence similarity threshold and Green Genes reference library was used to assign taxonomy with USEARCH (Edgar 2010). Removal of chimeras were also completed in this step as part of the UCHIME v 5.2.236 USEARCH algorithm.

4. Pick_rep_set.py: One representative sequence was picked for each OTU; this file was used in downstream analysis.

5. Align_seqs.py: Alignment of the representative sequences generated in the previous step was performed using the PyNAST method of alignment (Caporaso et al. 2009).

6. Assign_taxonomy.py: Taxonomy was assigned to each aligned representative sequence with BLAST.

7. Filter_alignement.py: Low quality reads, long sequences, zero ambiguous base calls, zero primer sequence mismatch and OTU representative sequences with no BLAST hits were filtered and removed.

8. Make_phylogeny.py: A phylogenetic tree comprised of the OTUs was created based on a multiple sequence alignment with FastTree (Price et al. 2009).

9. Make_otu_table.py: An OTU dataset which predicted the frequency of OTUs in each sample was generated as a biom table file for use in downstream analysis.

10. Alpha_rarefaction.py: Alpha-rarefied tables based on the OTU biom data set were generated and collated to create observed species, Chao1, phylogenetic diversity, and Shannon Index plots. These plots were used to compare bacterial composition (abundance, richness and evenness) across samples.

11. Jaccknifed_beta_diversity.py: A beta diversity analysis to compare bacterial composition between samples. The sample containing the smallest number of OTUs was used as the baseline number for selecting random sequences from each sample to be compared. UPGMA (unweighted pair group method with arithmetic mean) distance matrices were used to generate consensus trees. The make_bootstrapped_trees.py command was used to create both un-weighted and weighted jackknifed bootstrapped trees.

Appendix B: Command Scripts for R Studio

1. Read.table: To specify the data files used for downstream processing (the bacterial abundance and enzyme activity response files, and presence/absence data predictor file)

2. Library(vegan): To call the installed vegan package used for the diversity analysis, ordination methods, and analysis of dissimilarities

3. Decostand (method="Hellinger"): To perform a Hellinger transformation on the bacterial abundance data file to remove species with low or zero counts

4. Rda(response, predictor): An RDA multivariate analysis was performed on the bacterial abundance and presence/absence data files

5. Plot: To generate a figure based on the output of the RDA command script. Bacterial species, GIT sites and enzymes were plotted on this ordination to view the degrees of dissimilarity between these parameters

Appendix C: Blank PCR Validation Test

The blank sample collected during extractions with the Stool and DNEasy kits were tested for contamination using PCR with the universal bacterial primers (Sigma-Aldrich Co., Woodlands, Texas) 338/341F-785R (V3 hypervariable region of the bacterial 16S rRNA) and 967F-1177R (V6 hypervariable region) that had been resuspended to a concentration of 100 µM in RNAse and DNAse free molecular water and stored at - 20°C. Primer design was based on those by Baker et al. (2003) and Watanbe et al. (2001) for the V3 and V6 region primers, respectively (Table 3). PCR was used to amplify the V3 and V6 regions of bacteria to test for their presence in the blank, positive control which was a gDNA sample, and negative control containing only the PCR master mix. The master mix contained 6.25 µl Dreamtaq PCR master mix (Thermo-Fisher Scientific; Waltham, Massachusetts), 1.25 µl forward primer, 1.25 µl reverse primer, 1.75 µl molecular water, and 2 µl blank sample, gDNA or molecular water for the blank, positive, and negative control PCR tests, respectively. PCR was performed using the Bio-Rad MyCycler (Bio-Rad Laboratories Limited, Mississauga, Ontario) using the following PCR protocol: a 3-minute initial denaturation at 95°C, a 30 second repeated 95°C denaturation cycle, 45 second annealing step at 57-58°C, a 1-minute elongation step at 72°C, a final elongation 72°C for 5 minutes, and finally holding at 4°C until sample retrieval. PCR productions for the blank, positive, and negative control were examined by running samples on a 1.5% agarose gel in a Tris-HCl-acetic acid-EDTA buffer including 0.5µg/ml of ethidium bromide and imaging the resulting gel run using a MiniBis Pro Imager (FroggaBio Scientific Solutions, Toronto, Ontario). Presence of bands indicating bacterial presence in the blank or negative control resulted in re-extraction of the gDNA from experimental sample set using a brand-new kit and a new PCR master mix was used to re-test samples

Table 3. Bacterial primer sequences for the V3 and V6 hypervariable regions

Hypervariable region	Primer sequence for region	Source
V3	Forward: 338 = ACTCCTACGGGAGGCAGC 341= CCTACGGGAGGCAGCAGTG Reverse: 785 = CTACCAGGGTATCTAATCC	Baker et al. 2003
V6	Forward: 967 = CAACGCGAAGAACCTTACCT Reverse: 1177 = GACGTCATCCCCACCTTCCT	Watanabe et al. 2001

Appendix D: Fish Feed Composition

Table 4. Tropic Aquaria Ltd. Fish Feed "Tropical Energy Pelleted Tropical Fish Food" composition

Nutrient	Percentage of feed
Min. Crude Protein	37.5%
Min. Crude Fat	8%
Min. Crude Fibre	5%
Added Minerals	1.5%
Min. I.U. Vitamin A	180000/K